

SHAG Test Series

Seismic Research on an Aged United States Gate Valve
and on a Piping System in the Decommissioned
Heissdampfreaktor (HDR): Summary

Prepared by R. Steele, Jr., J. G. Arendts

Idaho National Engineering Laboratory
EG&G Idaho, Inc

Prepared for
U.S. Nuclear Regulatory
Commission

AVAILABILITY NOTICE

Availability of Reference Materials Cited in NRC Publications

Most documents cited in NRC publications will be available from one of the following sources:

1. The NRC Public Document Room, 2120 L Street, NW, Lower Level, Washington, DC 20555
2. The Superintendent of Documents, U.S. Government Printing Office, P.O. Box 37082, Washington, DC 20013-7082
3. The National Technical Information Service, Springfield, VA 22161

Although the listing that follows represents the majority of documents cited in NRC publications, it is not intended to be exhaustive.

Referenced documents available for inspection and copying for a fee from the NRC Public Document Room include NRC correspondence and internal NRC memoranda; NRC Office of Inspection and Enforcement bulletins, circulars, information notices, inspection and investigation notices; Licensee Event Reports; vendor reports and correspondence; Commission papers; and applicant and licensee documents and correspondence.

The following documents in the NUREG series are available for purchase from the GPO Sales Program: formal NRC staff and contractor reports, NRC-sponsored conference proceedings, and NRC booklets and brochures. Also available are Regulatory Guides, NRC regulations in the *Code of Federal Regulations*, and *Nuclear Regulatory Commission Issuances*.

Documents available from the National Technical Information Service include NUREG series reports and technical reports prepared by other federal agencies and reports prepared by the Atomic Energy Commission, forerunner agency to the Nuclear Regulatory Commission.

Documents available from public and special technical libraries include all open literature items, such as books, journal and periodical articles, and transactions. *Federal Register* notices, federal and state legislation, and congressional reports can usually be obtained from these libraries.

Documents such as theses, dissertations, foreign reports and translations, and non-NRC conference proceedings are available for purchase from the organization sponsoring the publication cited.

Single copies of NRC draft reports are available free, to the extent of supply, upon written request to the Office of Information Resources Management, Distribution Section, U.S. Nuclear Regulatory Commission, Washington, DC 20555.

Copies of industry codes and standards used in a substantive manner in the NRC regulatory process are maintained at the NRC Library, 7920 Norfolk Avenue, Bethesda, Maryland, and are available there for reference use by the public. Codes and standards are usually copyrighted and may be purchased from the originating organization or, if they are American National Standards, from the American National Standards Institute, 1430 Broadway, New York, NY 10018.

DISCLAIMER NOTICE

This report was prepared as an account of work sponsored by an agency of the United States Government. Neither the United States Government nor any agency thereof, or any of their employees, makes any warranty, expressed or implied, or assumes any legal liability of responsibility for any third party's use, or the results of such use, of any information, apparatus, product or process disclosed in this report, or represents that its use by such third party would not infringe privately owned rights.

SHAG Test Series

Seismic Research on an Aged United States Gate Valve
and on a Piping System in the Decommissioned
Heissdampfreaktor (HDR): Summary

Manuscript Completed: July 1989
Date Published: August 1989

Prepared by
R. Steele, Jr., J. G. Arendts

Idaho National Engineering Laboratory
Managed by the U.S. Department of Energy

EG&G Idaho, Inc.
P.O. Box 1625
Idaho Falls, ID 83415

Prepared for
Division of Engineering
Office of Nuclear Regulatory Research
U.S. Nuclear Regulatory Commission
Washington, DC 20555
NRC FIN A6322
Under DOE Contract No. DE-AC07-761D01570

ABSTRACT

The Idaho National Engineering Laboratory (INEL) participated in an internationally sponsored seismic research program conducted at a decommissioned experimental reactor facility, the Heissdampfreaktor (HDR), located in the Federal Republic of Germany (FRG). The research program included the study of the effects of excitation, produced during a simulated seismic event, on (a) the operability and integrity of a naturally aged 8-in. motor-operated gate valve installed in the Versuchskreislauf (VKL), an existing piping system in the HDR, (b) the dynamic response of the VKL and the operability of snubbers, and (c) the dynamic responses of various piping support systems installed on the VKL. The INEL work, sponsored by the U.S. Nuclear Regulatory Commission (USNRC), contributes to earthquake investigations being conducted by the Kernforschungszentrum Karlsruhe (KfK) and is part of the general HDR Safety Program performed in behalf of the FRG, Federal Ministry for Research and Technology. This report presents the results of the KfK-designated SHAG (Shakergebäude) test series; these are the first in situ experiments involving an actual nuclear power plant and a full scale piping system under simulated seismic loading.

INEL modified the VKL by installing a mid-life gate valve from a U.S. nuclear power plant and by designing and installing a piping support system typical of U.S. commercial design. Six other piping support systems of varying flexibility, from stiff to flexible, were also installed at various times during the experiments. Valve loadings, in addition to the seismic excitation, included internal hydraulic pressure, flow, and, during one series of experiments, elevated temperature.

Building response in terms of zero period accelerations (ZPA) reached 0.3 g and exceeded building design limits. The VKL response averaged over 1 g, with amplification at the valve exceeding 3 g. One manufacturer's snubbers experienced ASME Code Level C loadings. The valve response to dynamic motion showed unexpected amplification and frequency content. Also, the valve motor operator developed a functional problem. Near the end of the valve closing cycle, the motor stalled when the closing torque switch failed to open.

In all, twenty-five representative seismic experiments were conducted on the gate valve and seven piping support configurations. Results of the testing will contribute to the technical basis used for support and development of equipment qualification standards and procedures sponsored by the NRC.

FIN No. A6322—Environmental Qualification of Mechanical and Dynamic
(Including Seismic) Qualification of Mechanical and
Electrical Equipment Program (EDQP)

SUMMARY

During the summer of 1986, the Idaho National Engineering Laboratory (INEL), under contract with the United States Nuclear Regulatory Commission (USNRC), participated with the Kernforschungszentrum Karlsruhe (KfK), the Argonne National Laboratory (ANL), Staatliche Materialprüfungsanstalt (MPA), Kraftwerk Union (KWU), and the Electrical Power Research Institute (EPRI) in the KfK-designated SHAG (Shakergebäude) test series at the Heissdampfreaktor (HDR), a decommissioned experimental reactor facility located in the Federal Republic of Germany (FRG). This seismic research program consisted of a series of tests to evaluate the structural response, thermal-hydraulic performance, and fracture mechanics behavior of the HDR and the components and systems within the facility during simulated seismic excitation.

Specifically, the INEL investigated the operability of the piping supports and an 8-in. gate valve and assumed responsibility for the instrumentation and data collection of the portion of the testing associated with the Versuchskreislauf (VKL), a piping system located in the HDR. Our investigation included (a) monitoring the operability, integrity, and response characteristics of the mid-life gate valve during a series of simulated seismic events, (b) monitoring the operability of typical nuclear industry snubbers in the in situ environment, (c) providing data for the EPRI snubber replacement devices, and (d) recording the piping system response data for use by ANL to verify the SMACS (Seismic Methodology Analysis Chain with Statistics) computer code.

The experimenters mounted a large, collapsing twin-arm rotary mass coastdown shaker on the operating floor (30-m level) of the HDR reactor building to generate and transmit mechanical energy to the building. Force and motion were transmitted from the building floors and internal structures to the piping systems and components in the building.

The USNRC provided an aged 8-in. gate valve from the decommissioned Shippingport Atomic Power Station. The valve was refurbished, instrumented, and tested to the applicable sections of ASME/ANSI Standard B16.41 for installation in the HDR.

We performed a typical U.S. seismic analysis of the existing VKL at the HDR. The results of this analysis formed the basis for the piping system design modifications. The modifications consisted of installing the refurbished gate valve and installing snubbers and struts to set up a dynamic piping support system typical of U.S. stiff nuclear piping support systems; subsequent modification during the SHAG test series allowed us to test six additional piping support systems. INEL

enhanced the VKL instrumentation system by installing 103 instruments to measure acceleration, strain, displacement, force, temperature, pressure, valve stem position, valve operator motor current and voltage, and valve differential pressure. The VKL is constructed of stainless steel (approximately equivalent to U.S. Type 347) in four pipe sizes (equivalent to 10, 8, 5, and 4 in.). The system is located between the 18- and 24-m elevations in the HDR facility. The piping system internal fluid is electrically heated, and the system is capable of operating at Pressurized Water Reactor (PWR) secondary or Boiling Water Reactor (BWR) primary pressure/temperature. A maximum differential pressure of 385 psid was achieved across the valve.

Twenty-five individual coastdown tests were performed with initial shaker starting frequencies, at the beginning of coastdown, of 1.6 to 8 Hz. Only five of the seven support systems were installed for the 6- and 4.5-Hz tests, and only the most flexible support system was installed for the 1.6-Hz tests. Internal piping fluid temperatures included both ambient (25 to 40°C) and elevated (210°C) temperatures. Tests were conducted with and without hydraulic pressure in the piping system, and with and without flow through the valve.

For each experiment, INEL and MPA collected the data from the U.S. instruments installed to monitor the response of the VKL and the U.S. gate valve, reciprocally shared data with KfK (who had also installed instruments), and committed the data to permanent record.*

The response of the VKL was strongly influenced by the motion of a large vessel called the Heissdampfumformer (HDU), to which part of the VKL was attached. HDU movement was greater than the dynamic restraint anchorage movement and was the primary forcing function influencing VKL behavior. Input to the piping system exceeded typical U.S. East Coast safe shutdown earthquakes (SSEs) and West Coast operational basis earthquakes (OBEs).

The starting frequencies important to valve and piping response provided sufficient loading in the piping system to determine the influence of piping support methodology on pipe and valve response. The VKL response did not reach high levels of measured strain in the piping system. However, it did reach levels that loaded some of the installed snubbers to their ASME Code Level C rating, and it provided sufficient loading on the valve that in situ performance could be assessed. The responses were also high enough to permit identification of distinct modes of response for the various piping support systems and to allow assessment of their performance.

Pacific Scientific mechanical snubbers, the most popular mechanical snubber used in nuclear power plant applications, were used in the U.S. stiff piping support system during most of the tests. These snubbers generally performed to the manufacturer's specifications. Four of the other piping support systems used energy absorbing devices in place of the snubbers. The ANCO system was stiffer than the snubbed U.S. stiff system, and the EPRI Cloud, EPRI Bechtel, and GERB of Berlin systems were all softer than the snubbed system.

The naturally aged U.S. gate valve developed a motor operator anomaly during the program. The operator failed to open the closing torque switch on closing, and the motor went into a stall. Posttest

investigations revealed that the motor operator torque spring had taken a permanent set so that the motor operator was not producing the rated torque for a given torque switch setting (NRC Information Notice 89-43). #

Motor heating also reduced the operator's output. Later analyses showed that external circuit resistance contributed significantly to the motor operator's poor performance at HDR (NRC Information Notice 89-11). #

The analysis of the valve's dynamic response revealed amplification at frequencies other than those determined from seismic bench tests performed for valve qualification standards. The response above 33 Hz was not expected. Other full-scale, triaxially excited valve system responses compared with HDR results show similar results.

(708) 825-9500 list

ACKNOWLEDGMENTS

The efforts of many people and organizations were required to successfully conduct the SHAG Test Series of the HDR Seismic Research Program. For the portion of the HDR research reported herein, we wish to thank personnel from KfK PHDR, particularly Hr. Dr. L. Malcher and Hr. Schrammel; from HDR, Herren H. Wenzel, L. Lohr, and R. Machad; from MPA, Herren S. Hass and W. Ehling; and from the Fraunhofer Institut, Hr. Dr. H. Steinhilber. USNRC provided early planning assistance by allowing Dr. Shafik Iskander time to assist us; Drs. G. H. Weidenhamer and J. F. Costello, the onsite NRC Program Managers, assisted us throughout the program. We also express gratitude to Dr. C. Kot of ANL for his contributions to the program and his cooperation in this multinational, multilaboratory effort, and to M. J. Russell of the INEL for his insights and assistance.

CONTENTS

ABSTRACT	ii
SUMMARY	iii
ACKNOWLEDGMENTS	v
NOMENCLATURE	viii
1. INTRODUCTION	1
1.1 Background	1
1.2 Objectives	1
1.3 Qualification Standards and Regulatory Guides	2
2. TEST DESCRIPTION	3
2.1 The Heissdampfreaktor (HDR)	3
2.2 Seismic Simulator	3
2.3 VKL Piping Support Systems	3
2.4 Gate Valve	10
2.5 Instrumentation	10
3. TEST RESULTS	13
3.1 Building Response	13
3.2 HDU Vessel Response	15
3.3 VKL Piping System Response	18
3.4 Performance of Snubbers and Snubber Replacement Devices	20
3.4.1 Performance of Pacific Scientific Mechanical Snubbers	20
3.4.2 Performance of the Bergen Paterson Hydraulic Snubber	30
3.4.3 Performance of Snubber Replacement Devices	30
3.5 Comparison of Piping Support Systems	32
3.6 Valve and Motor Operator Response	34
3.6.1 Structural Integrity of the Motor-Operated Valve	35
3.6.2 Valve Response	35
3.6.3 Performance of the Motor Operator	35
3.6.4 Valve Dynamic Analysis	44

4. CONCLUSIONS	52
4.1 Building and Piping System Responses	52
4.2 Snubber Responses	52
4.3 Snubber Replacement Devices Compared	52
4.4 Valve Response	53
4.5 Valve Dynamic Analysis	53
5. REFERENCES	54

NOMENCLATURE

ANCO	ANCO Engineers, Inc.	KfK	Kernforschungszentrum Karlsruhe
ANL	Argonne National Laboratory	KWU	Kraftwerkunion AG (German architect-engineer)
ASME/ANSI	American Society of Mechanical Engineers/American National Standards Institute, Standard B16:41	LBF	Fraunhofer Institut für Betriebsfestigkeit Darmstadt
ASME Code	The American Society of Mechanical Engineers Boiler and Pressure Vessel Code, Section III	LOFT	Loss of Fluid Test Facility located at INEL
Baseline Functional	A functional test performed without dynamic loading to establish a normal measurement	MPA	Staatliche Materialprüfungsanstalt, Universität Stuttgart
Bechtel	Bechtel Power Corporation	Nupipe II	A piping analysis computer code developed by the Quadrex Corporation, Campbell California
Cloud	Robert L. Cloud Associates, Inc.	OBE	Operational basis earthquake (IEEE 344)
CPS	Containment penetration system, a design basis and severe accident study performed under FIN 6322	psid	Pounds per square inch differential
DIN Standards	Deutsche Institute für Norming	SHAG	Shakergebäude (building shaker)
EPRI	Electric Power Research Institute	SHAM	Servohydraulische Anregung Maschinetechnik
FRG	Federal Republic of Germany	SMACS	Seismic Methodology Analysis Chain with Statistics Computer Code
g	Acceleration equal to the acceleration of gravity	SSE	Safe shutdown earthquake (IEEE 344)
GERB	The GERB Company Berlin	Starting Frequency	The frequency in Hz at which the shaker was stabilized before the explosive bolt was fired
HDR	Heissdampfreaktor (superheated steam reactor)	T40.XX	The numbering system assigned to each SHAG test
HDU	Heissdampfumformer (steam convertor)	USNRC	United States Nuclear Regulatory Commission
Hydro	Hydrostatic Test per ASME Code	VKL	Versuchskreislauf (experimental piping system)
Hz	Herz (cycles per second)	ZPA	Zero period acceleration (IEEE 344)
INC	International NuclearSafeguards Company	ΔP	Differential pressure
INEL	Idaho National Engineering Laboratory		

SHAG TEST SERIES

SEISMIC RESEARCH ON AN AGED UNITED STATES GATE VALVE AND ON A PIPING SYSTEM IN THE DECOMMISSIONED HEISSDAMPFREAKTOR (HDR)

1. INTRODUCTION

The United States Nuclear Regulatory Commission (USNRC) requires qualification of certain equipment in U.S. nuclear power plants to ensure that the equipment will operate as designed when subjected to design basis loadings throughout its design life. Nuclear equipment qualification is typically performed to industry standards, some of which are justified by only an analytical or extrapolated basis. This is especially true of qualification standards for line-mounted equipment, for which dynamic input is always analytically determined. The SHAG Test Series provides in situ data from a prototypical piping system subjected to seismic-like loads.

1.1 Background

The Idaho National Engineering Laboratory (INEL), Environmental and Dynamic Qualification of Mechanical and Electrical Equipment Program, is performing research to establish a technical basis for assessing the adequacy of qualification standards and for recommending improvements. The research is performed under the auspices of the USNRC, Office of Nuclear Research. Dynamic qualification of line-mounted mechanical equipment is one area of the research where industry standards are still in draft form. Results from the USNRC/INEL participation in the HDR studies can provide a technical basis for contributions to the effort to finalize equipment qualification standards.

The current HDR test program is called the HDR Phase II Sicherheitsprogramm (Safety Research Program). The program is being conducted by Kernforschungszentrum Karlsruhe (KfK) in behalf of the Federal Republic of Germany (FRG) Federal Ministry for Research and Technology. The SHAG test series constitutes part of the seismic portion of the HDR Safety Research Program. Researchers from the INEL joined with researchers from the Argonne National Laboratory (ANL), the Electrical Power Research Institute (EPRI), Kraftwerk Union (KWU), and the Staatliche Materialprüfungsanstalt (MPA) in partici-

pating with KfK in the SHAG test series. These tests are the first in situ experiments involving an actual nuclear power plant and a full scale piping system under simulated seismic loading.

The SHAG tests at HDR provided a unique opportunity to study the behavior of a complete full-scale nuclear piping system that is supported in a manner representative of a U.S. installation. During the SHAG test series, it was possible to subject a valve to normal fluid loads and seismic-like loads, in combination. It was also possible to compare the response of the piping system when supported by the typical U.S. stiff support system to its response when supported by six other support systems ranging from very flexible to stiff.

The INEL equipment qualification involvement with the HDR Seismic Research Program began in FY-1984 with pretest planning. A test plan was drafted, and piping support design completed in FY-1985. Construction, instrumentation, and testing took place in FY-1986.

1.2 Objectives

The objectives for INEL's participation in the HDR Seismic Research Program were determined by reviewing the purpose of equipment qualification and the functional requirements of nuclear piping systems. The first objective was to measure the effects of various dynamic and hydraulic loads on gate valve operability, integrity, and response characteristics during a series of representative seismic events in an in situ environment. The dynamic loads were varied by modifying the piping support configurations from a base (typical) U.S. stiff piping support system to form six other systems ranging from a very flexible support system to a very stiff energy absorbing support system (described in Section 2), and by varying the magnitude and frequency of the excitation.

The second objective was to obtain data so that valve response to multiaxial, in situ seismic loads could be

compared with valve response to single effects loadings typical of valve qualification testing.

The third objective was to obtain piping system response data (strain, acceleration, force, and displacement) for the base system and the six other support systems during a series of reasonably representative simulated seismic events. The information is to be used to evaluate support system methodology, snubber performance, and snubber replacement device performance, and to verify the SMACS (Seismic Methodology Analysis Chain with Statistics) computer code.

Because of the large amount of information generated by the SHAG Test Series, this report is published in two volumes. Volume 1 presents a summary of the tests and the results, and Volume 2 contains appendices that present details and specifics.

1.3 Qualification Standards and Regulatory Guides

The following equipment qualification standards and regulatory guides are potentially affected by HDR research results.

- American Society of Mechanical Engineers, *Functional Qualification Requirements for Power Operated Active Valve Assemblies for Nuclear Power Plants*, ANSI/ASME B16.41, currently being revised as ANSI QV-4
- American Society of Mechanical Engineers, *Self-Operated and Power-Operated Safety-Related Valves Safety Specification Standard*, ANSI/ASME N278.1-1975
- Institute of Electrical and Electronic Engineers, *Recommended Practices for Seismic Qualification of Class 1E Equipment for Nuclear Power Generating Stations*, IEEE Standard 344, 1975
- Institute of Electrical and Electronic Engineers, *Qualification of Safety-Related Valve Actuators*, IEEE Standard 382, 1980
- Institute of Electrical and Electronic Engineers, *Design Qualification of Safety Systems Equipment Used in Nuclear Power Generating Stations*, IEEE Standard 627, 1980
- United States Nuclear Regulatory Commission, *Development of Floor Design Spectra for Seismic Design of Floor-Supported Equipment or Components*, Regulatory Guide 1.122
- United States Nuclear Regulatory Commission, *Damping Values for Seismic Design of Nuclear Power Plants*, Regulatory Guide 1.61
- United States Nuclear Regulatory Commission, *Functional Specification for Active Valve Assemblies in Systems Important to Safety in Nuclear Power Plants*, Regulatory Guide 1.148
- United States Nuclear Regulatory Commission, *Seismic Qualification of Electric Equipment for Nuclear Power Plants*, Regulatory Guide 1.100
- United States Nuclear Regulatory Commission, *Qualification Tests of Electric Valve Operators Installed Inside the Containment of Nuclear Power Plants*, Regulatory Guide 1.73
- United States Nuclear Regulatory Commission, *USNRC Standard Review Plan, Section 3.9.3., ASME Code Class 1, 2, and 3 Components, Component Supports, and Core Support Structures*, NUREG-0800, 1981
- United States Nuclear Regulatory Commission, *Qualification and Acceptance Tests for Snubbers Used in Systems Important to Safety*, Draft Regulatory Guide SC 708-4, Rev. 1, 1981
- American Society of Mechanical Engineers, *Examination and Performance Testing of Nuclear Power Plant Dynamic Restraints (Snubbers)*, ANSI ASME OM4, 1982
- American Society of Mechanical Engineers, *Boiler and Pressure Vessel Code, Section XI, Subsection IWF, Requirements for Class 1, 2, 3 and MC Component Supports of Light-Water Cooled Power Plants*, 1986 edition.

2. TEST DESCRIPTION

2.1 The Heissdampfreaktor (HDR)

The HDR is a decommissioned experimental reactor facility located near Frankfurt in the Federal Republic of Germany (FRG). The facility (Figure 1) was modified in two areas for the SHAG portion of the HDR Safety Research Program. One, we mounted a very large twin-arm rotary mass coastdown mechanical shaker or seismic simulator (Figure 2) to the operating floor at the 30-m level. Two, we modified an existing piping system called the Versuchskreislauf (VKL) by installing an aged 8-in. motor-operated gate valve of U.S. nuclear origin, a dynamic pipe support system typical of U.S. nuclear design, and 103 instruments on the piping system and on the Heissdampfumformer (HDU), a large vessel, similar to a steam generator, to which part of the piping system is attached (Figure 3). HDR pipe sizes, internal pressure, temperature, flow media, valve operation, and dynamic supports all represent reasonable commercial nuclear conditions and provide an outstanding test bed for in situ seismic research.

2.2 Seismic Simulator

The SHAG Test Series conducted at the HDR facility consisted of mechanical excitation of the HDR building and the resulting excitation of the systems and components inside the structure. Excitation of the building was accomplished by a large, twin-arm, eccentric mass coastdown shaker designed by ANCO Engineers, Inc. Various amounts of weight can be bolted to the revolving arms to produce different amounts of input energy to the building. The shaker was spun up with its weighted arms in balance (at 180 degrees) to the desired starting frequency, and then the motor was disengaged for coastdown. Then an explosive bolt was set off to allow the arms to swing together, creating a revolving eccentric mass that imparted the mechanical loading to the highest structural floor [30 m (100 ft)] in the building.

Tests were performed with starting frequencies from 1.6 to 8 Hz. Shaker input to the building for the 8 Hz tests exceeded 90 s in duration. The complex dynamic response of the building caused the components and systems in the building to respond with both vertical and horizontal motion.

For each experiment, the shaker was weighted with a specified amount of weight bolted to the shaker arms. In general, the amount of weight varied inversely with the starting frequency scheduled for the experiment.

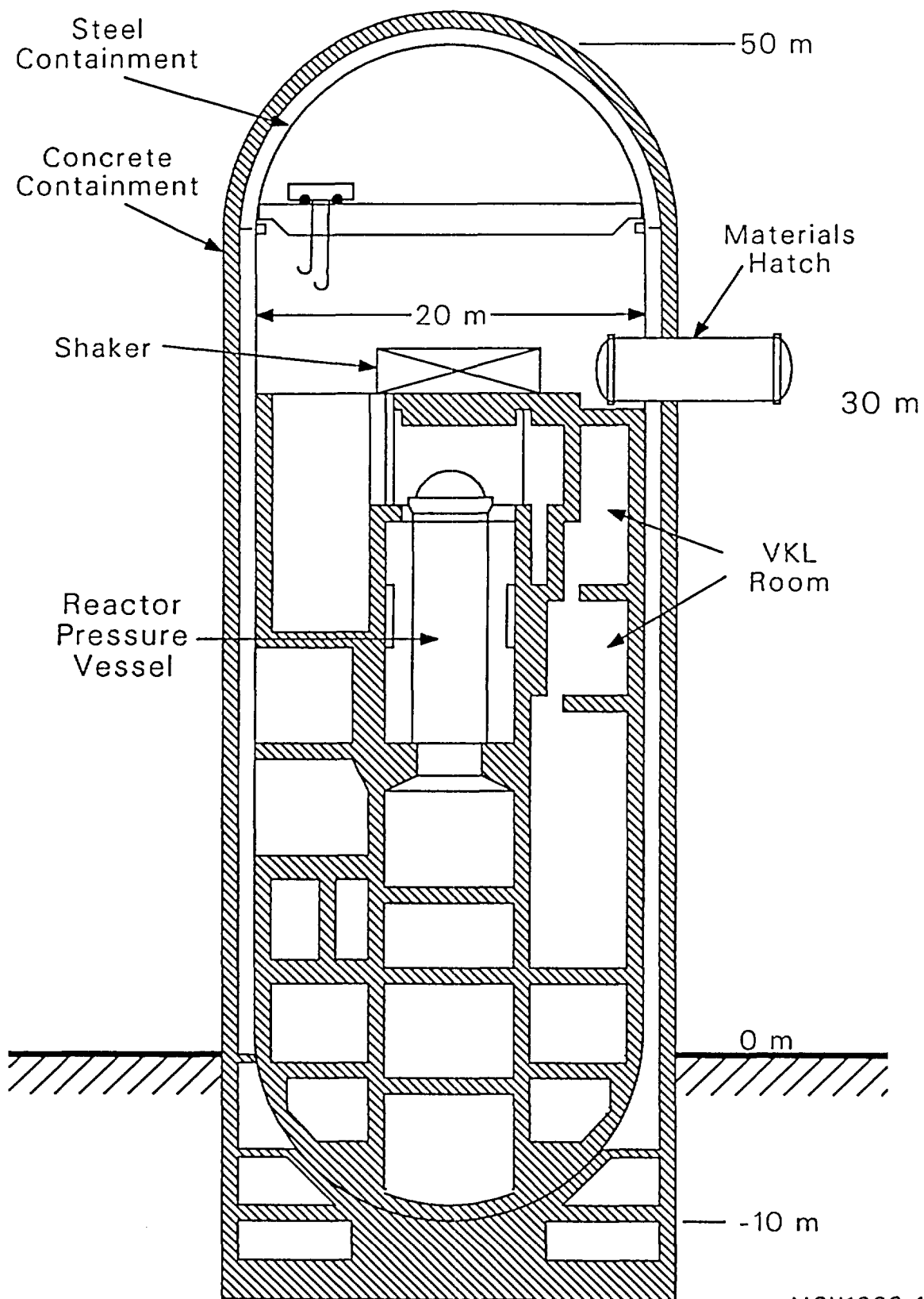
Twenty-five experiments were performed, as shown in Table 1 and as summarized in the following list:

Starting Frequency	Number of Tests	Starting Frequency	Number of Tests
1.6 Hz	3	5.6 Hz	1
2.1 Hz	1	6 Hz	6
4.5 Hz	6	8 Hz	8
Total	25		

2.3 VKL Piping Support Systems

The VKL is located between the 18- and 24-m elevations in the HDR facility, as shown in Figure 1. The VKL consists basically of two parallel flow loops connected to the HDU and to a manifold or header (DF 16), as shown in Figure 3. The VKL is constructed of stainless steel in four pipe sizes. Fluid in the system is electrically heated, and the system is capable of operating at pressurized water reactor (PWR) secondary or boiling water reactor (BWR) primary pressure and temperature conditions. One of the parallel flow loops was orificed to provide maximum differential pressure across the installed valve. USNRC provided the aged, 8-in., motor-operated gate valve from the decommissioned Shippingport Atomic Power Station, where it had served approximately 25 years as a feedwater safety injection isolation valve. INEL thoroughly refurbished the valve and added a total travel valve position device to the valve stem, which supplemented the limit switches to aid in valve signature analyses. Deutsche Institute für Norming (DIN Standards) apply for installations in German plants. The ASME code and ANSI B16.41 were acceptable substitutes. Testing included hydro, proof, leakage, and baseline functional tests and seismic fundamental frequency determination.

INEL analyzed the VKL, and, using the NUPIPE-II computer code, the response spectra analysis techniques, and equations of NC-3600, summer 1979 addenda of the ASME code, designed a dynamic piping support system for the VKL that was representative of a typical U.S. stiff support system. It was designed using typical U.S. struts and snubbers, sized for predicted loads at Level B allowables. Upset allowables were used owing to the uncertainty of KfK's input spectra. The manufactured supports, snubbers, struts, pipe clamps, pins, etc. were purchased from U.S. nuclear suppliers. The framework and anchors were purchased locally in Germany. HDR craftsmen



MGH1088-1

Figure 1. A simplified cross section of the HDR facility, showing the locations of the shaker, the VKL, and the reactor pressure vessel.

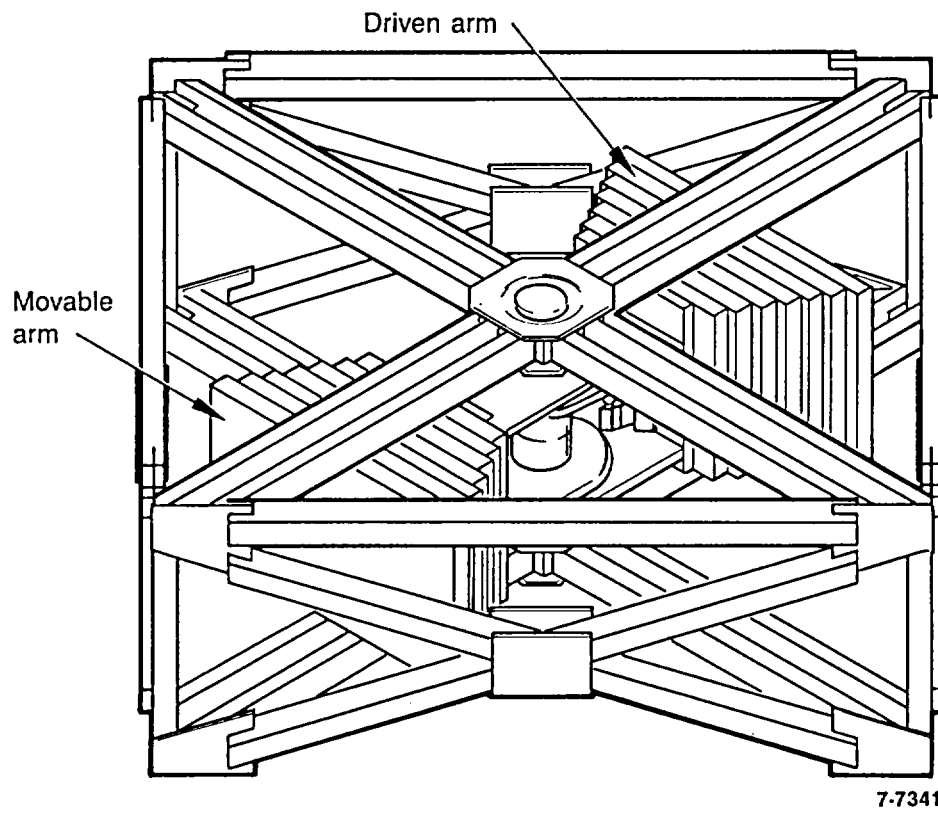


Figure 2. The large twin-arm rotary mass coastdown mechanical shaker used to produce the simulated seismic excitation.

Table 1. Test matrix

Test	Temperature (C)	Support Configuration	Eccentricity (kg/m)	Frequency (Hz)	VKL Flow (tons/h)	Valve Operation
T 40.34	20	3	4700	6.0	90	Cycle
T 40.35	20	3	4700	8.0	90	Cycle
T 40.36	20	3	8200	5.6	90	Cycle
T 40.37	20	3	27800	2.1	90	Cycle
T 40.40	20	4	4700	8.0	90	Cycle
T 40.20	20	2	4700	8.0	90	Cycle
T 40.60	20	6	4700	8.0	90	Cycle
T 40.50	20	5	4700	8.0	90	Cycle
T 40.70	20	7	4700	8.0	90	Cycle
T 40.10	20	1	4700	8.0	90	Cycle
T 40.30	20	3	4700	8.0	90	Cycle
T 40.31	20	3	6450	6.0	90	Cycle
T 40.41	20	4	6450	6.0	90	Cycle
T 40.21	20	2	6450	6.0	90	Cycle
T 40.11	20	1	6450	6.0	90	Cycle
T 40.51	20	5	6450	6.0	90	Cycle
T 40.52	210	5	8200	4.5	90	Cycle
T 40.32	210	3	8200	4.5	90	Cycle
T 40.42	210	4	8200	4.5	90	Cycle
T 40.12	210	1	8200	4.5	90	Cycle
T 40.22	50	2	8200	4.5	90	Cycle
T 40.12A	210	1	8200	4.5	90	Cycle
T 40.14	40	1	33000	1.6	90	Cycle
T 40.16	30	1	54000	1.6	0	Open
T 40.13	30	1	67000	1.6	0	Open

a. Support configuration:

- 1 = KfK very flexible
- 2 = KWU moderately flexible
- 3 = U.S. stiff
- 4 = EPRI/Bechtel energy-absorbing
- 5 = EPRI/Cloud impacting
- 6 = GERB energy-absorbing
- 7 = ANCO energy-absorbing

installed the supports under supervision of INEL engineers. This support system, by component removal or replacement, also formed the basis for the six other participants' piping support configurations.

Six struts and six snubbers (5 mechanical and 1 hydraulic) were added to the existing dead weight support system to constitute the U.S. stiff piping support system. The dead weight system included six Grinnell spring and constant force supports and one threaded rod hanger. An additional spring hanger (H-13) was

installed to account for the added weight of the U.S. gate valve that was installed. The dead weight supports were typical of those in U.S. nuclear piping systems. Figure 3 identifies the locations of the supports. The dead weight support configuration was not changed during the program.

Six other dynamic piping support systems were tested in addition to the U.S. stiff system. These additional piping support systems included a very flexible system (designed by KfK), a moderately flexible

system (designed by KWU), and four energy-absorbing support systems. The four energy-absorbing systems included an impact system [sponsored by the Electrical Power Research Institute (EPRI) and designed by Robert L. Cloud Associates, Inc.], a ductile flexure system (sponsored by EPRI and designed by Bechtel Power Corporation), and two viscous mass energy-absorbing designs (one by GERB Berlin, and the other by ANCO Engineers, Inc.). The energy absorbing systems varied in design stiffness from the flexible EPRI-Bechtel system to the ANCO system, which at ambient conditions was stiffer than the U.S. stiff system. We compared the seven systems by conducting several tests, at the same starting frequency and conditions but with different support systems, and measuring the operability of the valve and the responses of the piping system and of the valve in terms of acceleration, strain, force, and displacement. All seven systems were tested at the 8-Hz starting frequency. Five of the seven systems were tested at the 6-Hz and 4.5-Hz starting frequencies.

Descriptions of the seven support systems and the locations of specific items of equipment used in each support system are summarized in Table 2 and are given in the following list. Figure 3 shows the installed U.S. stiff system and identifies the locations (H-1, H-2, etc.) where the components were installed. In general, the U.S. stiff system, by component removal or replacement, served as the basis for the other systems. However, the GERB system included an energy-absorbing device placed at a location not shown in Figure 3. Figure 4 shows the installed GERB support configuration and identifies that additional location (near H-11).

Configuration 1 (KfK, very flexible). All snubbers and struts were removed except the two struts at H-4 and H-5.

Configuration 2 (KWU, moderately flexible). All snubbers and one strut, H-3, were removed.

Configuration 3 (U.S. stiff). The six struts and six snubbers (one hydraulic and five mechanical) were left in place. The struts, typical of those used in nuclear piping systems, were located at H-3, -4, -5, -9, -10, and -11. Initially, there were four International NuclearSafeguards Company (INC) mechanical snubbers, located at H-6, -7, -8, and -12; one Pacific Scientific mechanical snubber, located at H-1; and a Bergen-Patterson hydraulic snubber, located at H-2. After their failure during the preliminary tests, the four INC mechanical snubbers were replaced with Pacific Scientific mechanical snubbers for the comparison tests.

Configuration 4 (EPRI/Bechtel). The six snubbers were replaced with four energy absorbers at H-1, -6, -7, and -8. Snubber positions H-2 and H-12 were omitted. The six struts remained in place. The energy absorbers are pin-to-pin replacements for snubbers. The devices use ductile flexures to absorb dynamic energy.

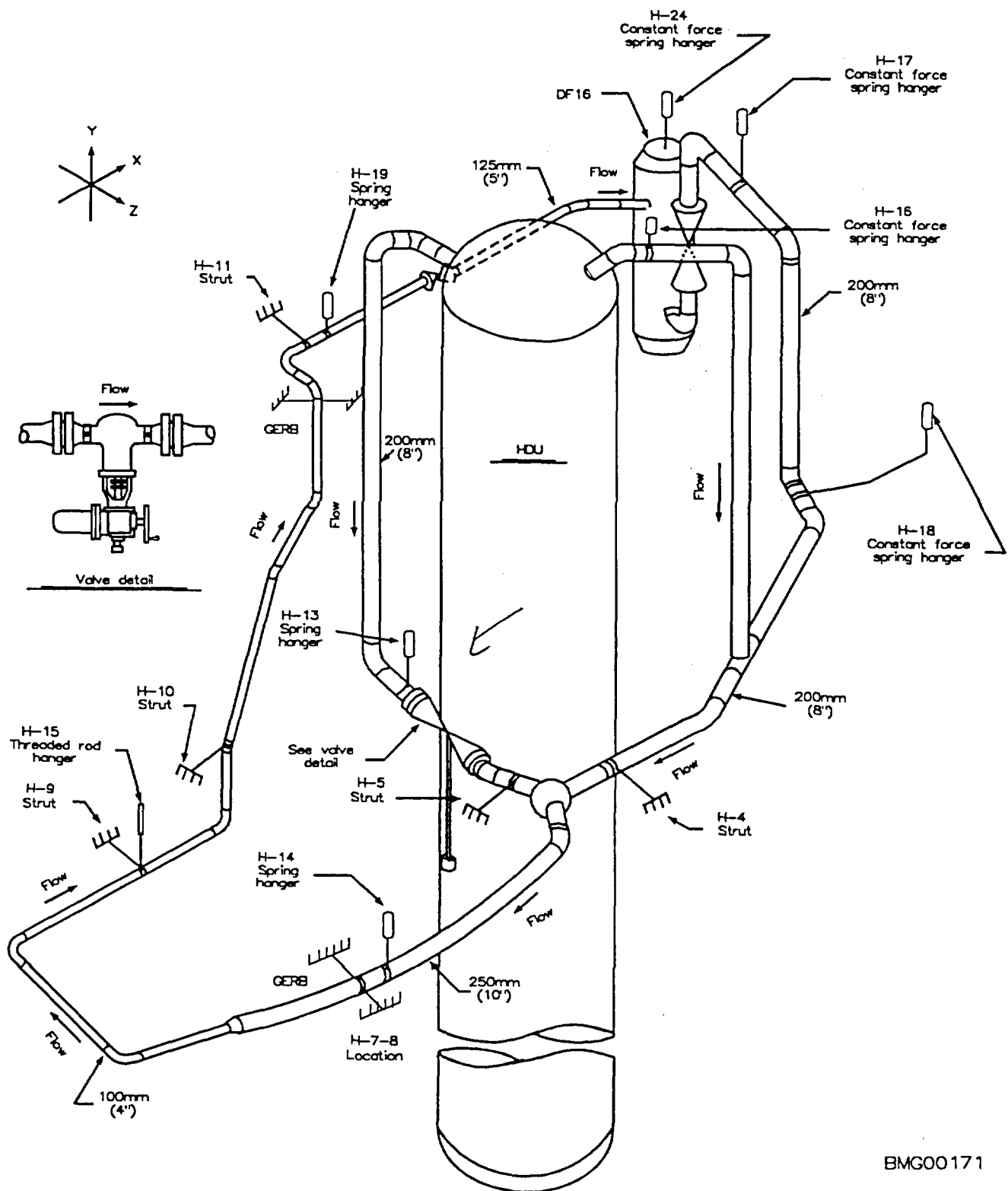
Configuration 5 (EPRI/Cloud). The six snubbers were replaced with six seismic-stop energy absorbers. The six struts were left in place. We expect the seismic stop to develop into a pin-to-pin replacement for snubbers. The devices absorb energy through impact in a manner typical of common box beam supports.

Table 2. Type of supports used in the HDR/VKL tests

Support System	System Number ^a	Struts	Snubbers	Viscous Mass Supports	Impact Supports	Flexure Supports
U.S. stiff	3	6	6 ^b	0	0	0
KfK very flexible	1	2	0	0	0	0
KWU flexible	2	5	0	0	0	0
EPRI/Cloud impacting	5	6	0	0	6	0
EPRI/Bechtel energy-absorbing	4	6	0	0	0	4
GERB energy-absorbing	6	5	0	2	0	0
ANCO energy-absorbing	7	6	0	6	0	0

a. We have retained the numbers chosen by KfK in order to facilitate cross-referencing among reports.

b. Five mechanical snubbers and one hydraulic snubber.



BMG00171

Figure 4. GERB VKL schematic showing the piping support system.

Configuration 6 (GERB). Five of the struts were retained; the one at H-3 was removed. The six snubbers were replaced with two biaxial viscous mass energy absorbers. The units were placed at the H-7 and -8 location and at a special location near the H-11 location (see Figure 4). This energy absorber uses a highly viscous bituminous liquid inside a small vessel with a damping rod. The system was tested only at the 8-Hz starting frequency.

Configuration 7 (ANCO). The six snubbers were replaced with six viscous mass energy absorbers, based on GERB viscous dampers, which were configured to be pin-to-pin replacements for snubbers. The six struts were retained. The system was tested only at the 8-Hz starting frequency.

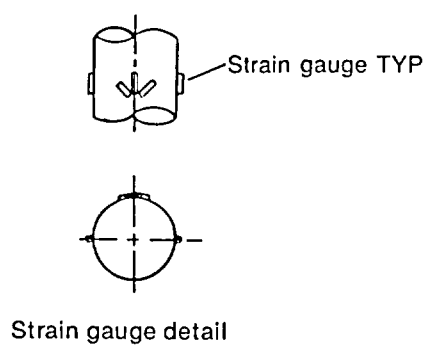
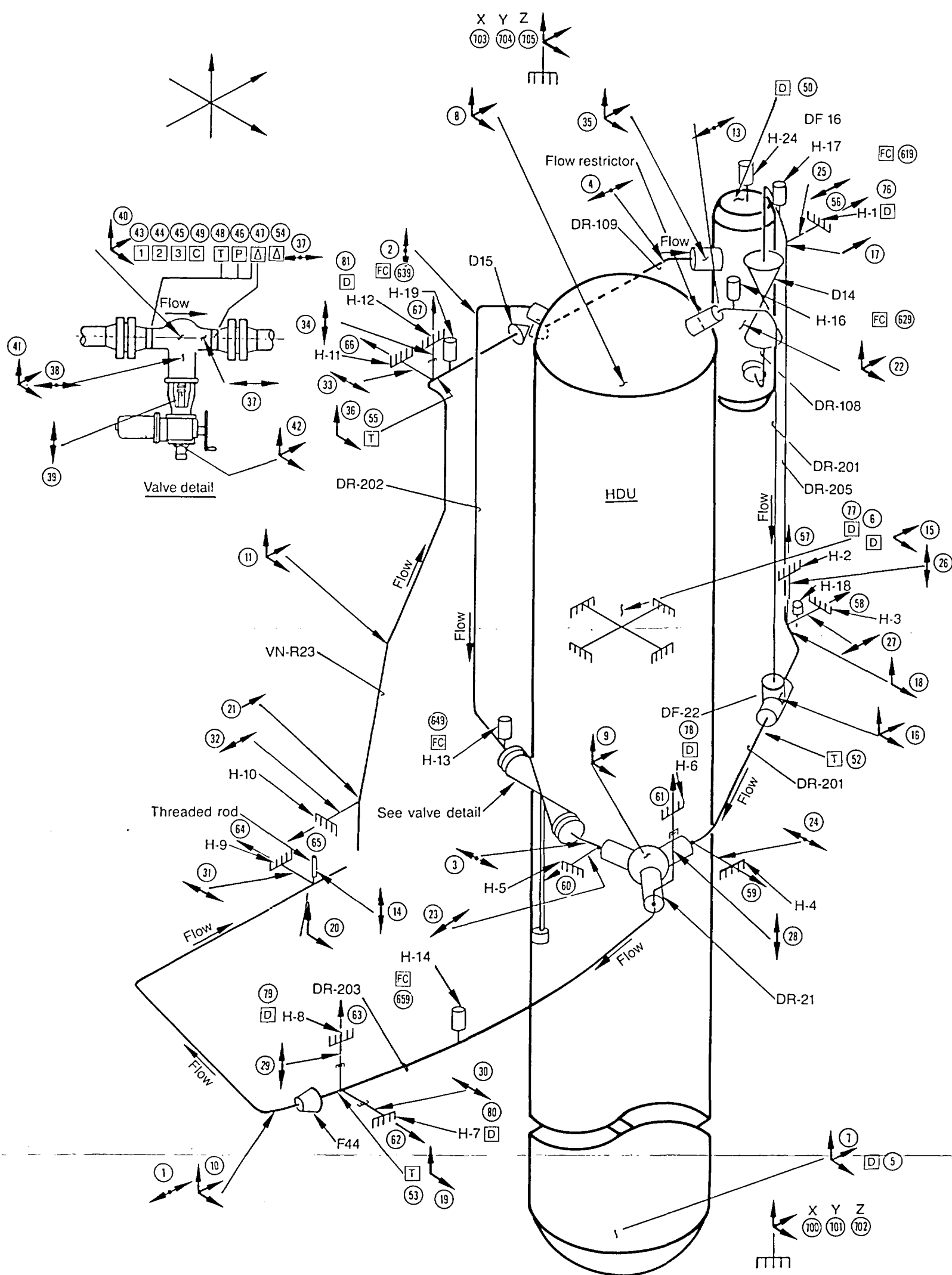
2.4 Gate Valve

USNRC provided the 8-in. motor-operated gate valve from the Shippingport Atomic Power Station. Prior to its use in the HDR Seismic Research Program, INEL disassembled and inspected the valve and subjected it to nondestructive examination as part of the USNRC Nuclear Plant Aging Research (NPAR) Program. After the nondestructive examination was completed, repairs were made to one of the valve's

sealing surfaces, a new safe end was welded on, and two new flanges were welded to the safe ends. The electrical components of the actuator were checked and cleaned, and the valve was reassembled and remated with the actuator. A more complete description of the valve is given in Appendix A, in Volume 2 of this report. Appendix A also describes the results of INEL's disassembly, inspection, and refurbishment of the gate valve in terms of the NPAR Program.

2.5 Instrumentation

INEL used 103 instruments, in addition to 57 installed by KfK, to monitor the response of piping system, the performance of the gate valve, snubbers, and snubber replacement devices, and the dynamic input of the support anchors to the VKL. Instrumenting the VKL and the HDU vessel was based on piping system analysis, system response characterization, and valve operability, piping system, and snubber requirements. The instrumentation (shown in Figure 5) measured acceleration, displacement, strain, force, temperature, pressure, differential pressure, valve position, and valve operator motor amperage and voltage. Appendix B (also in Volume 2) gives more information about the instrumentation of the piping system and equipment and a list of all the instruments installed.



Legend	
	Accelerometer and its detection axis
	Single strain gauge and its detection axis
	Strain gauges (see strain gauge detail)
	Displacement gauge
	Pressure
	ΔP
	Valve position
	Valve current
	Valve voltage
	Temperature
	Flowrate
	Video camera
	Force

Figure 5. HDR Instrumentation.

3. TEST RESULTS

Sections 3.1, 3.2, and 3.3 provide a general characterization of the HDR loadings and describe the behavior of the load path from the shaker to the VKL piping system. Sections 3.4 and 3.5 give a report on the performance of the piping support systems and their components, and Section 3.6 describes the performance and the dynamic response of the valve.

3.1 Building Response

Before the tests were conducted, calculations were performed to predict the maximum VKL excitation loadings for each starting frequency. These predictions were based on building safety studies and included calculations of input from the shaker to the building and input from the building to the VKL. The actual shaker output loads and building acceleration and strain loads as measured during the first four tests were used to verify predicted loads, and shaker output loads for subsequent tests were adjusted accordingly. These adjustments consisted of reductions in the loadings at mid to low frequencies, which correspond to the building's natural frequencies, to accommodate building strain limitations. The decreased inputs at the mid and low frequencies did not affect the piping and valve research because the maximum responses for the piping system were achieved at the 6- and 8-Hz shaker starting frequencies, which envelop most of the piping system natural frequencies.

Note that for the following discussion of HDR building and HDU vessel responses, all results are presented for 8-Hz starting frequency tests. Also, since building and HDU responses are independent of VKL piping support configuration, no designation is given concerning piping support configuration.

Building responses in the VKL area of the building were fairly uniform for each of the three axes; no part of the structure for a given direction participated more than another. Figures 6, 7, and 8 show acceleration responses of the building at a location near the bottom of the HDU; Figures 9, 10, and 11 show responses at a location near the top of the HDU; Figures 12 and 13 show building responses at support locations H-1 and H-4. Figure 14 provides locations, axes, and units of measurement for the responses shown in Figures 6 through 13. The figures show an average peak response of 0.25 to 0.3 g in the X and Z directions and 0.08 to 0.1 g in the vertical direction Y. Figure 15 shows a typical building acceleration in response spectrum format. The response is influenced primarily by the shaker frequency at 7 Hz and a

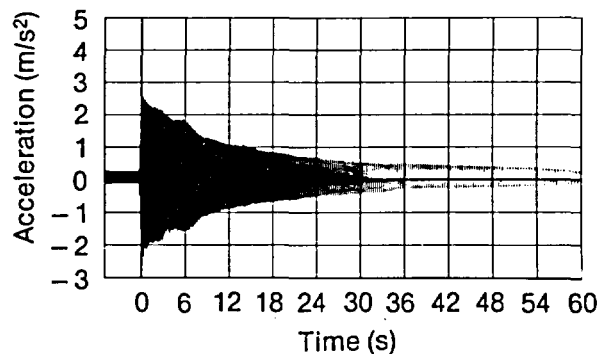


Figure 6. Building response, X axis, near bottom of HDU (instrument number 700).

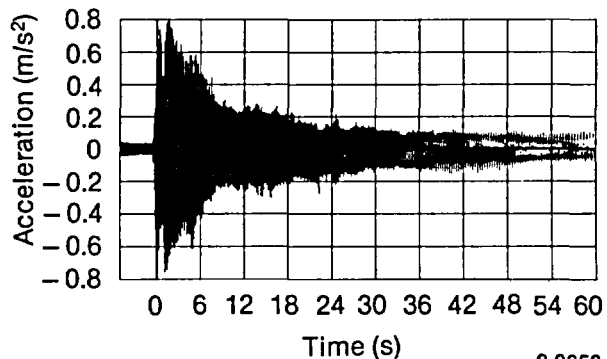


Figure 7. Building response, Y axis, near bottom of HDU (instrument number 701).

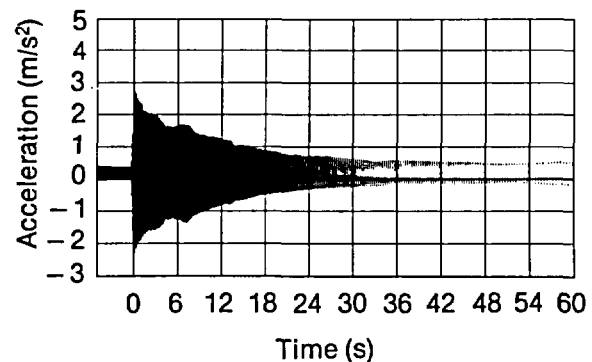


Figure 8. Building response, Z axis, near bottom of HDU (instrument number 702).

building frequency of 1.2 Hz, with a ZPA of 0.3 g. The spectrum was developed from an acceleration time history recorded at a building location near H-7, starting shortly after test initiation, and represents

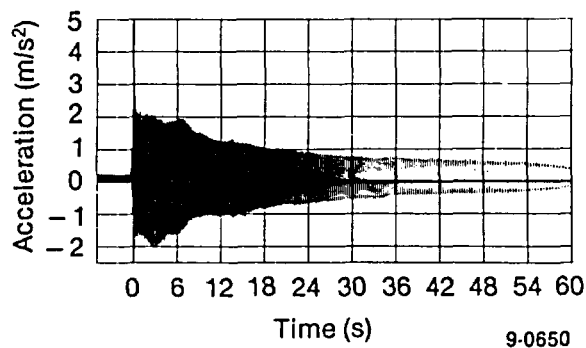


Figure 9. Building response, X axis, near top of HDU (instrument number 703).

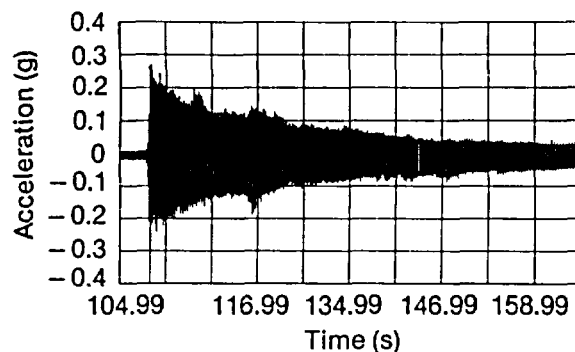


Figure 12. Building response, X axis, at piping support H-1 (instrument number 56).

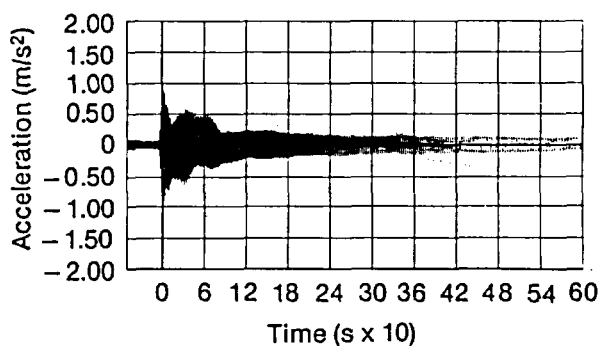


Figure 10. Building response, Y axis, near bottom of HDU (instrument number 704).

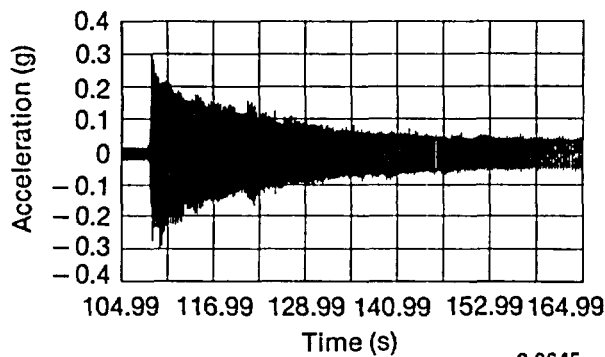


Figure 13. Building response, Z axis, at piping support H-4 (instrument number 59).

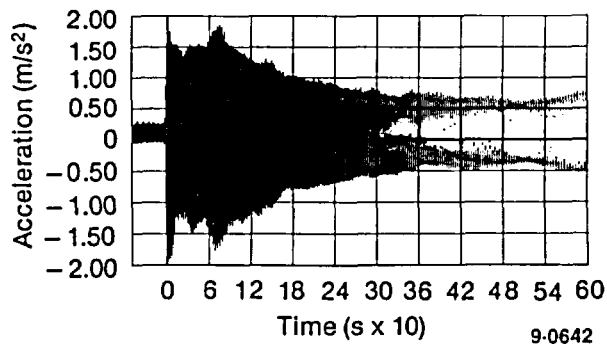


Figure 11. Building response, Z axis, near top of HDU (instrument number 705).

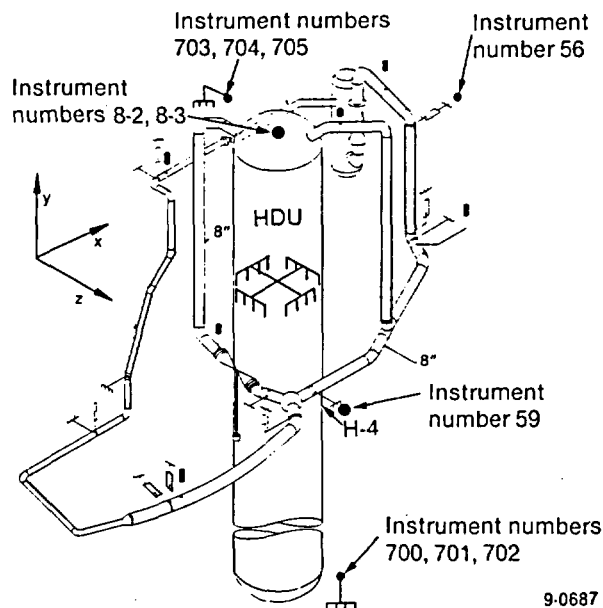


Figure 14. Instrument locations for Figures 6 through 13.

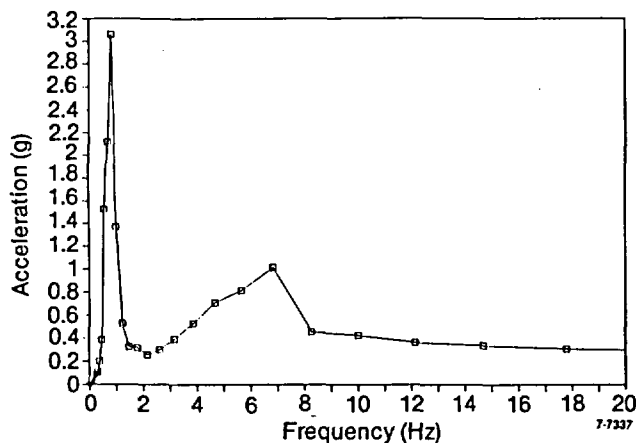


Figure 15. Typical acceleration response spectrum of the structure in the HDR building.

approximately a 7-s window. Figure 16 shows a typical shaker coastdown from 8 Hz; the shaker frequency is shown in the vertical axis and time in the horizontal axis, with a duration of 100 s. Comparison of this coastdown curve to the building acceleration histories (Figures 6 through 13) indicates that the highest responses were obtained in the early portion of the test. Figure 17 illustrates the settling of the reactor building in the ground before and after the SHAG experimental series. Figure 18 shows various cracks in the earth around the building after one of the lower starting frequency tests.

The actual forces applied to the building, in the frequencies of interest for piping and valve research (6 and 8 Hz), met the SHAG design requirements and provided significant excitation to the HDU and piping system. The building responses were uniform in each of the horizontal global axes. Vertical input to the

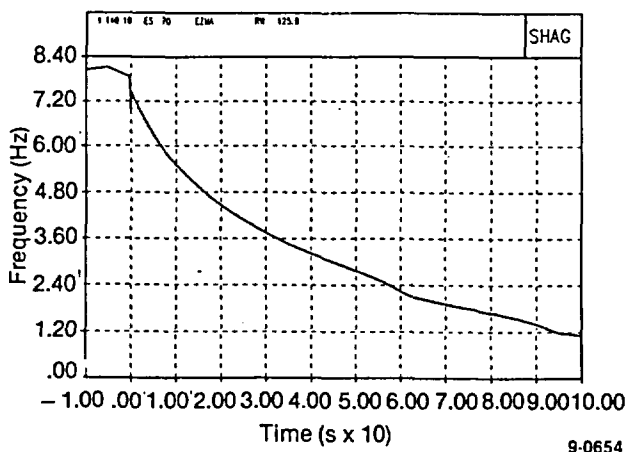


Figure 16. Shaker coastdown history from an 8-Hz starting frequency.

piping system was obtained, owing to the complex response of the building. ZPAs up to 0.3 g were input to the HDU and piping system supports. The resulting piping responses were more than adequate for the intended research.

3.2 HDU Vessel Response

The response of the VKL was influenced primarily by motion of the HDU vessel, not by the acceleration input at the support locations. Figure 19 compares anchor motion (in response spectrum format) in the two horizontal axes at the HDU mid-height support to the building response at support location H-4. The figure shows significantly more amplification in the HDU support than in the building. Figures 20, 21, and 22 present the acceleration responses recorded at the top of the HDU. Figure 23 provides locations of measurement, definition of axes, and units of measurement. A comparison of Figures 9, 10, and 11 with Figures 20, 21, and 22 shows that through the piping attached to the top of the vessel, the HDU had a greater influence on piping system response than did the supports connected to the building structure. The response of the vessel is 5 times greater, on an average in all axes, than the building response.

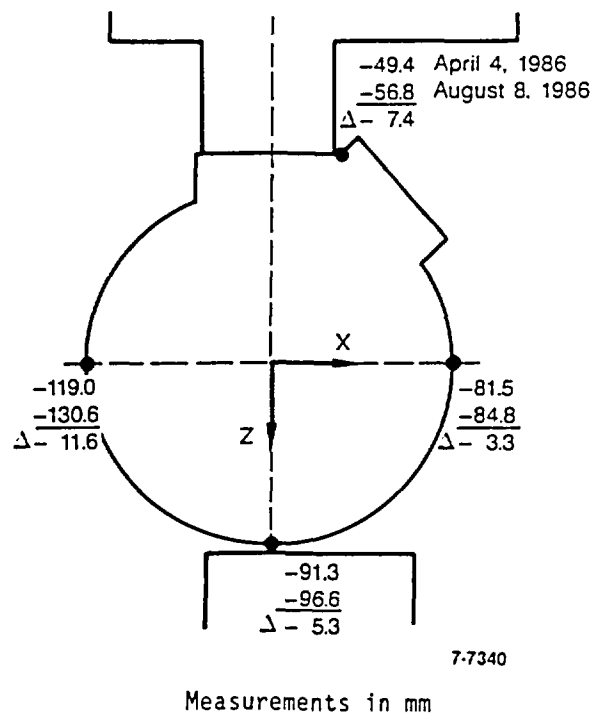


Figure 17. Comparison of building foundation elevation before and after the SHAG experiments.

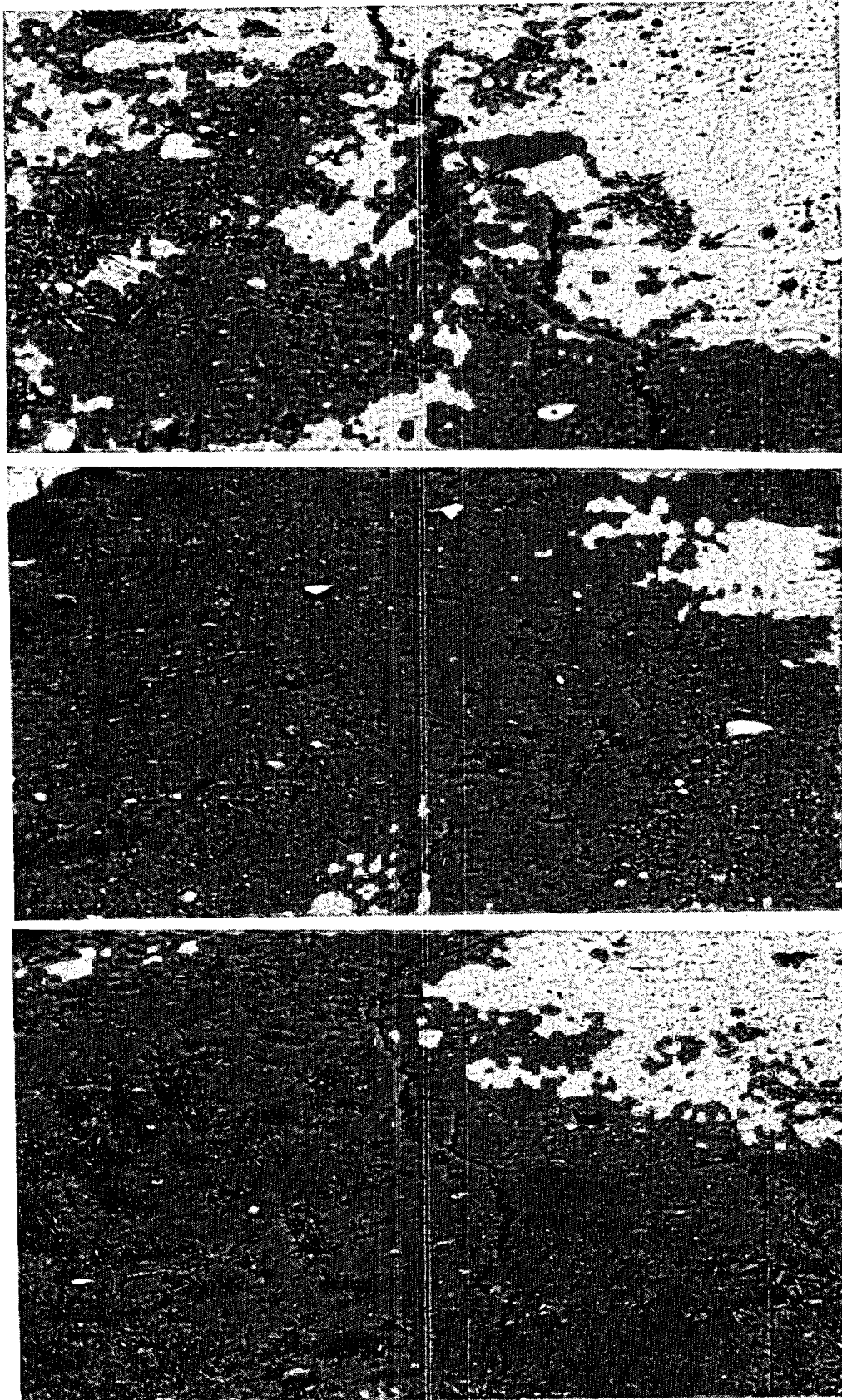


Figure 18. Ground damage 2 to 4 m from building foundation.

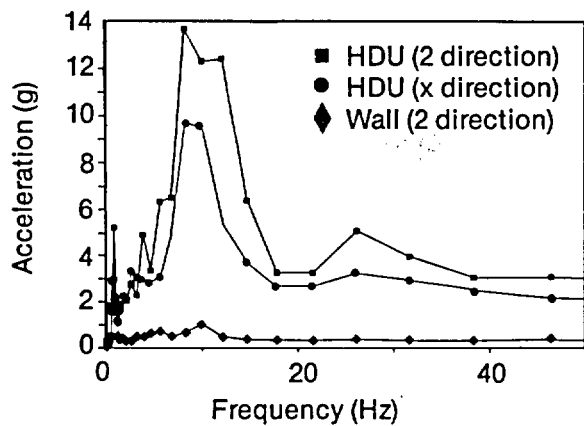


Figure 19. Response spectra derived from measurements taken from HDU supports (instrument number 15) and from a nearby wall (instrument number 59). Locations are shown on Figure 23.

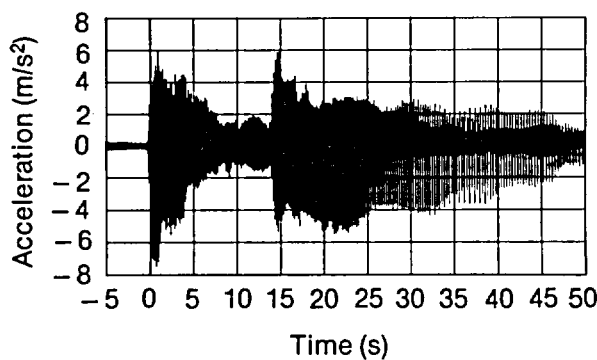


Figure 20. Acceleration history at the top of the HDU in the X direction (instrument number 8-1).

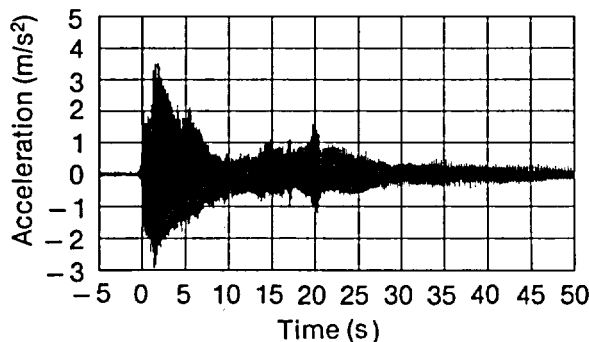


Figure 21. Acceleration history at the top of the HDU in the Y direction (instrument number 8-2).

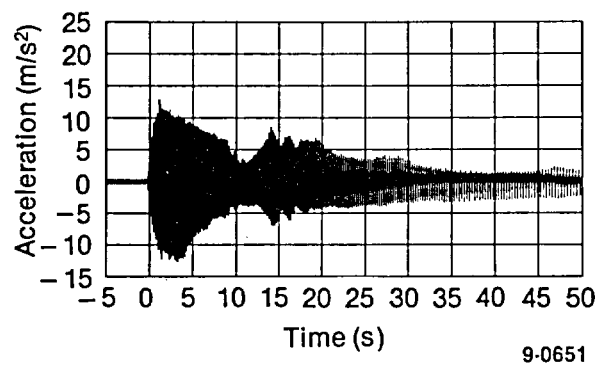


Figure 22. Acceleration history at the top of the HDU in the Z direction (instrument number 8-3).

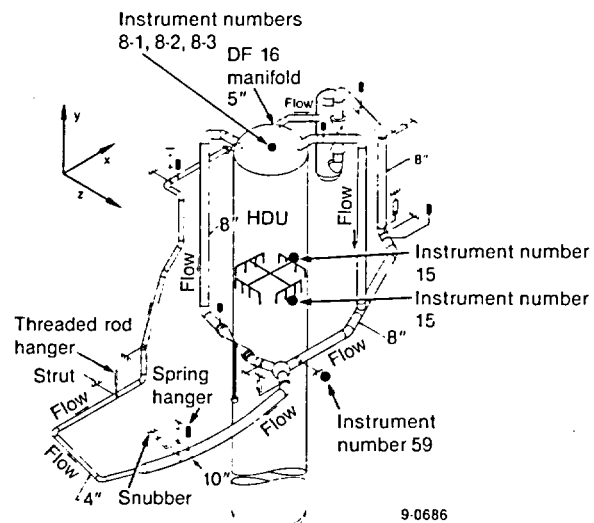


Figure 23. Instrument locations, axes, and units of measure for Figures 19 through 22.

The magnitude of the HDU vessel response was not anticipated from pretest analyses. The vessel input to the piping system provided loadings expected of SSE inputs. Note also that the response of the HDU vessel was not influenced by the support configuration installed on the piping; this response was the same with the U.S. stiff support system as it was with the flexible KfK support system. Because the HDU is the primary influence on piping system response, and is not influenced by the piping support configuration, we have a uniform basis, for a given starting frequency, on which to compare the influence that the various piping support configurations had on piping and valve responses.

3.3 VKL Piping System Response

Of the 25 seismic experiments conducted on the VKL, 17 are of interest for valve and piping response research. The 17 experiments included 7 tests performed at 8 Hz, 5 tests at 4.5 Hz, and 5 tests at 6 Hz. Of the remaining 8 tests, some were preliminary tests and the others had starting frequencies that were too low to excite the piping system to meaningful response levels.

It was assumed in the initial analysis that the most flexible system (KfK) and the most rigid system (U.S. stiff) enveloped the piping system responses. This proved true, except that one of the snubber replacement systems may have been stiffer than the U.S. stiff system. The snubber replacement systems are discussed in Sections 3.4.3 and 3.5.

The highest overall piping system responses were observed in the tests starting at 6 Hz with both the stiff system and the flexible system. The peak responses in the 8-Hz tests were slightly lower than those in the 6-Hz tests, and all levels of responses in the 4.5-Hz

starting frequency tests were significantly lower. The responses were largest in the 6-Hz tests because of the coincidence of a major piping system resonance near 6 Hz. These resonances are apparent in the 8-Hz tests, but the responses are not as large as those as achieved in the 6-Hz tests. Figures 24 through 27 are typical histories of shaker frequency and shaker force. As shown in Figures 24 and 25, during an 8-Hz test the shaker slows to 6 Hz about 5 s after test initiation, and the shaker input force was about 7000 kN at 5 s. Figures 26 and 27 are the frequency and force histories from a 6-Hz starting frequency test; in this test, 9000-kN input force was observed at the same 6-Hz frequency. We assume that the greater available input energy at resonance is the main reason for greater peak responses during the 6-Hz tests.

Figures 28 through 31 are acceleration histories recorded during the 8- and 6-Hz tests in the X direction just downstream from the H-7-8 snubber location, with either the flexible system or the stiff system installed. Figure 32 shows the location. Figure 28 is the acceleration history from the 8-Hz test with the KfK

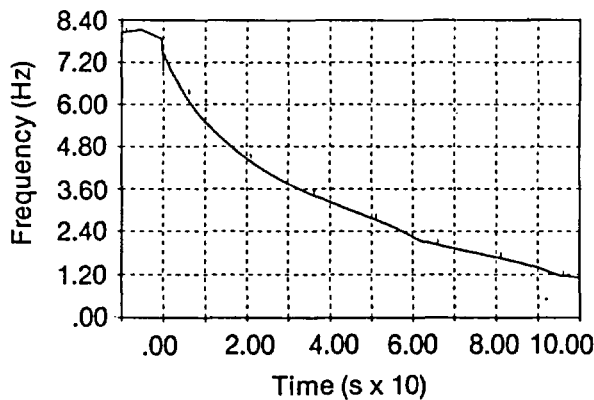


Figure 24. Shaker frequency coastdown history for an 8-Hz test.

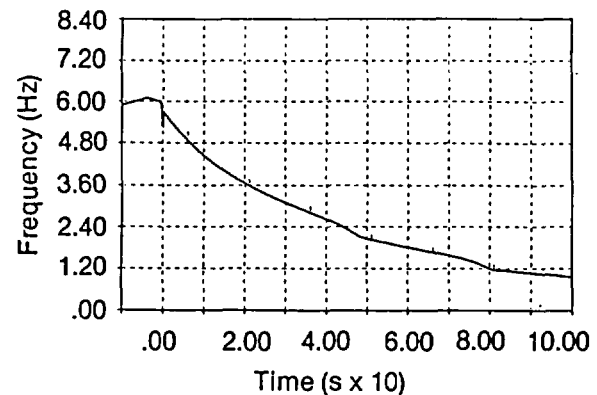


Figure 26. Shaker frequency coastdown history for a 6-Hz test.

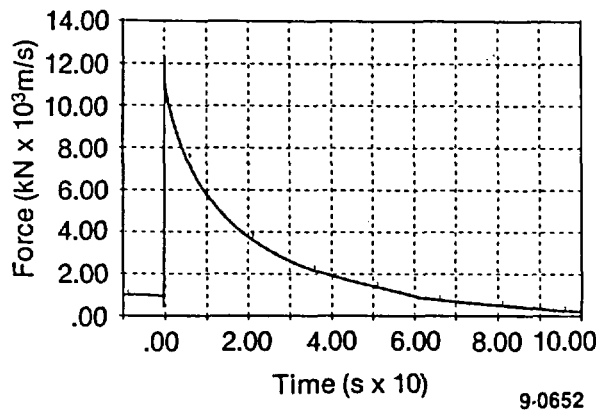


Figure 25. Shaker force history for an 8-Hz test.

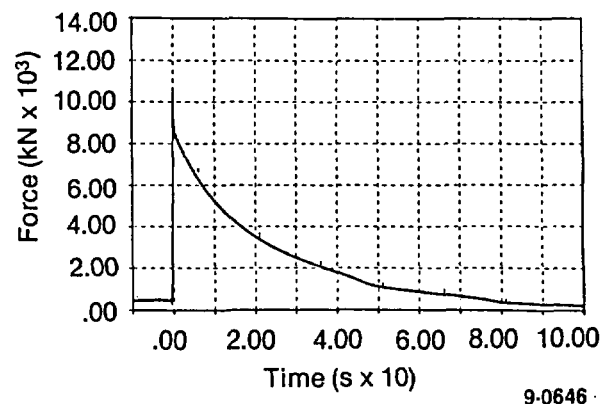


Figure 27. Shaker force history for a 6-Hz test.

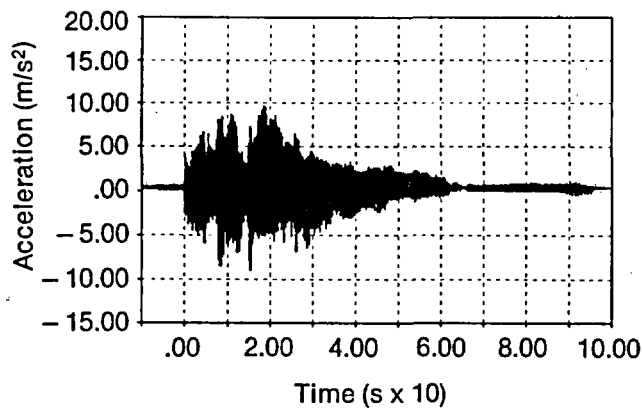


Figure 28. VKL acceleration history recorded at instrument location 10 in the X direction during an 8-Hz (starting frequency) test with the KfK flexible support system installed.

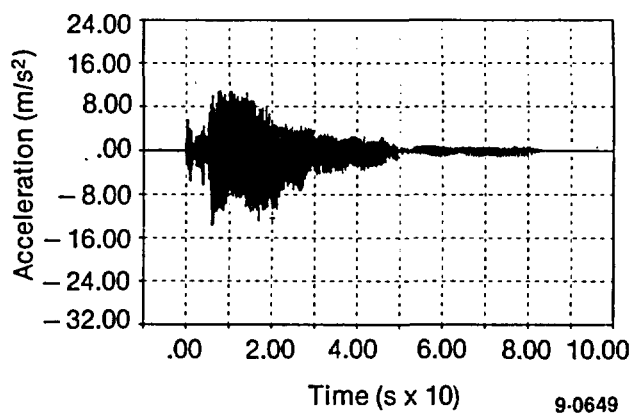


Figure 29. VKL acceleration history (at 10-X) recorded during a 6-Hz test with the KfK flexible support system installed.

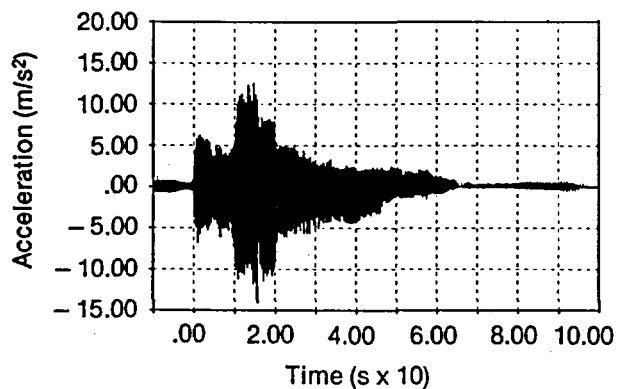


Figure 30. VKL acceleration history (at 10-X) recorded during an 8-Hz test with the U.S. stiff support system installed.

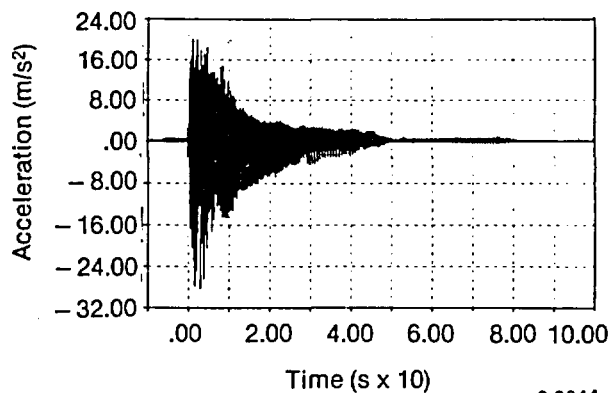


Figure 31. VKL acceleration history (at 10-X) recorded during a 6-Hz test with the U.S. stiff support system installed.

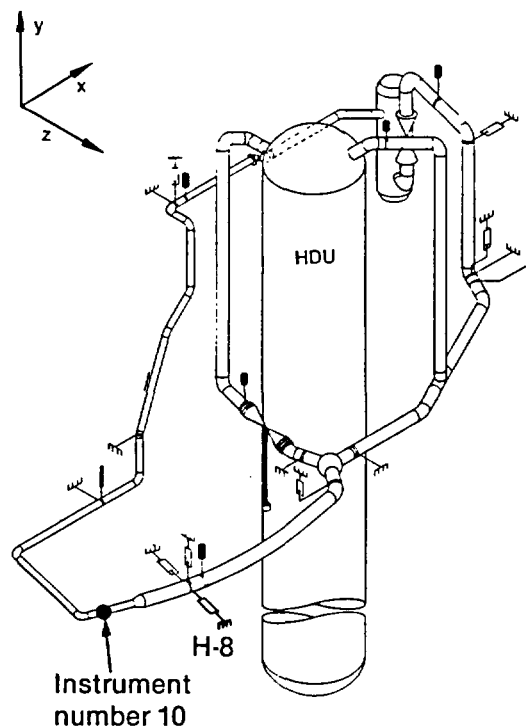


Figure 32. Instrument location for Figures 28 through 31.

flexible system, and shows resonance buildups occurring at shaker frequencies of near 6 and 4.5 Hz. Figure 29 shows the corresponding measurement from the 6-Hz starting frequency test. The near-6-Hz resonance is not excited; however, a 4.8-Hz resonance is. Figures 30 and 31 show the measurements from the 8- and 6-Hz starting frequencies with the U.S. stiff configuration. In the 8-Hz test, a major resonance is indicated at a shaker input frequency of 5.7 Hz. This resonance

point is below 6 Hz. In the 6-Hz stiff system test, this resonance point is excited to almost double the acceleration measured during the 8-Hz test. This comparison is fairly typical of measurements taken throughout the piping system. The flexible system has resonance points both above and well below the starting frequencies of 6 and 8 Hz, whereas the stiff system has a major resonance just below 6 Hz and is excited by this starting frequency.

This higher frequency resonance is expected from stiff support system design. Stiff piping systems were thought to be preferable to flexible piping systems because their natural frequencies are removed further from the significant frequencies associated with the building frequencies (normally low) than flexible systems, thus reducing the effect of resonance interaction between the building and the stiff systems.

Though greater acceleration response was measured with the U.S. stiff system than with the KfK flexible system, higher strains and forces were measured with the KfK flexible system. Frequency analyses of acceleration histories presented in Section 3.6.2 of this report indicate that a major vertical low-frequency response is present in the KfK system that is not present in the U.S. stiff system. It appears that the vertical responses are a primary influence on the strains and forces at the spherical tee with the KfK flexible system and may be attenuated by the vertical snubber (H-6) in the U.S. stiff system.

Tables 3 and 4 are peak response matrices for the seven 8-Hz and five 6-Hz starting frequency tests for all measured VKL responses. The matrices are designated according to global axes and are sequenced corresponding with fluid flow through the pipe starting at and returning to the HDU. These tables report average peak response. The matrices provide a comparison of all time responses for all seven support systems and for the two starting frequencies that had the greatest influence on piping response.

3.4 Performance of Snubbers and Snubber Replacement Devices

Two types of snubbers were used in the U.S. stiff piping support system—five mechanical snubbers and one hydraulic snubber. The hydraulic snubber was produced by Bergen-Patterson. Initially, four of the mechanical snubbers were of INC design, and the fifth was manufactured by Pacific Scientific.

The INC snubbers were in place during only the preliminary shakedown tests. During those tests, we discovered that the INC snubbers were functioning

erratically. We replaced the INC snubbers with Pacific Scientific snubbers for the remaining tests. Appendix C (Volume 2) describes the different kinds of snubbers, documents the poor performance of the INC snubbers during the preliminary tests, and presents the results of the investigation that followed. After checking with the NRC staff and the snubber manufacturers, we concluded that the once popular INC snubbers have been removed from operating utilities and are not a safety problem.

In general, four measured responses are of interest for each snubber location in the HDR test series. These are the force in the snubber, the pipe-to-wall relative displacement, the pipe absolute acceleration, and the wall absolute acceleration. Refer to Figure 3 for locations and orientations of snubbers. Figure 5 shows the instrumentation. Snubber locations are explained in Section 2.3.

The forces were sensed by pins (Figure 33) specially made for these tests by Tricoastal Industries of Seattle, Washington. The individual pins were sized to fit one of the snubber end connections. Strain gages within the pin were calibrated to measure the load transmitted through the snubber.

Displacements were measured with a CeleSCO PT101-20A position transducer (Figure 33). Piping accelerations were measured at locations adjacent to the support connection using PCB and Endevco piezoelectric transducers (Figure 33).

INEL and MPA recorded all measurements on analog and digital magnetic tape, with the exception of acceleration location 9, which was digitally recorded by KfK.

3.4.1. Performance of Pacific Scientific Mechanical Snubbers. Measurements of force through the snubber pins and acceleration of the piping indicate that the Pacific Scientific snubbers performed within the manufacturer's specified tolerances, except for the snubber at H-1 for a 3- or 4-s period during test T40.30, when the measured force dropped to nearly 100 lb (see Figure 34) and the acceleration increased. The anomaly was self-correcting, and the phenomenon did not occur again in this or other tests, nor did it occur at any of the other Pacific Scientific snubber locations.

Figure 35 provides an example of the four responses measured at one of the snubber locations. The force history plot for this Pacific Scientific snubber shows that it was resisting motion, but the displacement history shows that the snubber allowed greater dead band displacements than specified by the manufacturer, 0.1 in. peak to peak. This response was typical of all snubber locations, including the hydraulic snubber at the H-2 location. The displacements were measured

Table 3. Peak response matrix for all support systems at 8-Hz starting frequency

Instrument Number	Unit of Measure	Location	U.S. Stiff	ANCO	Bechtel	Cloud	KfK	KWU	GERB	Remarks
X AXIS										
15-1	A	HDU support	± 3 g peak ± 1.8 ave	± 3 g peak ± 1.8 ave	2 g peak ± 2.15 ave	± 3 g peak ± 1.9 ave	± 3.1 g peak ± 2.10 ave	± 3.3 peak ± 1.90 ave	± 2.85 peak ± 1.80 ave	
8-1	A	Top of HDU	± 6.5 m/s ²	± 6.5 m/s ²	± 10.5 m/s ²	M	± 6.0 m/s ²	± 8.0 m/s ²	8.1 m/s ²	
7-1	A	Bottom of HDU	M	M	M	± 7 m/s ²	M	M	M	
25	F	H-1	± 1200 lb	± 1250 lb	± 1300 lb	XX	XX	XX	XX	
76	D	H-1	$\pm .82$ in.	$\pm .60$ in.	$\pm .78$ in.	$\pm .56$ in.	$\pm .81$ in.	$\pm .70$ in.	$\pm .63$ in.	
17	A	H-1 pipe	± 2.75 g	± 1.6 g	± 2.0 g	± 4.0 g	± 3.95 g	± 4.40 g	± 4.35 g	
56	A	H-1 wall	$\pm .2$ g	$\pm .2$ g	$\pm .2$ g	$\pm .2$ g	$\pm .2$ g	$\pm .2$ g	$\pm .2$ g	
27	F	H-3	± 2400 lb	± 1750 lb	± 3125 lb	± 2125 lb	XX	XX	XX	
18-1	A	H-3 pipe	± 1.63 g	± 1.13 g	± 2.2 g	± 1.85 g	± 2.0 g	± 2.45 g	3.23 g	
58	A	H-3 wall	$\pm .3$ g	$\pm .3$ g	$\pm .3$ g	$\pm .3$ g	$\pm .3$ g	$\pm .3$ g	$\pm .3$ g	
16-1	A	Normal tee	± 1.5 g	$\pm .85$ g	± 1.5 g	± 1.43 g	± 1.40 g	± 1.1 g	± 1.1 g	
9-1	A	SP tee	± 10 m/s ²	± 6.5 m/s ²	± 7 m/s ²	± 10 m/s ²	± 8.5 m/s ²	8.6 m/s ²	7.25 m/s ²	
23	F	H-5	± 8000 lb	± 6300 lb	± 7500 lb	± 6750 lb	± 8400 lb	± 6900 lb	± 5300 lb	
60	A	H-5 wall	$\pm .2$ g	$\pm .2$ g	$\pm .2$ g	$\pm .2$ g	$\pm .2$ g	$\pm .2$ g	$\pm .2$ g	
3-2	S	Pipe bt H-5 and valve	± 180 u	± 175 u	± 37.5 u	± 170 u	± 265 u	± 145 u	± 300 u	
3-3	S	Pipe bt H-5 and valve	± 160 u	± 162 u	± 32.5 u	± 158 u	± 242 u	± 125 u	± 260 u	
37-2	S	Valve nozzle	± 90 u	± 80 u	± 117.5 u	± 100 u	± 140 u	± 85 u	± 80 u	
37-3	S	Valve nozzle	± 65 u	± 60 u	± 87.5 u	± 85 u	± 52.5 u	± 85 u	± 90 u	
40-1	A	Valve body	± 1.43 g	± 1.25 g	± 1.93 g	± 1.45 g	± 1.3 g	± 1.0 g	± 1.25 g	
41-1	A	Valve CG	± 1.25 g	± 1.05 g	± 1.90 g	± 1.10 g	± 1.33 g	± 1.05 g	± 1.33 g	
42-1	A	Valve actuator	—	—	± 2.40 g	± 2.30 g	± 2.05 g	± 2.2 g	± 2.7 g	
10-1	A	El dwn st of reducer	± 11 m/s ²	± 7.5 m/s ²	± 9 m/s ²	± 14.5 m/s ²	± 8.75 m/s ²	± 8.5 m/s ²	± 2.5 m/s ²	
32	F	H-10	± 750 lb	± 775 lb	± 825 lb	± 725 lb	XX	± 800 lb	± 975 lb	
21	A	H-10 pipe	± 1.10 g	$\pm .98$ g	± 1.10 g	± 1.45 g	± 2.10 g	± 1.35 g	± 1.20 g	
65	A	H-10 wall	$\pm .2$ g	$\pm .2$ g	M	$\pm .2$ g	$\pm .2$ g	M	M	
11-1	A	Pipe upstr of H-10	± 19 m/s ²	± 31.5 m/s ²	± 35 m/s ²	± 25 m/s ²	± 21 m/s ²	± 20 m/s ²	± 9.25 m/s ²	
2-2	S	Nozzle DF 16	± 33.5 u	± 35 u	± 52 u	± 29.5 u	± 38.5 u	± 37 u	37.5 u	
2-3	S	Nozzle DF 16	± 39.5 u	± 47.5	± 87.5 u	± 38 u	± 51 u	± 42 u	55 u	
35-1	A	Nozzle DF 16	± 12 m/s ²	± 11.5 m/s ²	± 12 m/s ²	± 11 m/s ²	11.75 m/s ²	± 13 m/s ²	11.5 m/s ²	
22-1	A	Body DF 16	± 1.15 g	± 1.30 g	± 1.30 g	± 1.15 g	± 1.43 g	± 1.95 g	± 1.75 g	

Table 3. (continued)

Instrument Number	Unit of Measure	Location	U.S. Stiff	ANCO	Bechtel	Cloud	KfK	KWU	GERB	Remarks
Y AXIS										
8-2	A	Top of HDU	$\pm 2.8 \text{ m/s}^2$	$\pm 2.75 \text{ m/s}^2$	$\pm 2.5 \text{ m/s}^2$	$\pm 2.6 \text{ m/s}^2$	$\pm 3.10 \text{ m/s}^2$	$\pm 2.25 \text{ m/s}^2$	$\pm 2.75 \text{ m/s}^2$	
7-2	A	Bottom of HDU	$\pm 2.25 \text{ m/s}^2$	$\pm 2.2 \text{ m/s}^2$	$\pm 2.2 \text{ m/s}^2$	$\pm 2 \text{ m/s}^2$	$\pm 2.2 \text{ m/s}^2$	$\pm 2.25 \text{ m/s}^2$	$\pm 2.2 \text{ m/s}^2$	
26	F	H-2	$\pm M 4000 \text{ lb}$	M	XX	XX	XX	XX	$\pm 1500 \text{ M}$	
77	D	H-2	$\pm .24 \text{ in.}$	$\pm .18 \text{ in.}$	$\pm .4 \text{ in.}$	$\pm .23 \text{ in.}$	$\pm .3 \text{ in.}$	$\pm .43 \text{ in.}$	$\pm .38 \text{ in.}$	
18-2	A	H-2 pipe	$\pm .60 \text{ g}$	$\pm .60 \text{ g}$	$\pm .67 \text{ g}$	$\pm .68 \text{ g}$	$\pm .75 \text{ g}$	$\pm .70 \text{ g}$	$\pm .65 \text{ g}$	
57	A	H-2 wall	$\pm .07 \text{ g}$	$\pm .08 \text{ g}$	$\pm .08 \text{ g}$	$\pm .08 \text{ g}$	$\pm .08 \text{ g}$	$\pm .08 \text{ g}$	$\pm .08 \text{ g}$	
16-2	A	Normal tee	$\pm .9 \text{ g}$	$\pm .9 \text{ g}$	$\pm .9 \text{ g}$	$\pm .9 \text{ g}$	$\pm .80 \text{ g}^*$	$\pm .63 \text{ g}$	$\pm .70 \text{ g}$	*High energy
9-2	A	SP tee	$\pm 6 \text{ m/s}^2$	6.25 m/s^2	$\pm 13 \text{ m/s}^2$	$\pm 12 \text{ m/s}^2$	$\pm 15.5 \text{ m/s}^2$	$\pm 10.5 \text{ m/s}^2$	$\pm 11.5 \text{ m/s}^2$	
3-1	S	BT SP tee and valve	$\pm 40 \text{ u}$	39 u	$\pm 34 \text{ u}$	$\pm 67 \text{ u}$	$\pm 92.5 \text{ u}$	95 u	$\pm 65 \text{ u}$	
3-6	S	BT SP tee and valve	$\pm 35 \text{ u}$	$\pm 35 \text{ u}$	$\pm 46 \text{ u}$	$\pm 50 \text{ u}$	$\pm 85 \text{ u}$	80 u	$\pm 80 \text{ u}$	
40-2	A	Valve body	$\pm .65 \text{ g}$	$\pm .60 \text{ g}$	$\pm .78 \text{ g}$	$\pm .95 \text{ g}$	$\pm .95 \text{ g}$	$\pm .95 \text{ g}$	$\pm 1.3 \text{ g}$	
41-2	A	Valve CG	$\pm .65 \text{ g}$	$\pm .53 \text{ g}$	$\pm .83 \text{ g}$	$\pm 1.2 \text{ g}$	$\pm .93 \text{ g}$	$\pm .95 \text{ g}$	$\pm 1.25 \text{ g}$	
42-2	A	Valve actuator	$\pm .68 \text{ g}$	$\pm .63 \text{ g}$	$\pm .80 \text{ g}$	$\pm 1.25 \text{ g}$	$\pm .93 \text{ g}$	$\pm .95 \text{ g}$	$\pm 1.33 \text{ g}$	
37-1	S	Valve nozzle	$\pm 65 \text{ u}$	$\pm 62 \text{ u}$	$\pm 102 \text{ u}$	$\pm 85 \text{ u}$	$\pm 50 \text{ u}$	$\pm 71.5 \text{ u}$	$\pm 95 \text{ u}$	
37-6	S	Valve nozzle	$\pm 25 \text{ u}$	$\pm 36 \text{ u}$	$\pm 63 \text{ u}$	$\pm 34 \text{ u}$	$\pm 50 \text{ u}$	$\pm 59 \text{ u}$	$\pm 60 \text{ u}$	
37-5	S	Valve nozzle	M	M	M	M	M	M	M	
37-4	S	Valve nozzle	$\pm 65 \text{ u}$	$\pm 67 \text{ u}$	$\pm 102 \text{ u}$	$\pm 90 \text{ u}$	$\pm 122.5 \text{ u}$	$\pm 80 \text{ u}$	$\pm 80 \text{ u}$	
2-1	S	Elbow HDU	$\pm 35.5 \text{ u}$	$\pm 38 \text{ u}$	$\pm 83 \text{ u}$	$\pm 36 \text{ u}$	$\pm 65 \text{ u}$	32 u	$\pm 70 \text{ u}$	
2-6	S	Elbow HDU	47.5 u	$\pm 55.5 \text{ u}$	$\pm 117 \text{ u}$	$\pm 45 \text{ u}$	$\pm 95 \text{ u}$	50 u	$\pm 100 \text{ u}$	
28	F	H-6	$\pm 2350 \text{ lb}$	$\pm 1575 \text{ lb}$	$\pm 2000 \text{ peak ave } 600 \text{ lb}$	XX	XX	XX	XX	
78	D	H-6	$\pm .37 \text{ in.}$	$\pm .55 \text{ in.}$	$\pm .58 \text{ in.}$	$\pm .4 \text{ in.}$	M	$\pm .42 \text{ in.}$	$\pm .42 \text{ in.}$	
61	A	H-6 wall	$\pm .1 \text{ g}$	$\pm .1 \text{ g}$	M	$\pm .1 \text{ g}$	M	$\pm .1 \text{ g}$	$\pm .1 \text{ g}$	
29	F	H-8	M	M	M	XX	XX	XX	XX	
79	D	H-8	$\pm .43 \text{ in.}$	$\pm .28 \text{ in.}$	$\pm .33 \text{ in.}$	$\pm .45 \text{ in.}$	$\pm .45 \text{ in.}$	$\pm .46 \text{ in.}$	$\pm .43 \text{ in.}$	
19-2	A	H-8 pipe	$\pm .4 \text{ g}$	$\pm .47 \text{ g}$	$\pm .90 \text{ g}$	$\pm .98 \text{ g}$	$\pm 1.35 \text{ g}$	$\pm 1.5 \text{ g}$	$\pm 1.0 \text{ g}$	
63	A	H-8 wall	$\pm .1 \text{ g}$	$\pm .1 \text{ g}$	M	$\pm .1 \text{ g}$	$\pm .1 \text{ g}$	$\pm .1 \text{ g}$	$\pm .1 \text{ g}$	
10-2	A	Pipe dwn st reducer	$\pm 6 \text{ m/s}^2$	$\pm 7.35 \text{ m/s}^2$	$\pm 9.5 \text{ m/s}^2$	$\pm 14 \text{ m/s}^2$	$\pm 17.5 \text{ m/s}^2$	$\pm 17 \text{ m/s}^2$	8.5 m/s^2	
1-1	S	EL dwn st reducer	$\pm 50 \text{ u}$	$\pm 85 \text{ u}$	$\pm 55 \text{ u}$	$\pm 111 \text{ u}$	$\pm 170 \text{ u}$	$\pm 115 \text{ u}$	95 u	
1-6	S	EL dwn st reducer	$\pm 35 \text{ u}$	$\pm 89 \text{ u}$	$\pm 50 \text{ u}$	$\pm 115 \text{ u}$	$\pm 185 \text{ u}$	$\pm 155 \text{ u}$	$\pm 100 \text{ u}$	
14	S	Threaded rod	$\pm 185 \text{ u}$	$\pm 185 \text{ u}$	$\pm 210 \text{ u}^*$	$\pm 220 \text{ u}$	$\pm 450 \text{ u}$	$\pm 410 \text{ u}$	$\pm 195 \text{ u}$	

Table 3. (continued)

Instrument Number	Unit of Measure	Location	U.S. Stiff	ANCO	Bechtel	Cloud	KfK	KWU	GERB	Remarks
Y AXIS (continued)										
20-2	A	Pipe at thrd rod	± 1.1 g	± 1.05 g	± 1.3 g	± 1.3 g	± 1.5 g	± 1.23 g	± 1.20 g	
11-2	A	Pipe dwn st H-10	± 7.75 m/s ²	± 13 m/s ²	± 13.5 m/s ²	± 13.5 m/s ²	± 14 m/s ²	± 10.5 m/s ²	11.5 m/s ²	
34	F	H-12	± 487 lb	± 475 lb	XX	M	XX	XX	XX	
81	D	H-12	$\pm .39$ in.	$\pm .64$ in.	$\pm .45$ in.	$\pm .4$ in.	M	$\pm .38$ in.	$\pm .35$ in.	
36-2	A	H-12 pipe	± 1.15 g	± 1.15 g	± 2.38	± 2.75	± 1.8 g	± 1.45 g	± 2.3 g	
67	A	H-12 wall	$\pm .1$ g	$\pm .1$ g	$\pm .1$ g	$\pm .1$ g	$\pm .1$ g	$\pm .1$ g	M	
4-1	S	DF 16 nozzle	± 92.5 u	± 82.5 u	± 312 u	± 95 u	± 200 u	± 135 u	± 100 u	
4-6	S	DF 16 nozzle	± 85 u	± 78.5 u	± 300 u	± 87.5 u	± 190 u	130 u	± 95 u	
35-2	A	DF 16 nozzle	± 6.5 m/s ²	M	± 5.75 m/s ²	± 7 m/s ²	± 6.6 m/s ²	± 7.0 m/s ²	± 6.5 m/s ²	
50	D	DF 16	$\pm .19$ in.	$\pm .17$ in.	$\pm .16$ in.	$\pm .18$ in.	$\pm .18$ in.	$\pm .18$ in.	$\pm .17$ in.	
Z AXIS										
22-2	A	DF 16 body	$\pm .43$ g	$\pm .39$ g	$\pm .7$ g	$\pm .38$ g	$\pm .42$ g	$\pm .42$ g	$\pm .39$ g	
15-3	A	H DU support	± 1.5 g	± 1.65 g	± 1.13 g	± 1.5 g	± 1.5 g	± 1.75 g	± 1.55 g	
8-3	A	Top of HDU	± 12 m/s ²	± 11 m/s ²	± 11 m/s ²	± 12 m/s ²	± 11.5 m/s ²	± 12 m/s ²	± 11 m/s ²	
7-3	A	Bottom of HDU	± 4 m/s ²	± 4 m/s ²	± 4 m/s ²	± 4 m/s ²	± 4 m/s ²	± 4 m/s ²	± 4 m/s ²	
16-3	A	Normal tee	± 1.25 g	± 1.0 g	± 1.75 g	± 1.63 g*	± 1.68 g	± 1.58 g	± 2.2 g	
24	F	H-4	± 3500 lb	± 3500 lb	± 4000 lb	± 3750 lb	± 8000 lb	± 7250 lb	± 5700 lb	
59	A	H-4 wall	$\pm .2$ g	$\pm .2$ g	$\pm .2$ g	$\pm .2$ g	$\pm .2$ g	$\pm .2$ g	$\pm .2$ g	
9-3	A	SP tee	± 6.7 m/s ²	± 4.95 m/s ²	M	± 7.5 m/s ²	± 6.75 m/s ²	M	M	
40-3	A	Valve body	$\pm .75$ g	$\pm .5$ g	$\pm .9$ g	$\pm .75$ g	$\pm .9$ g	$\pm .75$ g	$\pm .65$ g	
41-3	A	Valve CG	$\pm .75$ g	$\pm .75$ g	± 1.0 g	$\pm .8$ g	± 1.05 g	$\pm .75$ g	$\pm .7$ g	
42-3	A	Valve actuator	± 2.0 g	± 1.75 g	± 2 g	± 2.5 g	± 2.5 g	± 2 g	± 2.35 g	
2-1	S	Nozzle HDU	± 35 u	± 38.5 u	± 81.5 u	± 36 u	± 62.5 u	± 30 u	± 70 u	
2-6	S	Nozzle HDU	± 47 u	± 55.5 u	± 115 u	± 45 u	± 95 u	± 45 u	± 100 u	
30	F	H-7	± 2750 lb	± 1250 lb	± 1500 lb	XX	XX	XX	XX	
80	D	H-7	$\pm .31$ in.	$\pm .35$ in.	$\pm .35$ in.	$\pm .4$ in.	$\pm .43$ in.	M	$\pm .45$ in.	
19-3	A	H-7 pipe	M	M	± 1.28 g	M	M	± 1.10 g	± 1.3 g	
62	A	H-7 wall	$\pm .2$ g	$\pm .2$ g	$\pm .2$ g	$\pm .2$ g	$\pm .2$ g	$\pm .2$ g	$\pm .2$ g	
10-3	A	EL dwn st reducer	± 16 m/s ²	± 11.5 m/s ²	± 15 m/s ²	± 26 m/s ²	± 13.75 m/s ²	± 12.5 m/s ²	± 6.75 m/s ²	
1-2	S	EL dwn st reducer	± 117 u	± 72.5 u	± 80 u	± 90 u	± 290 u	± 132.5 u	± 80 u	
1-3	S	EL dwn st reducer	± 77.5 u	42.5 u	± 55 u	± 56 u	± 190 u	± 90 u	± 51 u	

Table 3. (continued)

Instrument Number	Unit of Measure	Location	U.S. Stiff	ANCO	Bechtel	Cloud	KfK	KWU	GERB	Remarks	
Z AXIS (continued)											
31	F	H-9	±700 lb	±1150 lb	±1500 lb	±950 lb	XX	±950 lb	±275 lb		
20-3	P	H-9	±.75 g	±.75 g	±1.15 g	±1.0 g	±1.88 g	±1.1 g	±1.0 g		
	A										
64	W	H-9	±.2 g	±.2 g	±.2 g	±.2 g	±.2 g	±.2 g	±.2 g		
	A										
11-3	P	Pipe up st H-10	28 m/s ²	±46 m/s ²	±55 m/s ²	±36 m/s ²	±20 m/s ²	±30 m/s ²	±11.5 m/s ²		
	A										
33	F	H-11	±450 lb	±5.25 lb	±1175 lb	±550 lb	±538 lb*	±600 lb	±875 lb	Support installed in error	
36-3	A	H-11 pipe	±1.13 g	±1.13 g	±.93 g	±1.38 g	±1.6 g	±1.25 g	±1.85 g		
66	A	H-11 wall	M	M	M	M	M	M	M		
4-2	S	DF 16 nozzle	±100 u	±117.5 u	±79 u	±108 u	±122 u	±117.5 u	±125 u		
4-3	S	DF 16 nozzle	±97.5 u	±120 u	±75 u	±110 u	±138 u	±127.5 u	±137 u		
35-3	A	DF 16 nozzle	±17.5 m/s ²	±17 m/s ²	±18.5 m/s ²	±17.5 m/s ²	±17.5 m/s ²	±17.5 m/s ²	±16.75 m/s ²		
22-3	A	DF 16 body	±1.13 g	±1.13 g	±1.6 g	±1.13 g	±1.39 g	±1.4 g	±1.3 g		
A = Acceleration D = Displacement S = Strain F = Force m/s ² = Meters per second square lb = Pounds force g = Acceleration measured in standardized gravitational units u = Microstrain XX = Not used in this confirmation M = Was not recorded or would not print out after digitizing											

Table 4. Peak response matrix for all support systems at 6-Hz starting frequency

Instrument Number	Unit of Measure	Location	U.S. Stiff	Bechtel	Cloud	KfK	KWU	Remarks
X AXIS								
700	A	Struct bottom HDU	$\pm 1.5 \text{ m/s}^2$	$\pm 1.7 \text{ m/s}^2$	$\pm 1.7 \text{ m/s}^2$	$\pm 1.7 \text{ m/s}^2$	$\pm 1.7 \text{ m/s}^2$	
703	A	Struct top HDU	$\pm 2 \text{ m/s}^2$	$\pm 2 \text{ m/s}^2$	$\pm 2 \text{ m/s}^2$	$\pm 2 \text{ m/s}^2$	$\pm 2 \text{ m/s}^2$	
15-1	A	HDU support	$\pm 2.5 \text{ g}$	$\pm 2.6 \text{ g}$	$\pm 2.40 \text{ g}^*$	$\pm 2.5 \text{ g}$	$\pm 2.4 \text{ g}$	
8-1	A	Top HDU	$\pm 6 \text{ m/s}^2$	$\pm 6.75 \text{ m/s}^2$	$\pm 6.9 \text{ m/s}^2$	$\pm 7 \text{ m/s}^2$	$\pm 7 \text{ m/s}^2$	
7-1	A	Bottom HDU	$\pm 3.5 \text{ m/s}^2$	$\pm 3.5 \text{ m/s}^2$	$\pm 3.5 \text{ m/s}^2$	$\pm 3.5 \text{ m/s}^2$	$\pm 4 \text{ m/s}^2$	
25	F	H-1	$\pm 2500 \text{ lb}$	$\pm 1400 \text{ lb}$	—	—	—	
76	D	H-1	$\pm .70 \text{ in.}$	$\pm .75 \text{ in.}$	$\pm .74 \text{ in.}$	$\pm .58 \text{ in.}$	$\pm .6 \text{ in.}$	
17	A	H-1 pipe	$\pm 4 \text{ g}$	$\pm 2.85 \text{ g}$	4.5 g	$\pm 5 \text{ g}$	$\pm 5.5 \text{ g}$	
56	A	H-1 wall	$\pm 2.1 \text{ g}$	$\pm .21 \text{ g}$	$\pm .21 \text{ g}$	$\pm .28 \text{ g}$	$\pm .25 \text{ g}$	
27	F	H-3	$\pm 1800 \text{ lb}$	$\pm 3150 \text{ lb}$	—	—	—	
18-1	A	H-3 pipe	$\pm 2.75 \text{ g}$	$\pm 2.25 \text{ g}$	1.75 g	$\pm 1.85 \text{ g}$	$\pm 2.10 \text{ g}$	
58	A	H-3 wall	$\pm .24 \text{ g}$	$\pm .24 \text{ g}$	$\pm 2.4 \text{ g}$	$\pm .24 \text{ g}$	$\pm .25 \text{ g}$	
16-1	A	Normal tee	$\pm 2.4 \text{ g}$	$\pm 1.55 \text{ g}$	1.53 g	$\pm 1.25 \text{ g}$	$\pm 1.8 \text{ g}$	
9-1	A	SP tee	$\pm 16.5 \text{ m/s}^2$	$\pm 10 \text{ m/s}^2$	15 m/s^2	$\pm 9.5 \text{ m/s}^2$	$\pm 13 \text{ m/s}^2$	
23	F	H-5	$\pm 4750 \text{ lb}$	$\pm 9250 \text{ lb}$	$\pm 11000 \text{ lb}$	$\pm 7750 \text{ lb}$	$\pm 11500 \text{ lb}$	
60	A	H-5 wall	$\pm .2 \text{ g}$	$\pm .2 \text{ g}$	$\pm .2 \text{ g}$	$\pm .2 \text{ g}$	$\pm .2 \text{ g}$	
3-2	S	Pipe bt H-5 and valve	$\pm 320 \text{ u}$	$\pm 300 \text{ u}$	200 u	175 u	260 u	
3-3	S	Pipe bt H-5 and valve	$\pm 270 \text{ u}$	$\pm 250 \text{ u}$	$\pm 180 \text{ u}$	150 u	225 u	
37-2	S	Valve nozzle	$\pm 135 \text{ u}$	$\pm 125 \text{ u}$	$\pm 117 \text{ u}$	$\pm 75 \text{ u}$	$\pm 120 \text{ u}$	
37-3	S	Valve nozzle	$\pm 110 \text{ u}$	$\pm 65 \text{ u}$	$\pm 75 \text{ u}$	$\pm 65 \text{ u}$	$\pm 75 \text{ u}$	
40-1	A	Valve body	$\pm 2.1 \text{ g}$	$\pm 1.85 \text{ g}$	$\pm 1.84 \text{ g}$	$\pm 1.15 \text{ g}$	$\pm 1.60 \text{ g}$	
41-1	A	Valve CG	$\pm 1.85 \text{ g}$	$\pm 1.58 \text{ g}$	$\pm 1.20 \text{ g}$	$\pm 1.1 \text{ g}$	$\pm 1.50 \text{ g}$	
42-1	A	Valve actuator	$\pm 2.5 \text{ g}$	$\pm 2.8 \text{ g}$	$\pm 2.5 \text{ g}$	$\pm 1.85 \text{ g}$	$\pm 2.45 \text{ g}$	
10-1	A	EL dwn st reducer	$\pm 22 \text{ m/s}^2$	$\pm 12 \text{ m/s}^2$	$\pm 16 \text{ m/s}^2$	11 m/s^2	15.5 m/s^2	
32	F	H-10	$\pm 1300 \text{ lb}$	$\pm 1300 \text{ lb}$	$\pm 1050 \text{ lb}$	XX	$\pm 1050 \text{ lb}$	
21	A	H-10 pipe	$\pm 1.20 \text{ g}$	$\pm 1.10 \text{ g}$	$\pm 1.40 \text{ g}$	3.05 g	1.15 g	
65	A	H-10 wall	$\pm .2 \text{ g}$	$\pm .2 \text{ g}$	$\pm .2 \text{ g}$	$\pm .2 \text{ g}$	$\pm .2 \text{ g}$	
11-1	A	Pipe upst of H-10	$\pm 30 \text{ m/s}^2$	$\pm 40 \text{ m/s}^2$	$\pm 28 \text{ m/s}^2$	$\pm 19 \text{ m/s}^2$	$\pm 23.5 \text{ m/s}^2$	
2-2	S	DF 16 nozzle	$\pm 40 \text{ u}$	$\pm 47 \text{ u}$	$\pm 36 \text{ u}$	38 u	50 u	
2-3	S	DF 16 nozzle	$\pm 55 \text{ u}$	$\pm 71 \text{ u}$	$\pm 40 \text{ u}$	50 u	68 u	
35-1	A	Nozzle DF 16	M	M	M	M	M	
22-1	A	Body DF 16	$\pm 1.55 \text{ g}$	± 1.85	M	$\pm 3 \text{ g}$	$\pm 2.55 \text{ g}$	

Table 4. (continued)

Instrument Number	Unit of Measure	Location	U.S. Stiff	Bechtel	Cloud	KfK	KWU	Remarks
Y AXIS								
701	A	Struct HDU	$\pm .5 \text{ m/s}^2$	$\pm .5 \text{ m/s}^2$	$\pm .5 \text{ m/s}^2$	$\pm .6 \text{ m/s}^2$	$\pm .6 \text{ m/s}^2$	
704	A	Struct HDU	$\pm .5 \text{ m/s}^2$	$\pm .5 \text{ m/s}^2$	$\pm .5 \text{ m/s}^2$	$\pm .5 \text{ m/s}^2$	$\pm .5 \text{ m/s}^2$	
8-2	A	Top HDU	$\pm 1.75 \text{ m/s}^2$	$\pm 2 \text{ m/s}^2$	$\pm 1.75 \text{ m/s}^2$	$\pm 3 \text{ m/s}^2$	$\pm 2.25 \text{ m/s}^2$	
7-2	A	Bottom HDU	$\pm 1 \text{ m/s}^2$	$\pm 1.5 \text{ m/s}^2$	$\pm 1.2 \text{ m/s}^2$	$\pm 1.75 \text{ m/s}^2$	$\pm 1.6 \text{ m/s}^2$	
26	F	H-2	$\pm 5000 \text{ lb}$	—	—	—		
77	D	H-2	$\pm .2 \text{ in.}$	$\pm .2 \text{ in.}$	$\pm .2 \text{ in.}$	$\pm .18 \text{ in.}$	$\pm .26 \text{ in.}$	
18-2	A	Pipe H-2	$\pm .82 \text{ g}$	$\pm .75 \text{ g}$	$\pm .95 \text{ g}$	$\pm .8 \text{ g}$	$\pm .85 \text{ g}$	
57	A	H-2 wall	$\pm .05 \text{ g}$	$\pm .05 \text{ g}$	$\pm .05 \text{ g}$	$\pm .05 \text{ g}$	$\pm .05 \text{ g}$	
16-2	A	Normal tee	$\pm .85 \text{ g}$	$\pm .78 \text{ g}$	1.02 g	$\pm .8 \text{ g}$	$\pm .85 \text{ g}$	
9-2	A	SP tee	$\pm 7 \text{ m/s}^2$	$\pm 7 \text{ m/s}^2$	$\pm 9.5 \text{ m/s}^2$	$\pm 8 \text{ m/s}^2$	$\pm 8 \text{ m/s}^2$	
3-1	S	BT SP tee and valve	M	M	M	M	M	
3-6	S	BT SP tee and valve	M	M	M	M	M	
40-2	A	Valve body	$\pm .65 \text{ g}$	$\pm .65 \text{ g}$	$\pm .75 \text{ g}$	$\pm .63 \text{ g}$	$\pm .53 \text{ g}$	
41-2	A	Valve CG	$\pm .60 \text{ g}$	$\pm .63 \text{ g}$	$\pm .75 \text{ g}$	$\pm .60 \text{ g}$	$\pm .54 \text{ g}$	
42-2	A	Valve actuator	$\pm .63 \text{ g}$	$\pm .63 \text{ g}$	$\pm .80 \text{ g}$	$\pm .65 \text{ g}$	$\pm .60 \text{ g}$	
37.1	S	Valve nozzle	$\pm 115 \text{ u}$	$\pm 80 \text{ u}$	$\pm 75 \text{ u}$	$\pm 60 \text{ u}$	$\pm 73 \text{ u}$	
37.6	S	Valve nozzle	$\pm 40 \text{ u}$	$\pm 59 \text{ u}$	$\pm 58 \text{ u}$	$\pm 36 \text{ u}$	$\pm 59 \text{ u}$	
37.5	S	Valve nozzle	$\pm 10 \text{ u}$	$\pm 17.5 \text{ u}$	$\pm 23 \text{ u}$	$\pm 15 \text{ u}$	$\pm 22 \text{ u}$	
37-4	S	Valve nozzle	$\pm 125 \text{ u}$	$\pm 112.5 \text{ u}$	$\pm 110 \text{ u}$	$\pm 68 \text{ u}$	$\pm 105 \text{ u}$	
2-1	S	Elbow HDU	$\pm 40 \text{ u}$	$\pm 62.5 \text{ u}$	$\pm 40 \text{ u}$	$\pm 43 \text{ u}$	$\pm 60 \text{ u}$	
2-6	S	Elbow HDU	$\pm 60 \text{ u}$	$\pm 82.5 \text{ u}$	$\pm 50 \text{ u}$	$\pm 60 \text{ u}$	$\pm 78 \text{ u}$	
28	F	H-6	$\pm 2750 \text{ lb}$	$\pm 1100 \text{ lb}$	XX	XX	XX	
78	D	H-6	$\pm .18 \text{ in.}$	M	$\pm .3 \text{ in.}$	$\pm .5 \text{ in.}$	$\pm .5 \text{ in.}$	
61	A	Wall H-6	$\pm .1 \text{ g}$	$\pm .1 \text{ g}$	$\pm .1 \text{ g}$	$\pm .1 \text{ g}$	$\pm .1 \text{ g}$	
29	F	H-8	M	M	XX	XX	XX	
79	D	H-8	$\pm .45 \text{ in.}$	M	$\pm .4 \text{ in.}$	$\pm .4 \text{ in.}$	M	
19-2	A	Pipe H-8	$\pm .58 \text{ g}$	$\pm .65 \text{ g}$	$\pm .75 \text{ g}$	$\pm .73 \text{ g}$	$\pm .70 \text{ g}$	
63	A	Wall H-8	$\pm .1 \text{ g}$	$\pm .1 \text{ g}$	$\pm .1 \text{ g}$	$\pm .1 \text{ g}$	$\pm .1 \text{ g}$	
10-2	A	Pipe dwn st reducer	$\pm 7.5 \text{ m/s}^2$	$\pm 8 \text{ m/s}^2$	$\pm 9 \text{ m/s}^2$	$\pm 10 \text{ m/s}^2$	$\pm 11.5 \text{ m/s}^2$	
1-1	S	El dwn st reducer	$\pm 80 \text{ u}$	$\pm 80 \text{ u}$	$\pm 95 \text{ u}$	$\pm 115 \text{ u}$	$\pm 79 \text{ u}$	
1-6	S	El dwn st reducer	$\pm 65 \text{ u}$	$\pm 60 \text{ u}$	$\pm 100 \text{ u}$	$\pm 102 \text{ u}$	$\pm 110 \text{ u}$	
14	S	Threaded rod	$\pm 225 \text{ u}$	$\pm 275 \text{ u}$	$\pm 338 \text{ u}$	$\pm 275 \text{ u}$	$\pm 300 \text{ u}$	

Table 4. (continued)

Instrument Number	Unit of Measure	Location	U.S. Stiff	Bechtel	Cloud	KfK	KWU	Remarks
Y AXIS (continued)								
20-2	A	Pipe at thrd rod	± 1.25 g	± 1.35	± 1.45 g	± 1.85 g	± 1.55 g	
11-2	A	Pipe dwn st H-10	± 17.5 m/s ²	± 18 m/s ²	± 20 m/s ²	± 17.5 m/s ²	± 12.5 m/s ²	
34	F	H-12	± 600 lb	XX	XX	XX	XX	
81	D	H-12	$\pm .4$ in.	$\pm .24$ in.	M	$\pm .4$ in.	M	
36-2	A	H-12 pipe	± 1.5 g	± 2.2 g	± 2.1 g	± 1.65 g	± 1.6 g	
67	A	H-12 wall	$\pm .1$ g	$\pm .1$ g	$\pm .1$ g	$\pm .1$ g	$\pm .1$ g	
4-1	S	DF 16 nozzle	M	M	M	M	M	
4-6	S	DF 16 nozzle	± 60 u	± 250 u	73 u	± 243 u	± 115 u	
35-2	A	DF 16 nozzle	M	M	M	M	M	
50	D	DF 16	$\pm .17$ in.	M	M	$\pm .08$ in.	$\pm .06$ in.	
22-2	A	DF 16 body	$\pm .66$ g	$\pm .75$ g	$\pm .68$ g	$\pm .66$ g	$\pm .75$ g	
Z AXIS								
702	A	Struct bottom HDU	± 1.65 m/s ²	± 1.65 m/s ²	± 1.65 m/s ²	± 1.65 m/s ²	± 1.65 m/s ²	
705	A	Struct top HDU	± 2.1 m/s ²	± 2.1 m/s ²	± 2.1 m/s ²	± 2.1 m/s ²	± 2.1 m/s ²	
15-3	A	HDU support	± 1.33 g	± 1.38 g	± 1.2 g	± 1.25 g	± 1.38 g	
8-3	A	Top HDU	± 7 m/s ²	± 9 m/s ²	± 9 m/s ²	± 8.5 m/s ²	± 8.25 m/s ²	
7-3	A	Bottom HDU	± 2.75 m/s ²	± 3.5 m/s ²	± 3 m/s ²	± 2.5 m/s ²	± 2.5 m/s ²	
16-3	A	Normal tee	± 2.35 g	± 2.0 g	± 1.98 g	± 1.9 g	± 1.85 g	
24	F	H-4	5350 lb	± 5000 lb	± 6750 lb	± 5750 lb	± 7200 lb	
59	A	H-4 wall	$\pm .2$ g	$\pm .2$ g	.29	$\pm .2$ g	$\pm .2$ g	
9-3	A	SP tee	± 10 m/s ²	± 8.5 m/s ²	± 8 m/s ²	± 8 m/s ²	± 8 m/s ²	
40-3	A	Valve body	± 1.33 g	$\pm .85$ g	± 1.0 g	$\pm .85$ g	$\pm .9$ g	
41-3	A	Valve CG	± 1.15 g	$\pm .85$ g	$\pm .98$ g	$\pm .75$ g	± 1.0 g	
42-3	A	Valve actuator	± 2.43 g	± 2.05 g	± 2.45 g	± 1.9 g	± 2.0 g	
2-1	S	Nozzle HDU	M	M	M	M	M	
2-6	S	Nozzle HDU	M	M	M	M	M	
30	F	H-7	M	± 1700 lb	—	—	—	
80	D	H-7	$\pm .35$ in.	M	M	$\pm .3$ in.	$\pm .60$ in.	Peak
19-3	A	H-7 pipe	—	M	± 42 g	—	—	
62	A	H-7 wall	$\pm .2$ g	$\pm .2$ g	$\pm .2$ g	$\pm .2$ g	$\pm .2$ g	
10-3	A	El dwn st reducer	± 20 m/s ²	± 19.5 m/s ²	37.5 m/s ²	± 12 m/s ²	13.5 m/s ²	
1-2	S	El dwn st reducer	± 135 u	± 115 u	± 135 u	405 u	± 140 u	

Table 4. (continued)

Instrument Number	Unit of Measure	Location	U.S. Stiff	Bechtel	Cloud	KfK	KWU	Remarks
Z AXIS (continued)								
1-3	S	El dwn st reducer	± 80 u	± 67.5 u	± 95 u	280 u	± 80 u	
31	F	H-9	± 1400 lb	± 1575 lb	± 1050 lb	XX	± 1000 lb	
20-3	A	H-9 pipe	± 1.15 g	± 1.0 g	M	± 1.88 g	± 1.05 g	
64	A	H-9 wall	$\pm .18$ g	$\pm .18$ g	$\pm .18$ g	$\pm .18$ g	$\pm .18$ g	
11-3	A	Pipe up st H-10	± 45 m/s ²	70 m/s ²	45 m/s ²	± 28 m/s ²	38 m/s ²	
33	F	H-11	± 675 lb	± 1100 lb	± 800 lb	XX	± 750 lb	
36-3	A	H-11 pipe	± 1.45 g	± 1.45 g	± 29 g*	± 2.85 g	± 1.65 g	Impact
66	A	DF 16 nozzle	$\pm .18$ g	$\pm .2$ g	$\pm .2$ g	$\pm .18$ g	$\pm .2$ g	
4-2	S	DF 16 nozzle	M	M	M	M	M	
4-3	S	DF 16 nozzle	± 87 u	± 90 u	± 105 u	350 u	± 158 u	
35-3	A	DF 16 nozzle	M	M	M	M	M	
22-3	Ac	DF 16 body	± 1.3 g	± 1.65 g	± 1.6 g	± 2.15 g	± 1.95 g	

A = Acceleration

D = Displacement

S = Strain

F = Force

m/s² = Meters per second square

g = Acceleration measured in standard gravitational units

lb = Pounds force

u = Microstrain

XX = Not used in this configuration

M = Was not recorded or would not print out after digitizing

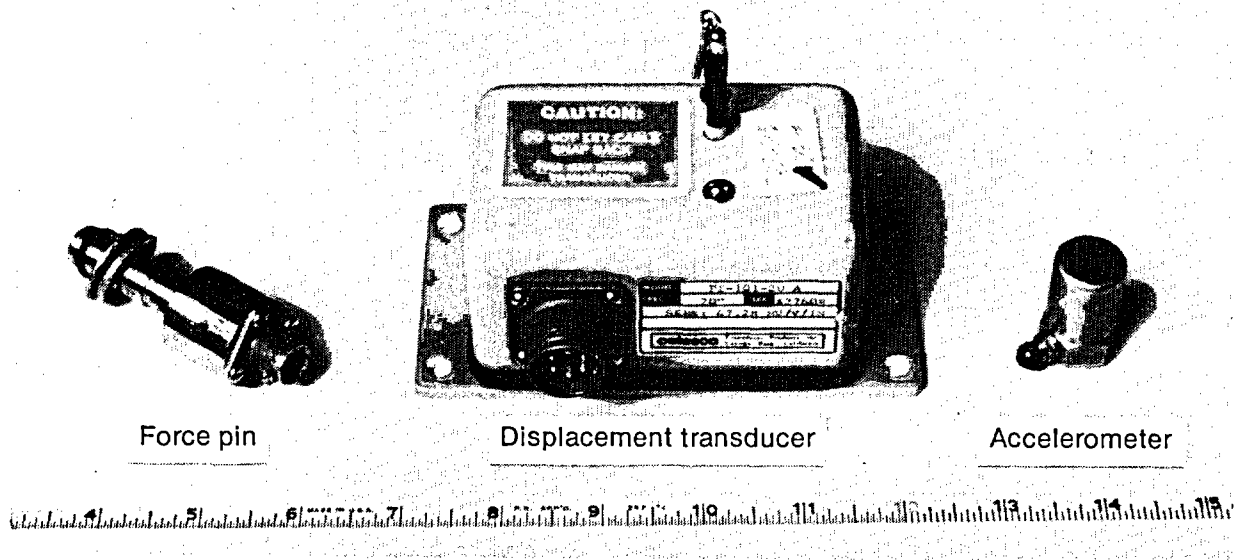
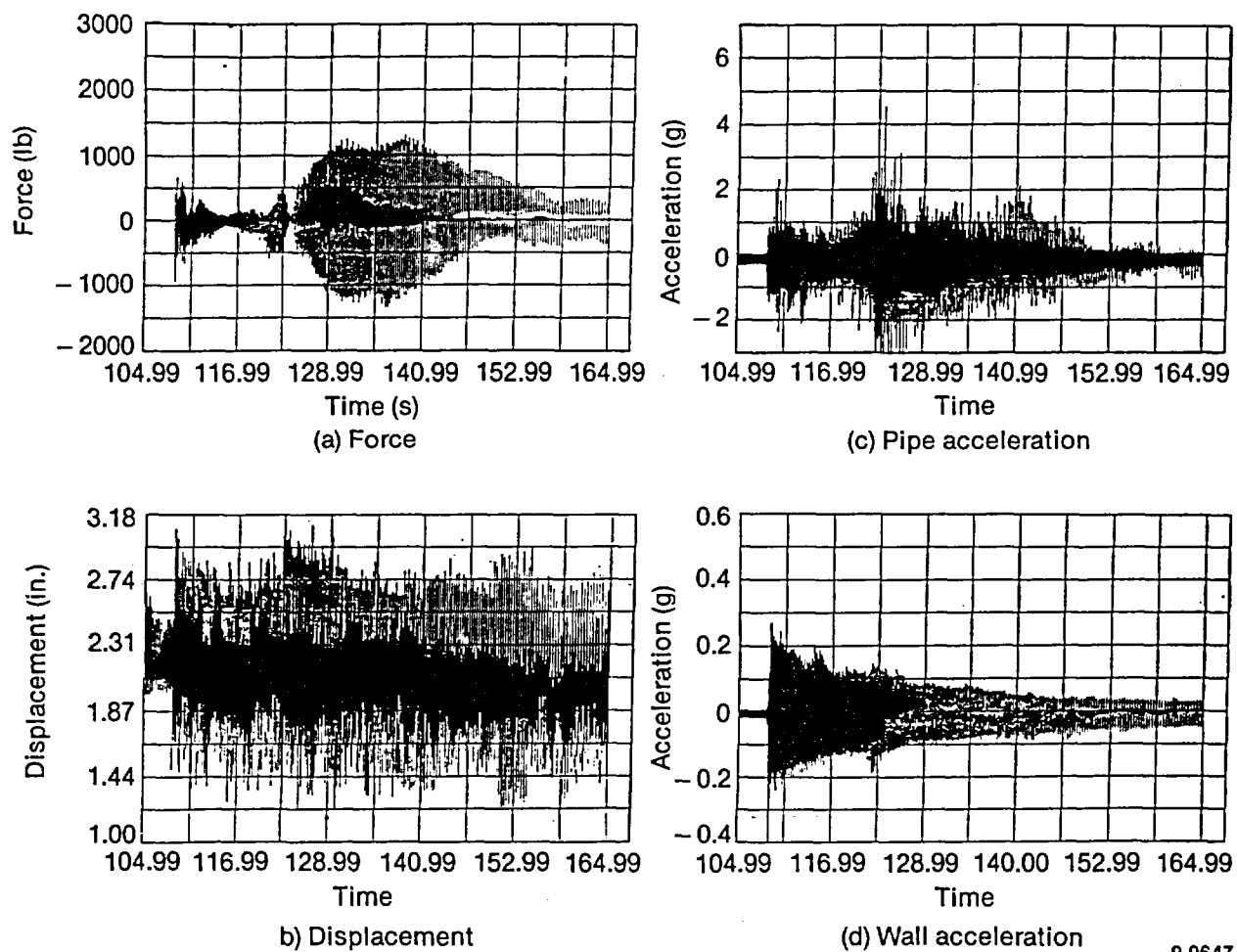


Figure 33. Force, displacement, and acceleration instruments.



9-0647

Figure 34. Responses recorded at Pacific Scientific snubber location H-1 during Test T40.30, 8-Hz starting frequency.

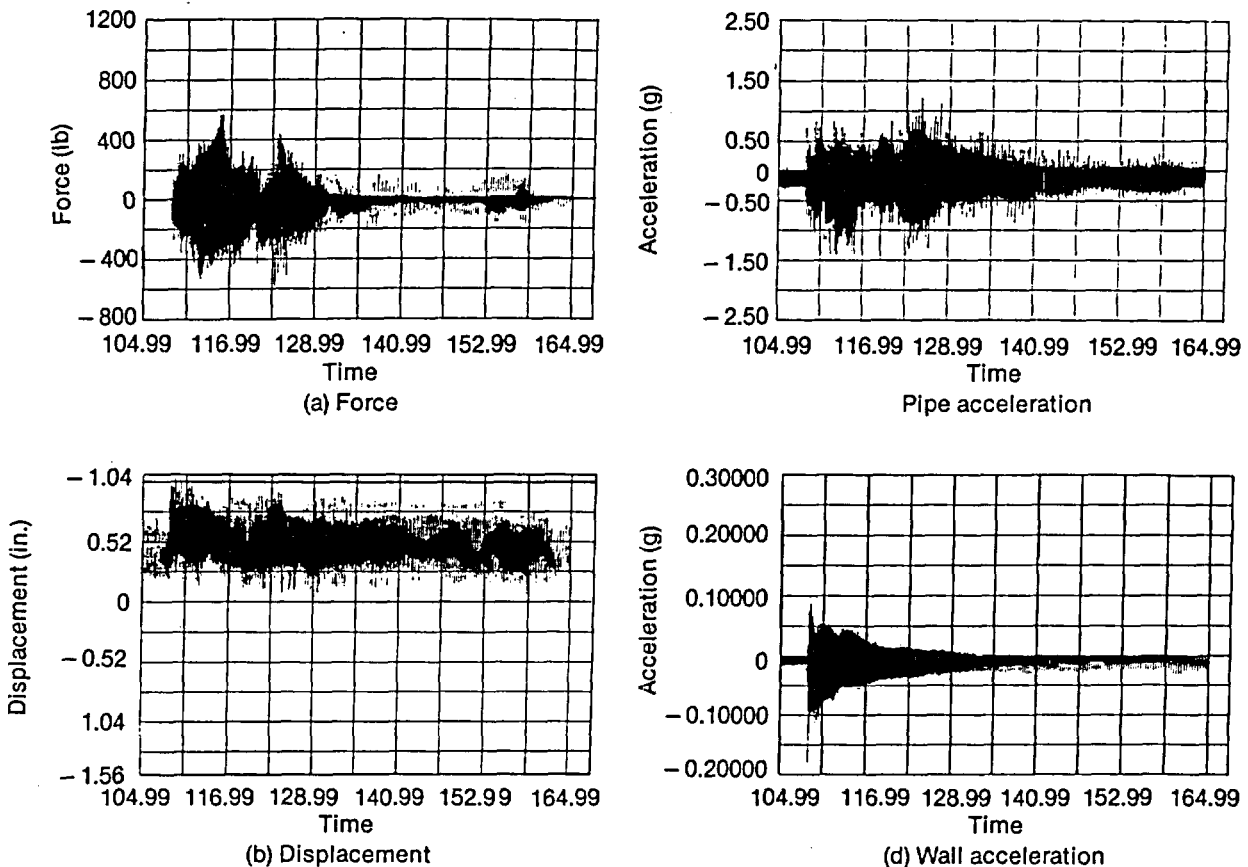


Figure 35. Responses recorded at Pacific Scientific snubber location H-12 during Test T40.30, 8-Hz starting frequency. 9-0643

by the Celesco displacement transducers described previously.

We conducted a posttest investigation at the INEL dynamics laboratory to determine if the Pacific Scientific snubbers were allowing displacements larger than the 0.1-in. peak-to-peak dead band specified by the manufacturer. A complete report of this investigation is included in Appendix C (Volume 2). The investigation indicated that the large displacement readings were a product of the Celesco transducers rather than the actual movement of the piping. The spurious transducer readings were probably a result of cable whip.

aging

3.4.2 Performance of the Bergen Paterson Hydraulic Snubber. Prior to installation in the HDR, the Bergen Paterson hydraulic snubber had been exposed to several seismic experiments at the INEL and was considered a functionally aged unit. Functionally, there was no problem with the unit during the test program, and there was no observed leakage. The large displacements recorded during the testing were, again, a product of the Celesco transducer.

3.4.3 Performance of Snubber Replacement Devices. Section 2.3 gives a description of the four piping support systems that used snubber replacement devices. We expect that EPRI and ANCO will evaluate their systems' performance against the performance of the typical snubber system (U.S. stiff system), and use the results, and other testing, to justify the use of the devices as replacements for snubbers in utilities. Since the GERB Company is primarily concerned with the European market, and the ANCO device is built using the GERB viscous mass device as its base and is expected to be the only GERB device potentially to be marketed in the U.S., the GERB system results will not be specifically discussed in this report.

The EPRI-sponsored devices and those built by ANCO have common features yet very diverse designs. All are meant to be pin-to-pin replacements for snubbers; all work on energy absorbing principles; and all are designed with the intention to provide higher reliability than conventional snubbers.

The EPRI/Bechtel device is based on the principle of dynamic energy absorption by ductile flexures. The EPRI/Cloud device is based on the principle of energy

absorption by impact, where the impacting takes place inside the device. During the SHAG test, the pipe behaved in a manner similar to the way pipes behave at common box beam supports. The ANCO device is based on the GERB viscous mass energy absorber. Figure 36 is a photograph of the EPRI/Cloud devices installed at locations H-7 and 8; Figure 37 is a functional schematic of the EPRI/Bechtel device; Figure 38 is a photograph of the ANCO device installed at location H-2.

Cloud and Bechtel devices were installed individually for tests at the three significant starting frequencies. ANCO installed their support system for one test at 8 Hz, but did not participate in the 4.5- or 6-Hz frequency tests.

Only a general qualitative discussion can be presented for the snubber replacement devices, because the only analyses made compared the total system response for each support system methodology. In general, the load ratings for all of the snubber

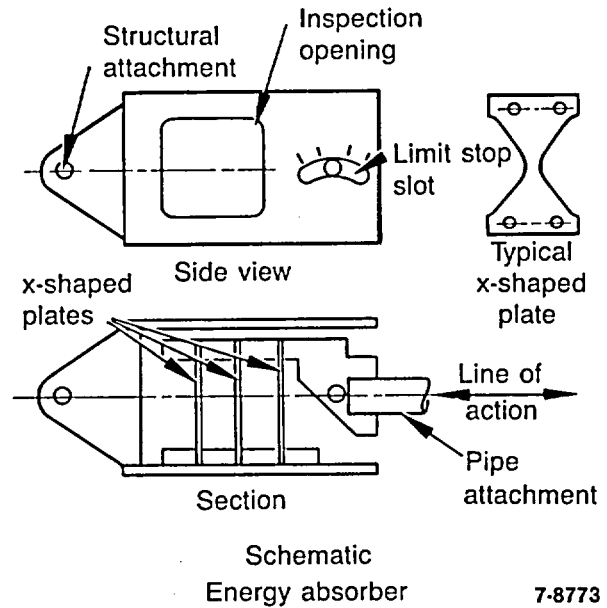


Figure 37. Functional schematic of the EPRI/Bechtel energy absorber.

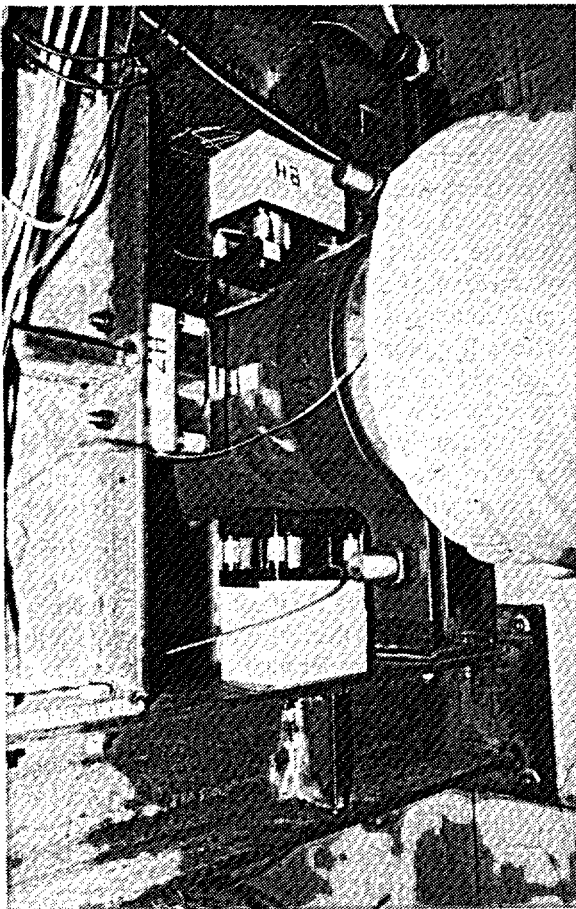


Figure 36. EPRI/Cloud seismic stops installed at locations H-7-8.



Figure 38. ANCO snubber replacement device installed at the H-2 location.

replacement devices were higher than the loads reached in the tests. Therefore, no damage was expected for any of the devices, and none was sustained. Research being performed for EPRI by Cloud and Bechtel is expected to detail the performance of their units, and ANCO Engineers have published reports on their findings. The following section presents a comparison of the piping support systems, including the four systems that used snubber replacement devices, and explains how modifications to the support system affected VKL response.

3.5 Comparison of Piping Support Systems

Aging The dynamic loading from the shaker exceeded design allowable strain limits for the concrete containment building. The VKL piping acceleration responses averaged from 1 to 3 g throughout the piping system. Some of the installed snubbers experienced loads approaching ASME code Level C allowables. Struts experienced loads of up to 11,000-lb force. However, the strains measured in the piping system and valve were fairly low in comparison to the forces and accelerations experienced in each of the piping support systems tested. The structural integrity of the piping and valve was not compromised. None of the support systems resulted in piping strain measurements that reached 50% of yield.

The responses were high enough to permit identification of distinct modes of response for the various piping support systems and to assess their performance. The U.S. stiff system performed as designed, raising the resonant frequency of the piping system. Generally, the flexible and U.S. stiff system responses did envelop the response of the VKL. However, they were not the best support systems based on stresses in the system. The KWU system had fewer high-peak responses than did either the stiff or the flexible system. This fact supports current thinking in the United States that the best design lies somewhere in between stiff and flexible.

Table 5 compares the forces and strains for the U.S. stiff snubbed, Cloud, and Bechtel piping support systems, the recorded measurements being average peak responses from the measured histories. The measurements include only those instruments that were used in all three support systems. The comparison shows that whereas the snubbed system has four of the highest measured values for a given location, the magnitudes are close to those of one or both of the other systems; however, several of the Cloud and Bechtel measurements are double those of the snubbed system responses. The snubbed system had 4 maxima of the 22 selected measurements, 3 of them for the 6-Hz

starting frequency. The Cloud system had 8 maxima, 5 of them for the 6-Hz starting frequency. The Bechtel system had 11 maxima, 7 for the 8-Hz starting frequency.

These results point out that changing pipe support types changes the response of a piping system when all other parameters remain the same. The results of the changes are not always beneficial, as shown. The ANCO system was tested only at the 8-Hz starting frequency and at ambient temperature. The ANCO pipe support system was stiffer than the U.S. stiff system, as indicated by evaluation of the measured responses. The ANCO system had typically lower forces and strains than the U.S., Bechtel, and Cloud systems. However, the ANCO system was tested only at the 8-Hz shaker starting frequency and, like the U.S. system, might have responded more at the 6-Hz starting frequency (see Section 3.3). The ANCO system was tested only with the piping system at ambient temperature. The containment environment was warmer when the piping system was at elevated temperature, and the high temperature might have lowered the viscosity of the viscous damper had it been tested at a higher temperature. Therefore, a direct comparison of the responses of a typical U.S. stiff system with those of the ANCO system cannot be made.

Each of the four energy-absorbing support systems resulted in different response frequencies in the piping. Also, the expected plant-specific input spectra must be considered when judging the effectiveness of the support system in reducing loads in the piping. We infer from the results of the SHAG experiments that one system cannot be chosen over another without careful consideration of the input excitation to the piping system. It appears that appropriate analyses should be conducted before snubbers in existing support systems are replaced with snubber replacement devices.

Posttest analyses of the KfK flexible and U.S. stiff system responses indicated, as would be expected, that stiff system dynamic response stresses were less than the corresponding flexible system stresses. However, the relative differences were not as great as would be expected. The moderately flexible KWU system, with 50% fewer supports than the typical U.S. stiff design, responded with a smaller total system stress than any of the other systems tested, including the energy-absorbing systems.

In general, if piping system dynamic input is significant and input excitation frequencies correspond with the natural frequencies of the piping system, the response of the system will be amplified. The philosophy underlying present U.S. nuclear piping system seismic design is to avoid amplification and reduce resonant response by using snubbers and struts to stiffen the systems so that the natural frequencies are higher than

Table 5. Comparison of system device forces and strains for different support configurations

Instrument No.	Unit of Measure	Location	Shaker Starting Frequency (Hz)	U.S. Stiff Snubbed System	Bechtel System	Cloud System
X AXIS						
27	lb Force	H-3	8	2400	3125	2125
27	lb Force	H-3	6	1800	3150	— ^a
23	lb Force	H-5	8	8000	7500	6750
23	lb Force	H-5	6	4750	9250	11000
3-2	Micro Strain	Pipe Between Tee & Valve	8	180	370	170
3-2	Micro Strain	Pipe Between Tee & Valve	6	320	300	200
3-3	Micro Strain	Pipe Between Tee & Valve	8	160	330	160
3-3	Micro Strain	Pipe Between Tee & Valve	6	270	250	180
32	lb Force	H-10	8	750	825	725
32	lb Force	H-10	6	1300	1300	1050
Y AXIS						
1-1	Micro Strain	El Below Reducer	8	50	55	110
1-1	Micro Strain	El Below Reducer	6	80	80	95
1-6	Micro Strain	El Below Reducer	8	35	50	115
1-6	Micro Strain	El Below Reducer	6	65	60	100
14	Micro Strain	Threaded Rod	8	185	210	220
14	Micro Strain	Threaded Rod	6	225	275	338
Z AXIS						
24	lb Force	H-4	8	3500	4000	3750
24	lb Force	H-4	6	5350	5000	6750
31	lb Force	H-9	8	700	1500	950
31	lb Force	H-9	6	1400	1575	1050
33	lb Force	H-11	8	450	1175	550
33	lb Force	H-11	6	675	1100	800

a. Measurement not available.

the amplified building excitation frequencies. This design philosophy has disadvantages. The relative movement of the anchors in a stiff support system can actually add stress to a piping system during a seismic event, and stresses caused by thermal expansion during normal operation may be large, especially if snubbers malfunction by locking up when they should not.

The following "time at frequency" rationale may explain why the moderately flexible KWU system experienced lower total system stresses than the U.S. stiff system. The test excitation method, a decaying sinusoidal input to the HDR building, ensured that, with the exception of the very flexible system, the lowest natural frequencies of all systems were excited with large input frequency content, and the systems

with lower natural frequencies were excited with greater energy. However, the time required for maximum resonant response to be generated in the piping system is largely dependent on the natural frequency of the excited mode: the lower the natural frequency, the longer the time required to obtain maximum response. Apparently the duration of excitation was not long enough for the lower frequency modes of the moderately flexible KWU system to reach maximum response. This would explain why the moderately stiff system developed lower total system stresses than the U.S. stiff system even though the U.S. stiff system had the highest natural frequencies and would therefore be expected to respond with less amplification. We believe that this result is valid for systems subjected to true

earthquake excitation as well; because of complex building response filtering imposed on the system by the test, the excitation frequency content was very "earthquake-like," and the duration of maximum excitation, approximately 30 s, was conservatively representative of the duration of earthquake strong motion.

Further analysis of experimental results is needed, since the conclusions presented here are based on limited data analyses. However, these analyses results suggest the advantages of more flexible designs for U.S. nuclear piping systems.

Aging

3.6 Valve and Motor Operator Response

One of the objectives of the HDR testing was to subject the refurbished 8-in. motor-operated gate valve to combined loads. The valve was tested under normal internal hydraulic loads (pressure and flow loads) in combination with dynamic excitation to determine how effectively the normal equipment qualification single effects testing used in the U.S. can model or envelope in situ conditions. Tests were conducted both at ambient and at elevated temperatures.

The valve was baseline functional tested at the INEL with and without pressure loads prior to its use in the SHAG dynamic test series. Important valve parameters were recorded at that time, including valve stroke time, motor current and voltage, system pressure, valve differential pressure, valve stem position and strain, and system fluid temperature. Similar baseline functional tests, with the addition of flow loads, were performed after the valve was installed in the VKL at the HDR. Those tests were performed at ambient temperature just before the SHAG dynamic testing and again at elevated temperatures (200°C) just before the hot dynamic tests. These pretest parameters were compared with parameters recorded during pre-SHAG functional testing. From the quick look data, satisfactory agreements were obtained.

Dynamic testing of the valve consisted of opening and closing the valve during and after the simulated seismic excitation of the piping system. Dynamic tests were conducted both at ambient and at elevated temperatures with the valve subjected to various pressure and flow loads. The same parameters recorded during the baseline functional tests were recorded during the dynamic tests. In addition, acceleration, displacement, and strain were measured on the valve to record its response to dynamic excitation. Figure 39 shows the valve instrumentation, and Figure 40 shows the installed valve.

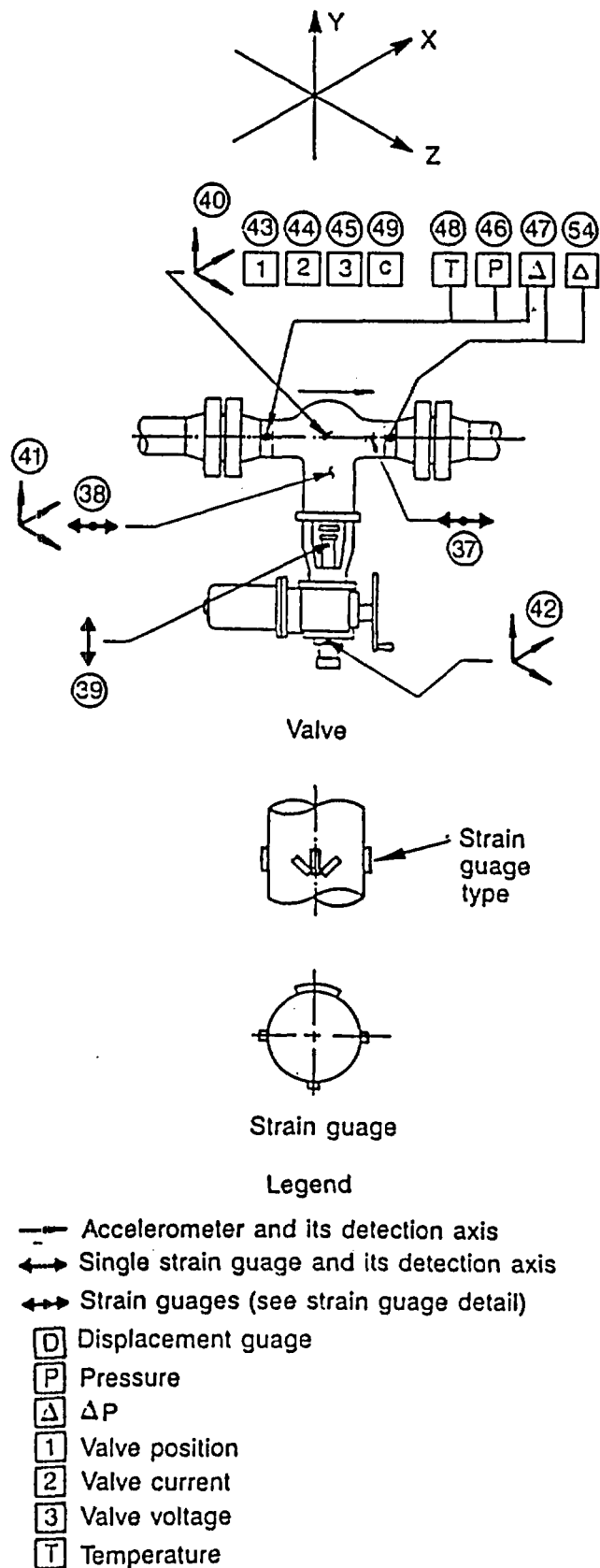


Figure 39. Valve instrumentation detail.

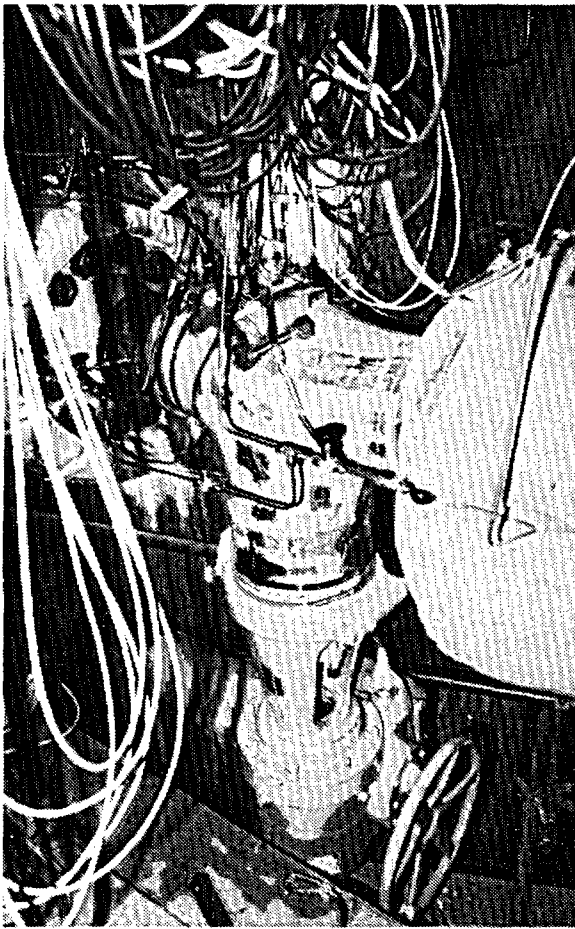


Figure 40. Installed gate valve and part of the installed instrumentation.

A motor-operated valve consists of two sub-assemblies: the valve itself and the motor operator. In the following discussion, Section 3.6.1 reports on the structural integrity of both the valve and motor operator subassemblies. Section 3.6.2 reports on the operability of the valve subassembly, and Section 3.6.3 reports on the performance of the motor operator and documents the operator's anomalous performance. Section 3.6.4 reports the valve's (and the operator's) amplified dynamic response to the tests.

3.6.1 Structural Integrity of the Motor-Operated Valve. The structural integrity of the valve and motor operator was not affected by SHAG dynamic excitation. Structurally, valves are inherently rugged. From the loadings input at HDR and the strains measured during the tests, we infer that considerably higher loadings could have been applied without reaching near yield stresses of the valve and motor operator.

3.6.2 Valve Response. The valve subassembly performed quite well throughout the test program, as determined from the posttest data review and analysis. None of the data provides any indication of measurements different than they should be for the given test conditions and loading. The valve stem packing was replaced during refurbishment at INEL, and no packing leakage was observed during the test program.

The dynamic excitation experienced by the valve did not adversely affect its operability. In fact, the closing currents recorded during the hot dynamic tests were lower than those recorded during the hot functional tests (which were conducted without dynamic input to the system), indicating that the load was actually smaller. We assume that the vibration during the dynamic tests helped to break the valve disc to body guide friction.

3.6.3 Performance of the Motor Operator.

Table 6 gives a summary of the measurements taken of valve functions during the SHAG tests. From the column labeled "stall," one can see that the motor operator failed to torque out at the end of the closing stroke during several of the tests. This anomaly is discussed at length in the following paragraphs.

Initially, the motor operator appeared to perform quite well. The stroke times and valve currents varied with internal valve loadings as expected, with the exception of the slower closing times during hot functional tests. They are slower than the closing times during hot dynamic test. The seismic excitation caused no measurable increase in operator load and may have actually reduced that load in some cases. The spread of valve functional responses (current and stroke times) was very good. The failure of the operator to torque out is apparently unrelated to the dynamic loads imposed on the valve during the tests.

3.6.3.1 Torque-out Failure. Normally, the high torque produced by the motor when the valve reaches the fully closed position causes the motor operator to torque out; that is, the closing torque switch opens and, through the motor controller, interrupts current to the motor. Figure 41 shows the major components involved in this process. The splined output shaft drives the worm, which turns the worm gear and the stem nut. The stem nut drives the threaded valve stem. As the valve seats and the worm gear resists motion, the worm climbs the worm gear, floating on the splined shaft and compressing the torque spring until the shoulder of the worm contacts and rotates the arm of the torque switch and opens the torque switch. The higher the torque switch setting, the further the worm must compress the spring before the torque switch opens and interrupts current to the motor. If the torque switch fails to open,

Table 6. Valve function parameters

Test T40	Temp (°C)	Current in Amps							Pressure (psi)	
		Stroke Time (s)		Closing			Opening			
		Closing	Opening	Run	Peak	Stall	Peak	Run	System	ΔP
Ambient	20	14.4	14.4	12	12+	—	16.41	10.94	73.95	384
34	20	—	14.7	12	14	—	17.67	10.6	73.95	377
35	20	—	—	12.5	15	—	17	11	15.0	333
36	20	—	15	11	13.5	—	14	9.5	55.5	330
37a	20	—	—	12	13.5	—	17	11	67	333
b	—	—	—	11.5	—	35	13	10	—	—
40a	20	15.5	15.5	12	17	—	17	10	67	259
b	—	—	15.5	12	—	38	20	9	—	371
20a	20	—	15.6	13.5	18	—	24	12	74	344
b	—	17	17	12.5	16	38	25	12.5	—	351
60a	20	—	—	14	19	—	23	11	74	340
b	—	—	16	13.5	—	—	—	—	—	344
50a	20	—	15	12.5	14	—	20	9	67	333
b	—	15.5	16	11	—	38	20	9	—	263
70a	20	—	—	11	13	—	19	7	67	333
b	—	—	16	11.5	—	37	18	7.5	—	263
10a	20	—	—	—	—	—	24	8	70	362
b	—	—	16	12.5	—	38	25	10	—	329
30a	20	—	—	—	—	—	25	10	70	362
b	—	—	16	12.5	—	38	25	10	—	340
31a	20	—	—	—	—	—	25	11	70	348
b	—	—	16	12.5	—	38	25	11.5	—	333
41	20	—	16	12.5	13.5	—	25	11.5	70	333
21	20	—	16	12	13	—	25	10.5	70	325
11	20	—	14	12.5	13	—	25	11.5	70	329
51a	20	—	—	12.5	—	38	25	11	70	322
b	—	—	17	12.5	—	37	25.5	11	—	333
Hot a	210	22	12	17	27	40	12	7	924	313
Func b	—	22	12	17	27	38	12	7	—	313
52a	210	—	—	12.5	25	37	10	6	924	301
b	—	—	12.5	12.5	25	36	10	7	—	301
32a	210	—	12.5	12.5	25	37	10	5	924	301
b	—	—	12.5	12.5	26	36	11	6	—	301
42a	210	—	12.5	12.5	25	36	10.5	5	924	305
b	—	20	12.5	13.5	25	37	10.5	6	—	305
12	210	19.5	12.5	13	25	38	11	6	924	305
22	50	—	13.5	—	—	—	18	7	70	359
12A	210	20	12.5	13	25	37	10	5.5	924	313
14	40	—	14	10	17	—	17	8	50	350
16	Valve tests were not performed during this dynamic test.									
13	Valves tests were not performed during this dynamic test.									
After a	40	14.5	14	13	19	—	20	12	74	359
Hot b	—	15	14	13	19	41	22	11	—	354

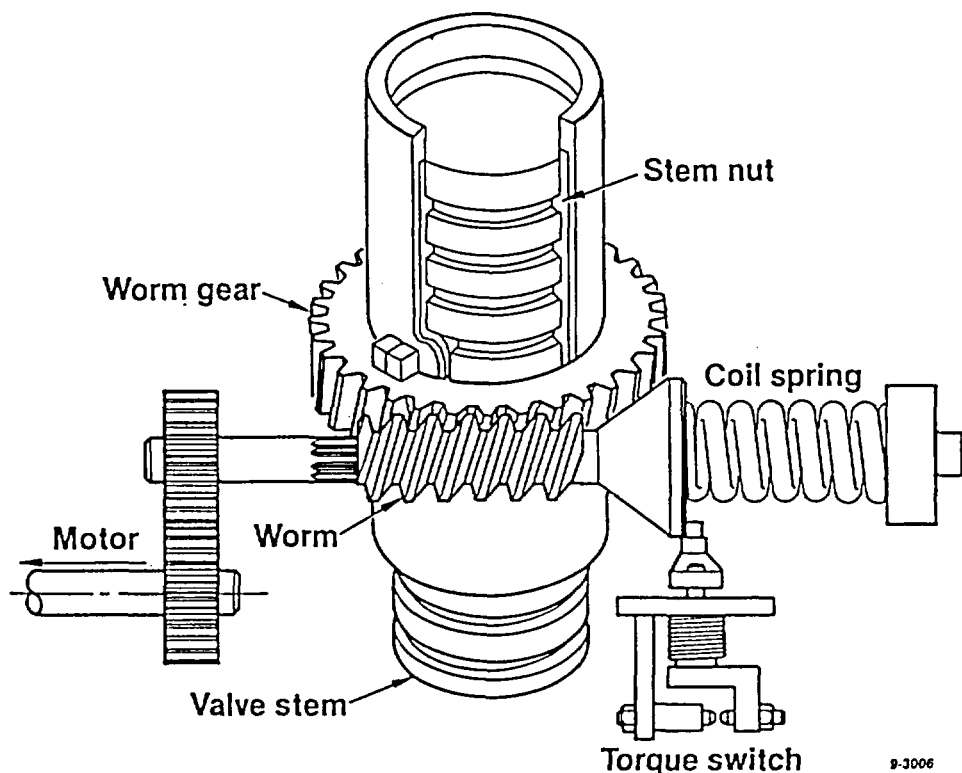


Figure 41. Simplified diagram showing some of the components of a motor operator.

the motor stalls and starts to overheat. If the thermal overload relay malfunctions, or if it has been bypassed, the result can be motor burnout and the functional loss of the valve.

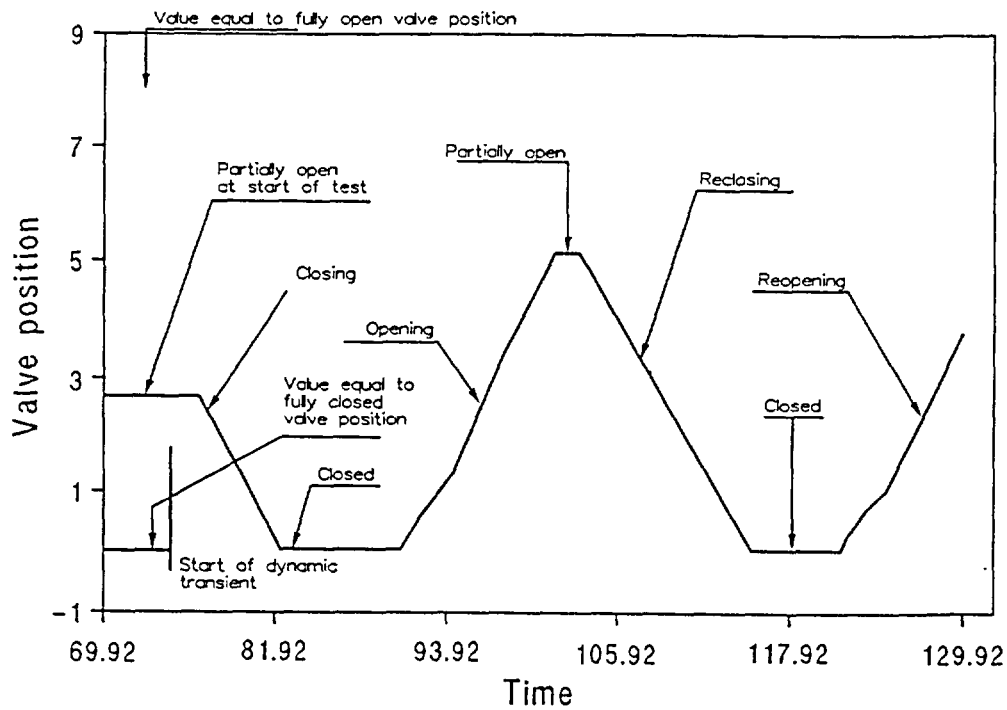
The sequence of valve operation at the HDR required the valve to be closed for no more than 10 s to accommodate system pressure control concerns. The reopening of the valve within 10 s after closing kept the motor from overheating and delayed detection of the problem until posttest data reduction. Figure 42 shows the output of the valve stem position transducer for two partial valve cycles during the fourth SHAG test (the first observance of the malfunction). Figure 43 shows the valve operator motor current history for the same test. Figure 43 shows that the motor operator performed normally during the first cycle, but during the second cycle the torque switch did not open, and the motor stalled.

This functional anomaly occurred repeatedly throughout the program. We determined early in our investigation that the problem was not caused by the torque switch being set too high. Further analyses of the measured valve response data from the SHAG tests indicated that the valve functional anomaly probably was

the result of more than one problem. The NRC and the INEL agreed to set up a review group to advise the further investigation and analyses of what might be a generic problem. The review group included representatives from the NRC staff, INEL, Oak Ridge National Laboratory (ORNL), and Limitorque.

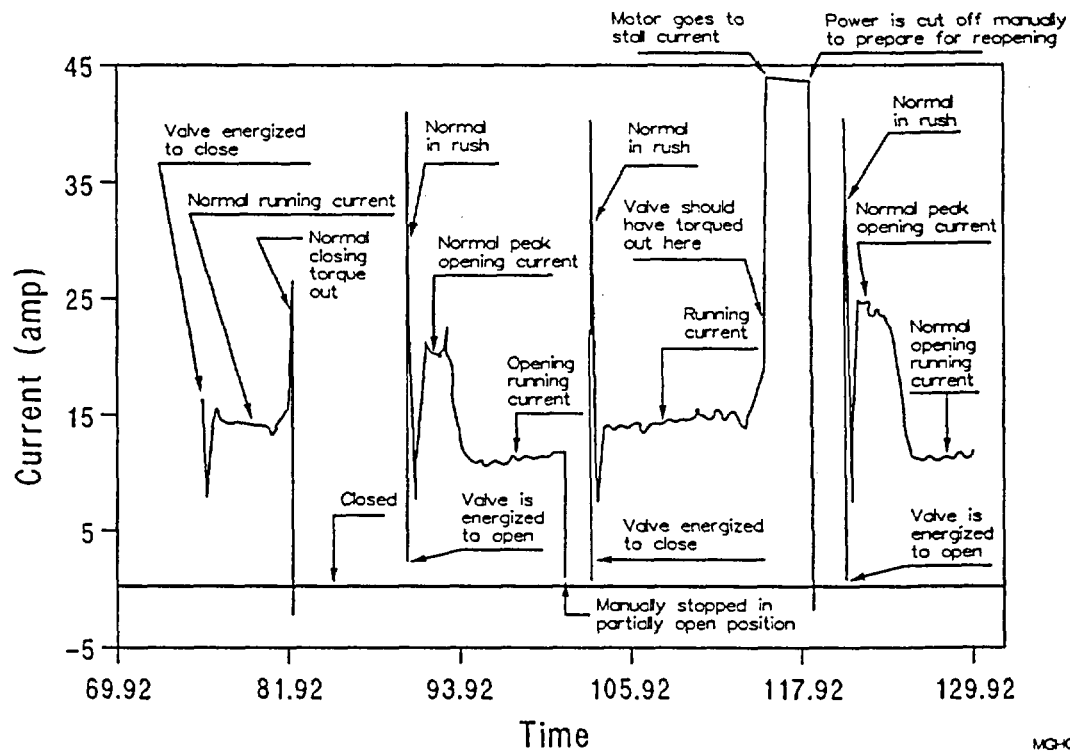
3.6.3.2 Additional In Situ Tests at HDR. The review group recommended that a parametric in situ test be conducted at the HDR to provide additional data. Limitorque agreed to support the tests from its European office. Table 7 provides the results of those tests.

These results showed that the functional anomaly was influenced by the internal valve hydraulic load. With internal static pressure alone, the valve functioned correctly. Figure 44 shows three valve stem position histories for the closing stroke for three internal valve static pressures. The plot shows linear closing response for the valve on each trace with a slightly longer total stroke time for each increasing pressure. Figure 45 shows the same three static pressure cases with flow through the valve. The flow and resulting differential pressure are the same for all three of the static pressures. In all three cases, the valve closure rate



MGH01355

Figure 42. Valve position versus time during in the fourth test.



MGH01354

Figure 43. Valve current versus time during the fourth test.

Table 7. HDR in situ valve testing summary

Test	Torque Switch Setting	Stroke Time Closing (S)	Stroke Time Closing Stall (S)	Stroke Time Opening (S)	Pressure (bar)	Flow (tons/hr)	Torque Switch Deflection Total (Degree)	Torque Switch Deflection Run (Degree)	Current Closing Run (amp)	Current Closing Peak (amp)	Current Closing Stall (amp)	Current Opening Peak (amp)	Current Opening Unseat (amp)	Current Opening Run (amp)	Voltage Closing Run (Vdc)	Voltage Closing Peak (Vdc)	Voltage Closing Stall (Vdc)	Voltage Opening Peak (Vdc)	Voltage Opening Unseat (Vdc)	Voltage Opening Run (Vdc)	Incomplete Closing (in.)
01	2.9	19.0		16.4	0	0	30.0	12.0	18.5	17.5		26.5		15.0	120.0	120.0		116.0		121.0	0.00
02	2.9	19.2		15.3	10	0	31.0	13.5	19.0	18.2		26.5	13.0	13.5	119.0	120.0		116.0	122.0	122.0	0.00
03	2.9	21.3		14.2	20	0	28.8	14.0	21.0	20.3		26.0	12.1	11.0	118.0	118.2		116.0	121.8	121.8	0.00
04	2.9	19.6		15.0	21	45	26.5	13.5	18.0	25.5		26.0	23.5	10.5	118.0	115.0		116.0	116.0	121.0	0.00
05	2.9	19.0		13.7	25	45	27.0	14.0	17.0	26.5		25.0	22.5	9.0	118.0	115.0		116.0	116.0	121.0	0.00
06	2.9	21.7		14.5	30	80	25.0	17.0	20.5	36.0		26.0	26.0	9.5	118.0	112.5		116.0	116.0	122.0	0.16
07	2.9	21.7		13.2	35	80	25.0	16.0	20.5	35.0		26.0	24.0	7.5	118.0	112.5		116.0	117.0	123.5	0.28
08	2.9	21.5		12.2	40	85	25.3	15.0	19.0	33.7		26.0	21.7	6.5	119.0	113.0		116.0	118.0	123.7	0.32
09	3.1		23.3	12.7	40	85	28.0	13.0	17.0		43.5	25.5	24.3	6.0	119.0		108.7	116.0	116.0	123.7	0.16
11	3.1	16.6		15.6	0	0	34.8	12.5	15.0	15.5		26.8		13.0	119.0	119.0		114.7		120.0	0.00
11A	2.9	17.4		15.4	0	0	34.5	12.0	16.0	15.0		26.5		13.0	119.0	119.0		116.2		120.0	0.00
12	2.0	16.4		15.4	0	0	24.0	8.0	15.5	13.0		26.5		14.0	121.8	122.0		117.2		121.9	0.00
13	2.5	16.7		15.6	0	0	28.3	9.0	15.5	14.0		26.5		14.0	120.0	120.5		116.3		121.0	0.00
14	3.0	16.6		15.6	0	0	29.0	7.5	15.5	15.0		26.5		14.0	121.0	121.0		116.2		121.0	0.00
15	3.5	16.6		15.6	0	0	32.5	7.4	15.0	19.7		27.0		14.0	121.0	117.9		117.2		121.0	0.00
16	4.0		16.8	15.6	0	0	36.0	9.0	15.5		45.5	26.5		14.0	120.0		108.6	116.2		121.0	0.00
17	2.5	16.3		15.4	0	0	30.0	9.0	15.5	13.0		27.0		14.0	121.8	125.0		118.0		122.8	0.00
18	2.5	18.4		15.4	10	0	30.5	14.0	17.5	15.0		27.0		13.5	120.0	120.0		116.2		121.0	0.00
19	2.5	19.0		14.0	20	0	25.3	9.5	18.0	16.4		27.0		11.0	120.0	121.0		117.2		122.7	0.00
20	2.5	20.8		13.7	30	0	23.7	9.5	19.0	17.7		27.0	10.2	9.0	120.0	120.0		116.6		124.0	0.00
21	2.5	22.2		12.2	40	0	24.5	11.0	22.0	18.5		27.0	9.0	7.0	118.0	119.0		116.3		123.7	0.00
22	2.5	20.4		12.0	40	80	16.5	9.5	19.0	27.5		26.0	19.5	6.5	118.0	114.5		116.2	118.0	122.0	0.40
23	2.5	17.7		13.5	30	80	16.5	8.0	17.0	28.0		26.0	22.5	7.5	119.0	114.4		116.2	118.0	122.0	0.32
24	2.5	17.5		13.8	20	80	15.5	6.0	15.0	28.0		25.5	26.5	8.5	120.0	114.4		116.3	115.0	122.0	0.24
25	2.5	17.0		15.5	10	80	18.3	5.8	14.5	24.0		25.5	28.0	10.0	120.0	116.3		116.3	114.4	121.5	0.00
26	3.0	17.0		15.5	10	72	24.0	6.3	14.5	28.8		26.0	27.5	10.5	120.0	114.0		116.0	114.0	121.0	0.00
27	3.0		19.0	14.6	20	80	22.0	7.0	16.0		44.0	25.5	27.5	8.0	119.0		108.2	116.0	114.0	121.8	0.00
28	3.0		20.3	13.7	30	80	21.8	7.8	16.0		42.5	25.0	26.0	7.0	119.0		108.7	116.0	115.0	122.0	0.12
29	3.0		22.2	12.7	40	80	23.0	10.0	18.0		43.5	25.0	22.7	6.5	118.0		108.5	116.0	116.0	123.0	0.16
30	3.0	19.7		11.9	40	0	30.0	11.5	17.0	19.8		26.0	9.0	6.5	120.0	119.0		116.0	122.0	123.6	0.00
31	3.0	18.3		12.7	30	0	27.4	7.4	16.0	18.0		26.0	9.4	7.4	120.0	119.0		116.0	122.0	123.7	0.00
32	3.0	16.7		12.8	20	0	27.0	8.0	14.0	17.0		26.0	10.4	8.0	121.0	120.0		116.0	122.0	122.5	0.00
33	3.0	15.5		13.4	10	0	27.4	5.7	13.0	16.5		26.0	11.4	9.5	121.5	120.0		116.5	122.0	122.5	0.00
34	3.0						27.0														
34A	3.5						34.0														
35	3.5	15.7		13.7	10	0	34.0	6.5	14.0	19.2		26.4	12.3	11.0	122.5	120.5		118.0	123.7	123.7	0.00
36	3.5		22.2	12.6	40	80	23.5	10.2	19.0		44.0	26.5	24.0	7.0	118.0		108.7	116.0	116.0	123.5	0.24
40	3.1		21.1	14.0	40	85	24.0	12.0	19.7		45.3	26.0	23.0	10.5	119.0		108.7	116.0	117.0	121.8	0.27
40A	3.1		20.2	13.7	40	85	21.0	9.0	18.0		44.7	26.0	22.5	10.0	119.0		108.7	116.0	117.0	121.8	0.30
40C	3.1	18.5		15.5	20	80	27.3	10.5	16.0	29.7		25.7	26.0	11.0	120.0	114.4		116.0	115.0	121.8	0.00
40D	3.1		18.2		20	80	24.8	8.3	15.5		44.5				120.0		108.7				0.00
40E	3.1	17.5		14.4	20	30	28.5	8.5	16.0	19.7		25.7	19.0	10.7	120.0	118.0		116.0	119.0	121.8	0.00
41	3.1	17.7		16.3	0	0	23.2	3.2	16.0	17.9		26.0		14.5	120.0	120.0		116.0		120.0	0.00
41A	3.1			15.8	0	0						26.0		13.5				116.0		120.0	0.00
42	3.0	21.8		14.2	40	80	20.7	9.2	20.0	42.5		26.0	26.2	9.0	119.0	110.6		116.0	116.0	123.0	0.21
42A	3.0	19.5		13.8	40	80	16.0	9.5	19.0	29.0		27.5	25.0	8.0	120.0	116.0		116.0	117.0	123.0	0.30
42B	3.1		21.7	14.7	40	80	21.6	9.4	18.0		45.5	26.0	30.5	8.5	119.0		108.7	116.0	116.0	122.0	0.16
42C	3.1		23.8	14.5	40	80	22.0	8.5	18.5		47.0	26.5	26.5	8.0	118.0		107.8	116.0	116.0	122.0	0.16
45	2.8	20.5		13.8	40	80	23.8	13.3	18.0	37.5		26.0	25.0	8.0	118.0	110.6		116.0	116.0	122.0	0.18
45A	2.8	20.5		13.7	40	80	19.5	9.5	18.5	38.2		26.0	25.0	8.0	118.0	110.6		116.0	116.0	122.0	0.18
46	2.8	19.3		16.3	0	0	24.9	6.0	18.0	18.0		26.5	16.5	9.0	120.0	120.0		116.0	121.0	122.0	0.00
46A	2.8	18.2			0	0	25.5	6.7	17.0	18.5					120.0	120.0					0.00

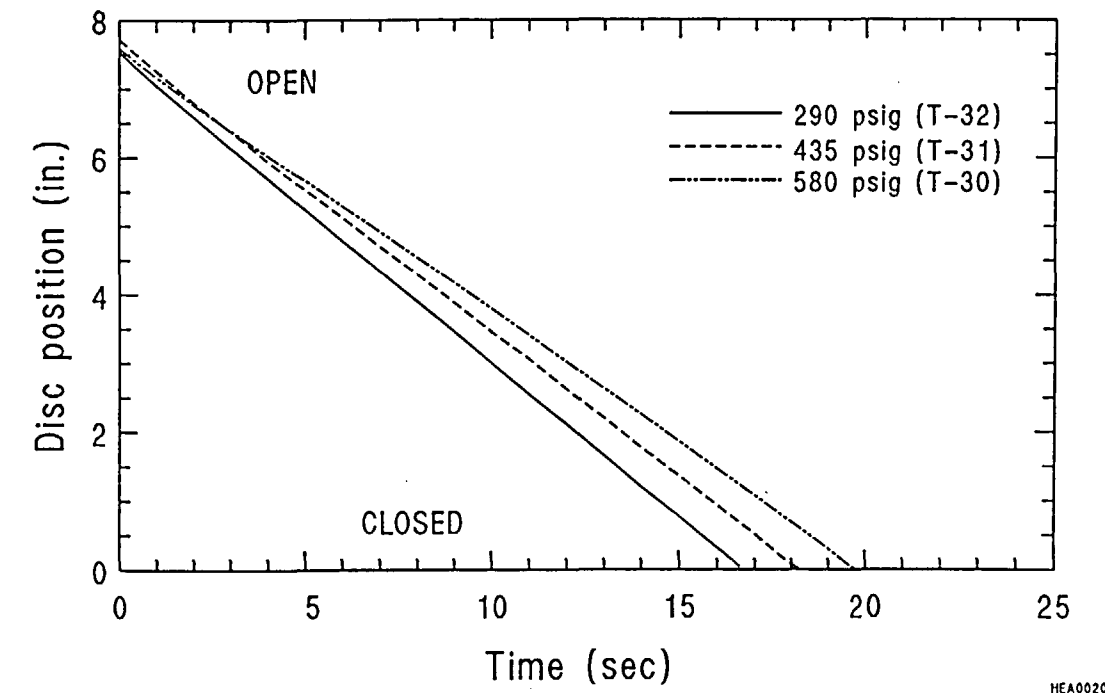


Figure 44. Valve position during closing stroke under three different static pressure loads with no flow.

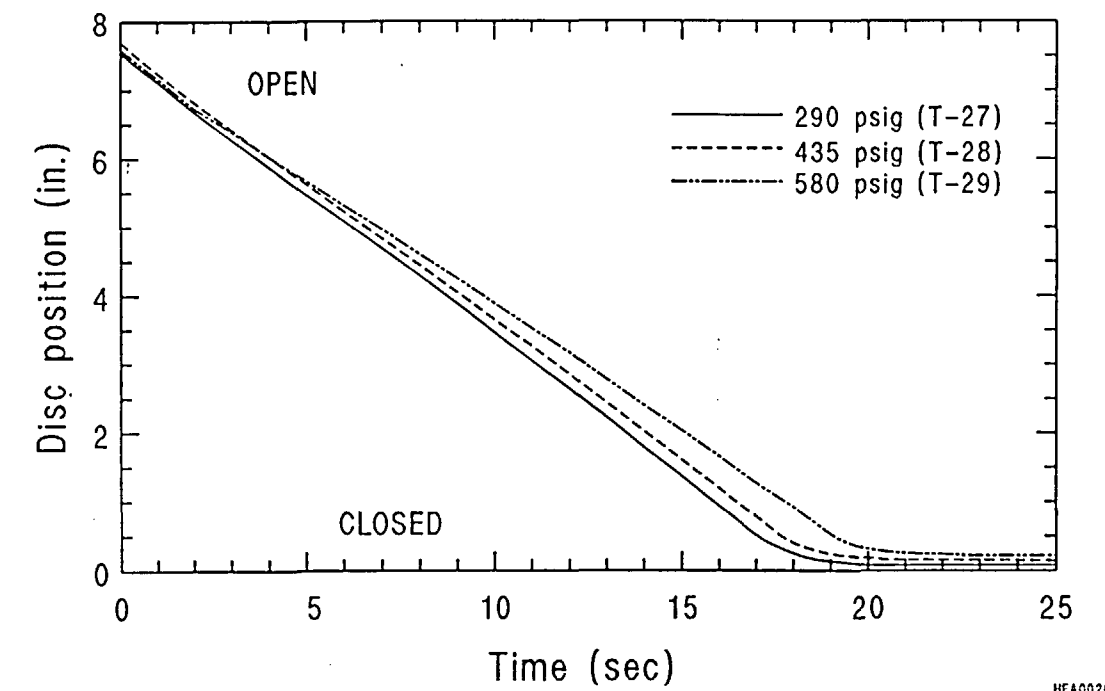


Figure 45. Valve position during closing stroke with flow (360 gpm) under three different static pressure loads.

slows down near the end of the stroke, and in all three cases the valve does not completely close. The extent to which the valve remains open is increasingly greater with each increase in pressure combined with the flow load. The static pressures applied at the HDR were all lower than design specifications for this 900-lb valve, and the differential pressure loads were only a small percentage of design specifications.

The parametric study showed that at lower torque switch settings the torque switch functioned, but the valve did not completely close at the higher pressures and flows. At higher torque switch settings the motor stalled. The valve closed farther with the higher setting, but the motor usually stalled before the valve was completely closed.

During the parametric study, we determined that the problem was not the result of inadequate lubrication, worn bearings, or high resistance in a field coil in the motor. At the end of the parametric in situ study, the cause of the problem had not been isolated. Voltages and currents during HDR tests were measured at the motor with three different measurement systems from two different laboratories. According to the data, the voltage at the motor did not drop below 107 Vdc at motor stall, and the motor voltage at stall was only slightly less than the running voltage. These voltage readings temporarily diverted our attention from the possibility that the power supply or power cabling might be the cause of the reduced performance at HDR. Later analyses showed that these voltage readings were unreliable because of the circuit design.

3.6.3.3 Dynamometer Testing at Limitorque Laboratories. The motor operator was removed from the valve and returned to the U.S. for testing at the Limitorque Facility in Lynchburg, VA. The results of those dynamometer tests are presented in Table 8.

Testing of the motor operator on the Limitorque dynamometer showed a marked improvement in performance at loadings above 35 amp. Locked rotor currents were 75 amp, compared to 50 amp at HDR. The published locked rotor current for the motor is 120 amp.

The tests also provided some insights on the torque switch position versus our power torques at HDR. The torque switch was set at the nominal value of 3. A torque switch setting of 3 should produce nearly 12,000 lb of thrust; the dynamometer tests showed that at a torque switch setting of 3 the motor operator produced only 8,000 lb of thrust. A setting of 3.75 was necessary to consistently achieve an output thrust of 12,000 lb.

3.6.3.4 Torque Spring Inspection. At the recommendation of the review group, the torque spring was

removed from the operator and inspected. We discovered that the torque spring had taken a permanent set, measuring approximately 1/2 in. shorter than specified. The shorter torque spring required the torque switch to be set to a value of 3.75 to produce the specified torque for the nominal torque switch setting of 3. A second Shippingport valve in the as-removed condition was located at Oak Ridge National Laboratory. The motor operator was disassembled and the torque spring removed for measurement. This spring also was short, by 3/16 in. Two springs are not a large sample, but these instances do suggest that the SMA coil springs may be susceptible to permanent set over time, and users should not rely on torque switch settings alone (NRC Information Notice 89-43).

3.6.3.5 Dynamometer Testing at Peerless. The motor manufacturer Peerless Winsmith agreed to dynamometer test the motor to quantify the motor-alone performance. During these dynamometer tests, the motor met all of the specified output parameters, including a locked rotor current of approximately 120 amp. Figure 46 compares the actual speed and current to predicted motor performance. We attributed the difference between the test results at Limitorque for the motor operator and those at Peerless for the motor alone to a difference in the test techniques, partly because of the way the INEL had requested them to perform the dynamometer test loadings. We had requested at both laboratories that the load be slowly increased to the specified test load as it would in the closing cycle of a valve. This type of load tends to heat the motor. Because the specified performance was for a relatively cool motor, the motor was cooled to ambient temperature before each test at Peerless. This was not done at Limitorque.

To quantify the effects of motor heating, a special test was performed during the electric motor dynamometer test. A 50 ft/lb load was set on the dynamometer, the motor was cooled to ambient temperature, the motor was energized and allowed to come to speed, the load was applied, and the current was monitored for 20 s. The loss of power on the motor was linear; the current decayed 1 amp per second. Two amp is roughly one ft/lb of torque on this motor. Thus, motor heating caused the motor to lose 10 ft/lb of output in 20 s. Figure 47 shows these results. These results partly explain the valve's failure to torque out on the second cycle during the HDR tests. The motor heated up during the first cycle and did not have the power to trip the torque switch in the second cycle.

The dynamometer testing results provide answers to several of the questions involved in the valve functional anomaly at the HDR; however, they do not explain the root cause of the valve stalling at near 50 amp at

Table 8. Results of motor operator testing at Limitorque Laboratory

Test No.	Torque Switch Setting	Set Voltage (Vdc)	Minimum Voltage ^a (Vdc)	Plotter Peak Current (amp)	Peak Torque (ft-lb)	Peak Thrust (lb)	Comments
1	—	—	—	9.0	—	—	No load/baseline
2	2.00	110	108	15.0	99	4480	
3	2.00	125	110	15.0	88	3982	
4	2.50	125	121	21.0	125	5656	
5	2.50	110	107	21.0	132	5973	
6	2.90	110	105	25.0	154	6969	
6.1	2.90	110	105	25.7	185	8371	
7	2.90	125	120	26.0	169	7647	Stall Stall
8	2.90	125	120	29.5	176	7964	
9	3.10	125	119	34.0	220	9955	
10	3.10	110	104	35.0	229	10362	
11	3.10	100	95	34.0	231	10453	
12	3.50	100	94	41.0	242	10951	
13	3.50	100	94	39.0	275	12444	
14	3.50	110	104	40.0	242	10951	
15	3.50	125	119	38.0	264	11946	
16	3.75	125	118	39.0	277	12534	
17	3.75	110	103	42.0	264	11946	
18	3.75	100	94	42.0	245	11086	
19	4.00	100	93	46.0	286	12942	
20	4.00	110	103	46.0	286	12942	
21	4.00	125	118	46.0	264	11946	
22	4.20	100	93	50.0	308	13937	
23	4.50	100	92	58.0	352	15928	
24	4.50	100	91	56.0	363	16426	
25	4.50	110	102	54.0	330	14933	
26	4.50	125	116	51.0	308	13937	
27	4.75	125	112	75.0	484	21901	
28	4.75	110	99	66.0	407	18417	
29	3.50	90	85	39.0	231	10453	
30	3.50	80	75	40.0	255	11539	
31	3.50	80	73	41.0	220	9955	
32	3.50	80	79	5.5	—	—	No-load
33	3.50	90	89	5.3	—	—	No-load
34	3.50	100	99	6.0	—	—	No-load
35	3.50	110	109	6.0	—	—	No-load
36	3.50	125	124	6.0	—	—	No-load

a. Derived from visual readings.

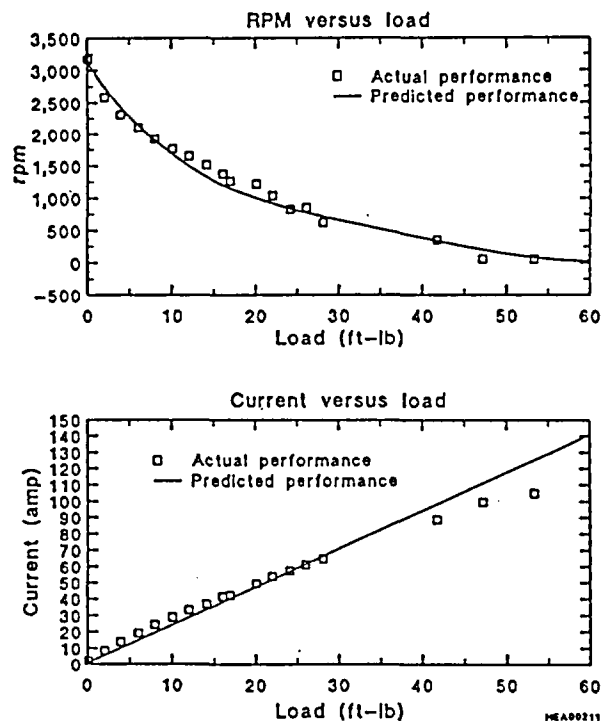


Figure 46. Results of motor dynamometer testing at Peerless.

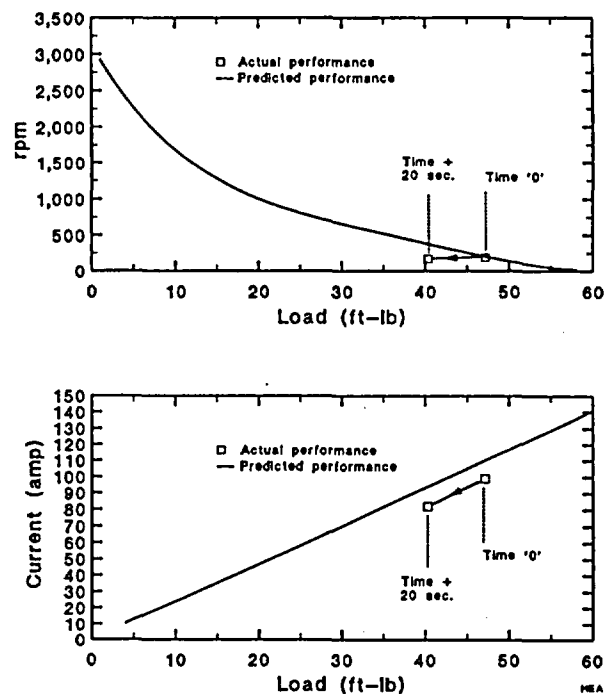


Figure 47. Effects of motor heating, as demonstrated during motor testing at the Peerless laboratory.

the HDR. Voltages during the dynamometer testing at Limitorque were dropped to 80 Vdc, 20 volts below minimums, in an attempt to reproduce the HDR motor operator performance, yet the results could not be duplicated.

3.6.3.6 Analysis of the HDR Power Circuit. Concurrent with Limitorque's assistance to the INEL with the HDR investigation, a utility called upon Limitorque to assist with similar dc motor-actuated valve problems. The utility was a two unit station, and all of the dc powered valve problems were associated with one unit. Several control circuit problems were found during the investigation, and the root cause of the dc motor failures had been attributed to those problems. Interestingly, the power cables in the unit having problems were smaller than those in the other unit. However, this difference was not highlighted in the investigation.

Shortly afterwards, Limitorque published a maintenance letter that contained an electrical circuit calculation basis for dc motor operated valves. This calculation was developed from Limitorque's investigations of dc motor problems at HDR and at the utility mentioned above. In most dc motor operated valve control circuits, the armature coil and the series fields are interconnected through the motor controller, and four power cables must be considered in the calculation,

not two as one might assume. Limitorque recommended using this calculation to determine voltage drop instead of trying to measure the voltage drop in the circuit. In attempts to measure the voltage drop, it is very difficult to load the circuit and sum the various voltage drops.

From this new methodology we developed an analytical model for the HDR valve power circuit to determine the influence of external circuit resistance on the HDR valve anomaly. The HDR in situ tests and the Limitorque tests were chosen for comparison, as the motor operator was operated a comparable number of times over the same period of time at both locations and the size of the large external circuit cabling at Limitorque should eliminate the influence of any external circuit resistance. Two different calculations of the HDR power conductor resistance were made: one was based on the size and approximate length of the cables, and the other on measurements of the current through the circuit and the voltage drop across the portion of the circuit that was measured. The calculations were comparable. Four times the calculated resistance for a single cable was inserted in the analytic model to account for the armature and the field being connected in series through the motor controller. The measured parameters from the HDR in situ testing and the Limitorque dynamometer testing were then

analyzed and actual motor resistances calculated. Very good comparisons were found. The results demonstrate that the differences between the motor operator performance at HDR and the performance at Limitorque were caused by external circuit resistances.

These results point out the significance of the external circuit resistance and motor heatup in reducing the safety margins of motor operator torque output. High external circuit resistance and motor heating are not usually detectable in normal plant in situ testing, where valves are tested with no load or with a static pressure load alone. This was quite apparent from HDR in situ testing, where the motor operator operated successfully with no pressure, static pressure alone, and with static pressure and very low differential pressure. When the differential pressure from the flow load was increased, the valve either failed to close all the way or the operator motor stalled, depending on the torque switch setting.

To understand this in situ problem, one must understand dc motors. These motors generate a back electromotive force (EMF) when turning. This back EMF acts like a bucking voltage in the circuit. Stated in an over-simplified way, this back EMF limits the current in the circuit much the way a resistance would. The back EMF is proportional to the motor speed and current. These high-torque compound-wound motors have a weak shunt field and act very much like a series wound motor in application. As the load is increased the motor slows down, reducing the back EMF. This allows more current to flow, thus producing higher torque. This behavior continues down to motor stall, where the dc resistance of the motor is the only internal resistance to current flow. These motor resistances at or near locked rotor are in the 1.0 to 1.5 ohm range for a 40 to 60 ft-lb output torque motor operating on 125 Vdc. Because the field and armature cabling are connected in series through the motor controller, four long cable runs, not two, contribute to the resistance of the external circuit. External circuit resistance of just 0.5 to 1.0 ohm can reduce the motor output torque by 1/3 to 1/2.

During normal valve testing or operation, the resulting motor loadings are in the 20 to 30% running torque range. The back EMF or effective motor resistance would be approximately 5 ohms, and a 0.5 to 1.0 ohm external resistance would not significantly degrade motor performance. This conclusion was supported by the results of the HDR static pressure testing. However, during a transient or a line break where isolation is required, the high differential pressure across the valve disc would require a higher motor output, and the external circuit resistance in series with the motor resistance could reduce the output torque of the

motor significantly, as it did at the HDR during tests with flow loads.

At the end of our investigation of the valve's anomalous performance at HDR, we had identified three separate problems. The potential safety implications of these problems are significant. Spring aging can result in a valve that torques out early and, depending on the extent of the degradation, can leave the valve partially open. Coil spring aging in the older SMA motor operators may go undetected, as there are fewer diagnostic test systems adaptable to these units. Motor heating can reduce motor operator output if the valve is cycled more than once without time for the windings to cool. If a marginally powered valve is subjected to high loads on closing, this reduced output can result in motor stall, probably with the valve partially open. External circuit resistance also can cause the motor to stall before the valve fully closes. Motor stall can cause the thermal overload switches to open and render the motor operator temporarily unavailable for use. If the thermal overload switches have been bypassed or set too high, or if they malfunction, the motor will burn out. High external circuit resistance in both the SMA and the newer SMB operators with dc motors can go undetected in normal in situ valve testing. The problem is detectable only at higher loadings when the motor is slowed down and momentum can not carry the unit through torque out.

A complete discussion of the anomalous performance of the valve is given in Appendix A (Volume 2). Appendix A also gives a description of the valve and its refurbishment and subsequent installation in the HDR.

3.6.4 Valve Dynamic Analysis. HDR SHAG test results indicated an unexpectedly large high-frequency response of the gate valve installed in the VKL. In addition, accelerations (transverse to the valve stem) were significantly amplified from the valve body to the valve operator. These results were not anticipated by bench testing.

Seismic qualification of line-mounted equipment is currently based on bench tests and analytical calculations. As part of its refurbishment, INEL dynamically tested the valve to Annex "E" Exploratory Vibration Test of ANSI B16.41, and determined the valve's natural frequencies. The lowest natural frequencies found were 28 Hz and 48 Hz, respectively, in the directions perpendicular and parallel to the valve flow axis. The valve perpendicular axis is X; the direction parallel to the flow axis is Z. Valve qualification standards define flexible and rigid valve assemblies by their fundamental frequency, and the qualification requirements differ accordingly. Valve assemblies having frequencies below 33 Hz are considered flexible and require rigorous testing as defined in the actuator

qualification standard. Valve assemblies having fundamental frequencies above 33 Hz are considered rigid, and seismic qualification can be as simple as a yoke deflection test. The standards also allow both rigid and flexible assemblies to be qualified by analyses without testing. Typically in industry, the decision as to whether a valve is flexible or rigid is made by comparing the fundamental frequency of the valve with the response spectra for the valve installation. If the fundamental frequency of the valve falls within the amplified portion of the spectra, it is considered flexible, and if it is above, it is considered rigid. The lowest frequency of this valve was 28 Hz, which was well above the amplified portion of the HDR installation. It was considered a rigid valve for the HDR and would have been also considered rigid for most U.S. plant applications.

The in situ environment at the HDR presented an excellent opportunity to compare valve dynamic performance determined by bench testing with actual in situ dynamic behavior. During posttest evaluation of the valve response data, examination of the valve acceleration histories revealed considerable amplification of response at the valve motor operator as compared to corresponding response of the valve body. Triaxial accelerometers were located on the body, at the center of gravity, and on the motor operator. Further evaluation of the responses in the frequency domain revealed amplification at frequencies above and below bench-tested lower-mode frequencies. The higher frequencies are considered important, as most seismic qualification addresses only frequencies less than 33 Hz. The maximum excitation frequency input to the HDR building was 8 Hz, and high-frequency (greater than 33 Hz) amplified response of the valve actuator was not expected.

3.6.4.1 Investigation of High-frequency Amplification

Owing to the potential significance of this finding on qualification requirements for valve-operator and operator-mounted valve control components, the phenomenon was investigated in detail. The objectives of the investigation were (a) to quantify and compare the measured response, (b) to determine if the response was influenced by piping support configuration, and (c) to determine, if possible, if the high-frequency response was generated within the valve or was an amplified response generated external to the valve.

The U.S. stiff and KfK flexible support systems were selected for study since they should envelope the piping system response. The 8-Hz starting frequency was selected so that the greatest input excitation frequency bandwidth was available. These tests were designated T40.30 (U.S. stiff) and T40.10 (KfK flexible).

As previously described, the data indicate that the excitation of the piping system was predominately caused by motion of the HDU vessel at the two nozzle connections to the VKL. Therefore, the accelerometer locations studied were those at the top of the HDU, at the valve, and at available intermediate VKL accelerometer locations. In this discussion, these locations are designated Top HDU, Standard T, Spherical T, Valve Body, and Valve Operator, corresponding to instrument locations 8, 16, 9, 40 and 42, respectively. These locations are shown in Figure 48. Since each of these five locations was instrumented with triaxial accelerometers, a total of fifteen transducer output records were studied for each of the two tests.

Frequency domain analysis was used to study and compare the behavior of the five locations. Standard procedures were used to calculate auto-spectra [power spectral densities, (PSDs)] of the acceleration records. Appendix E (Volume 2) contains a complete discussion of the valve dynamic analysis.

A standard technique in frequency analysis is to average the PSDs obtained from several sequential time frames in order to minimize the effect of noise in the measurements. However, for the measurements studied herein, several of the resonant peaks in the PSDs changed in frequency as a function of the time frame studied because of the coastdown of the shaker. Thus, averaging several sequential frames had the effect of smearing these variable PSD peaks. In order to reduce the smearing effect, analysts studied and compared the data on a frame by frame basis.

Subsequent discussion of analysis and results deals with the first 8 s of the transient. The data acquired by KfK was low-pass filtered at 30 Hz during acquisition; thus, the potential high-frequency (33 to 50 Hz) information present at the top of the HDU vessel and at the spherical tee may have been removed from the acceleration histories recorded for these locations. Data acquired by INEL was low-pass filtered at 200 Hz, so this is not a problem for the other measured points.

Figures 49 through 51 reproduce the first-frame PSDs found in frequency analysis of the 30 acceleration histories (X, Y, and Z directions for each of the five locations, and for each of the two tests). The figures present the PSDs of the major excitation source (the top of the HDU) on the left, then follow the load path from left to right through the standard tee, the spherical tee, the valve body, and the valve actuator (located on the far right). Each figure represents either the X, Y, or Z response direction, with the KfK flexible system shown at the top of the figure, and the U.S. stiff system shown below.

Figure 49, the X axis PSD matrix, shows essentially the same HDU response for both systems. Comparison of the standard tee responses shows for the

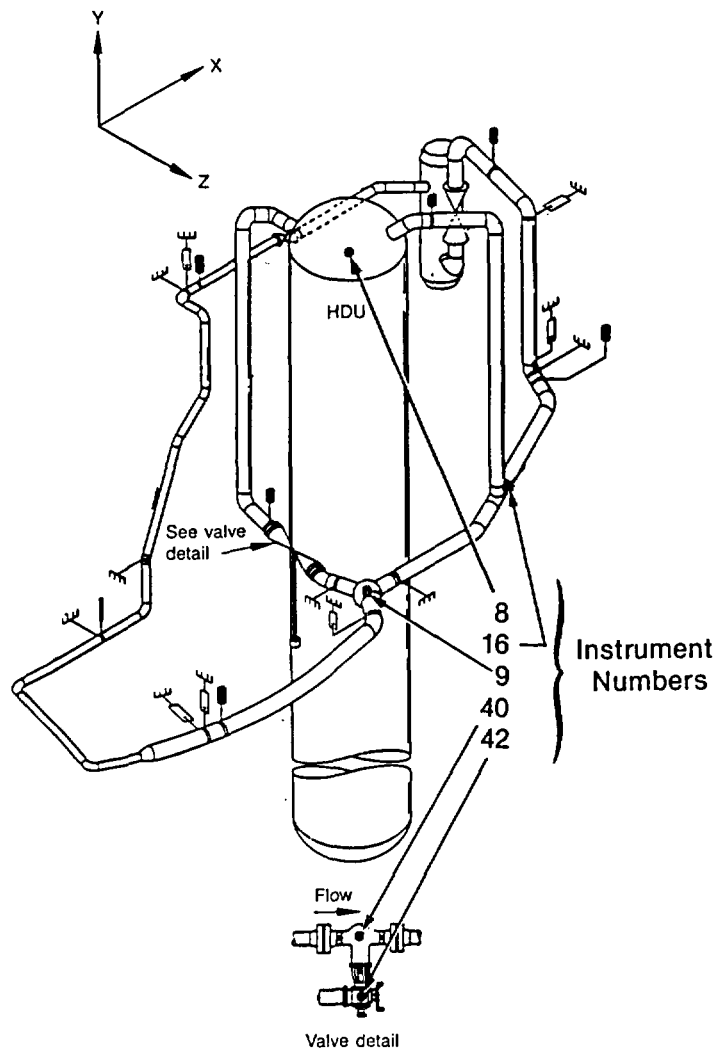


Figure 48. Instrument locations for the dynamic load path from the HDU vessel to the 8-in. gate valve.

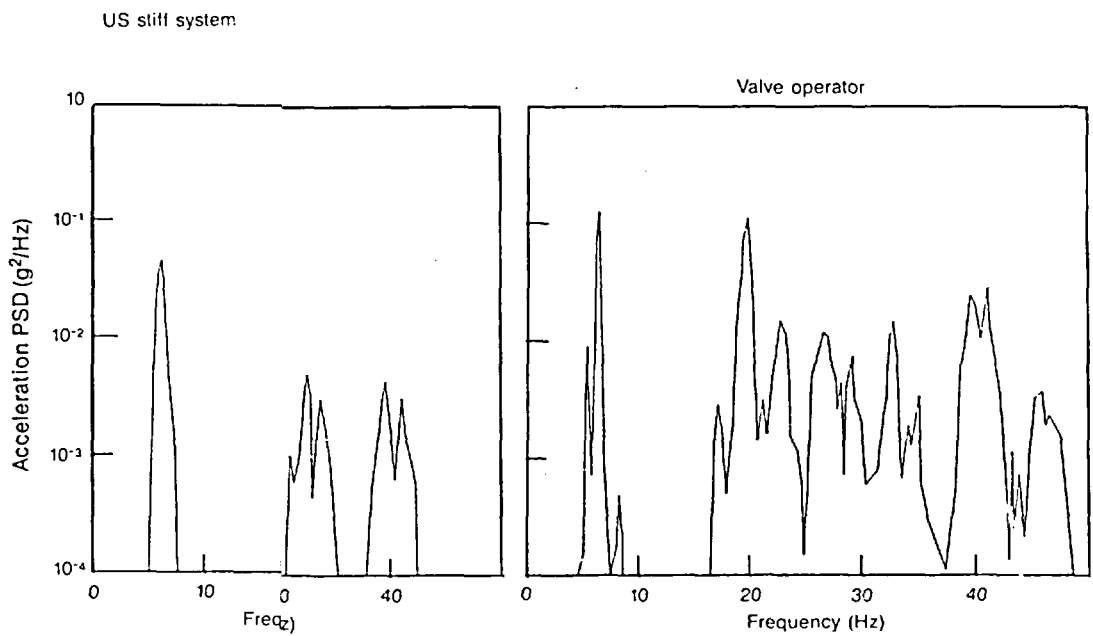
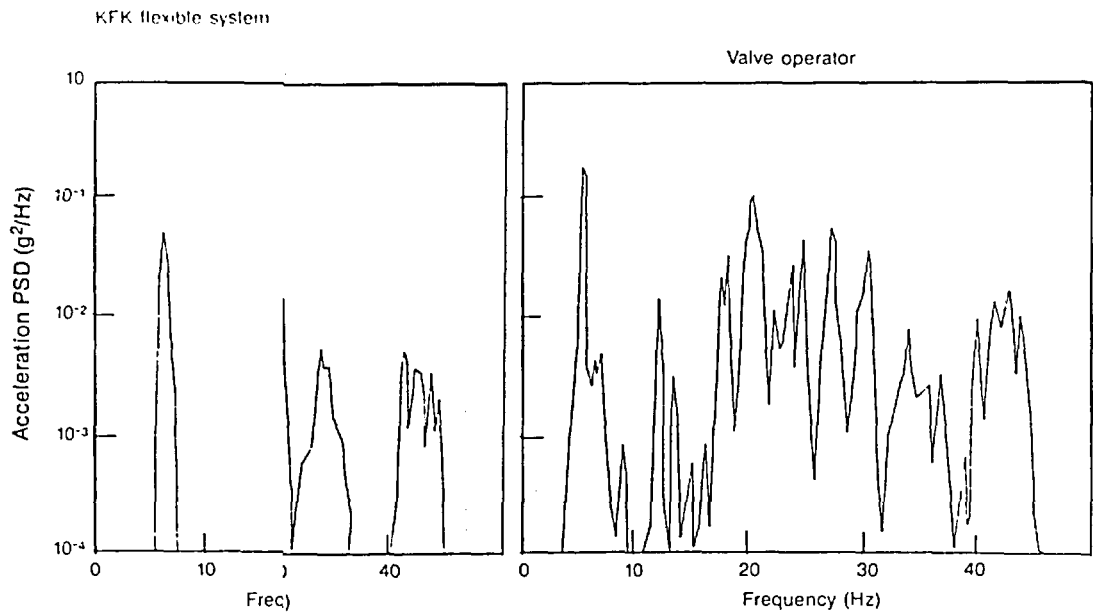
flexible system a greater response in the low-frequency range, as expected, with the higher-frequency distributions slightly different, but not significantly so. INEL/MPA monitored the standard tee instrumentation location. As previously discussed, these data were not filtered at 30 Hz; high-frequency content is shown. However, instrumentation located at the spherical tee was monitored by KfK and, for the most part, the high-frequency content of the response appears to have been filtered out.

For all instrument locations in the frequency range less than 10 Hz, the U.S. stiff system frequency distributions follow the HDU response with a narrow band response, whereas the flexible system response distribution is more broadbanded. For valve body and operator instrument locations, note again that response data are unfiltered at 30 Hz; high-frequency content is present. The valve responses also indicate a lower

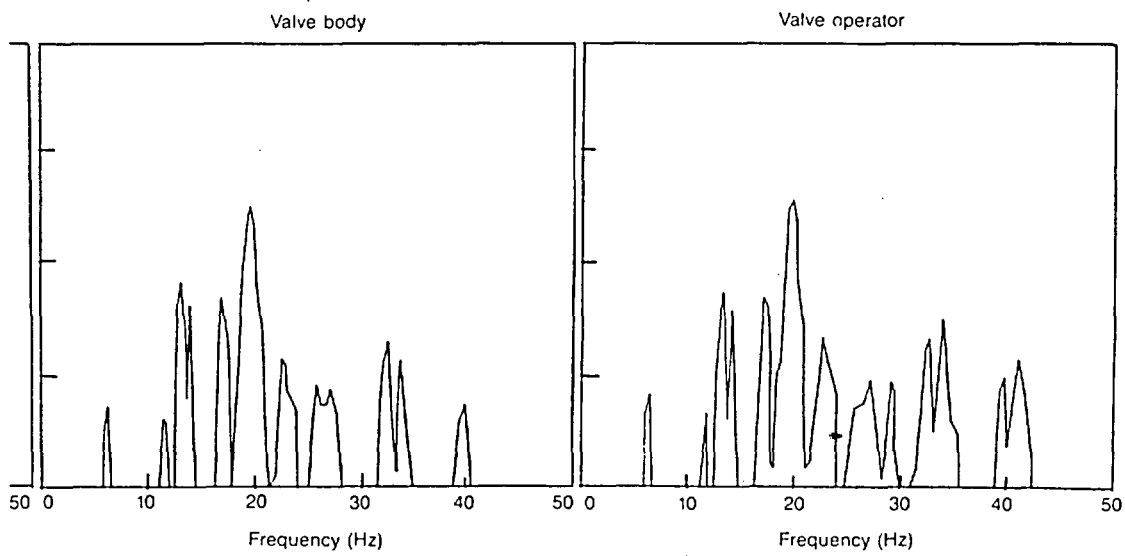
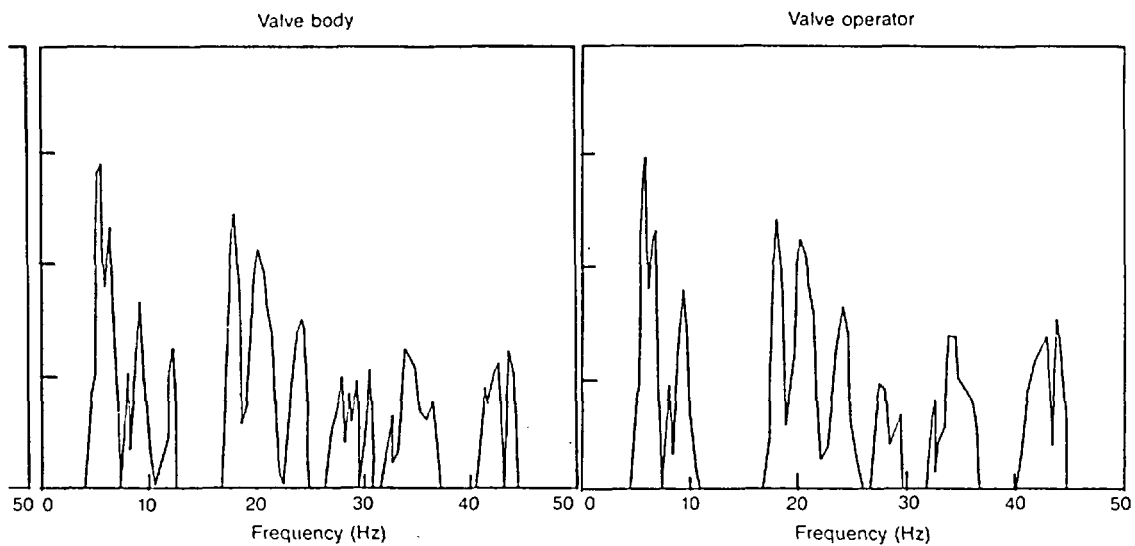
frequency content for the flexible system than is seen in the stiff system response.

Comparison of the valve operator responses with the valve body responses shows considerable amplification and band broadening, especially for frequencies above 10 Hz. We believe that the 8-Hz response peak appearing in all of the plots represents near rigid body motion of the entire VKL system and follows the shaker input excitation. The remainder of the response bands do not appear to be harmonic components of the shaker excitation; we assume that they represent dynamic response modes of the VKL system and HDU vessel. Note that no significant amplification occurs between the HDU and the valve body.

The most significant peak appearing in the operator responses, other than the shaker-induced 8-Hz peak, occurs near 20 Hz. We consider this amplification at 20 Hz to be the results of a resonance, since it appears



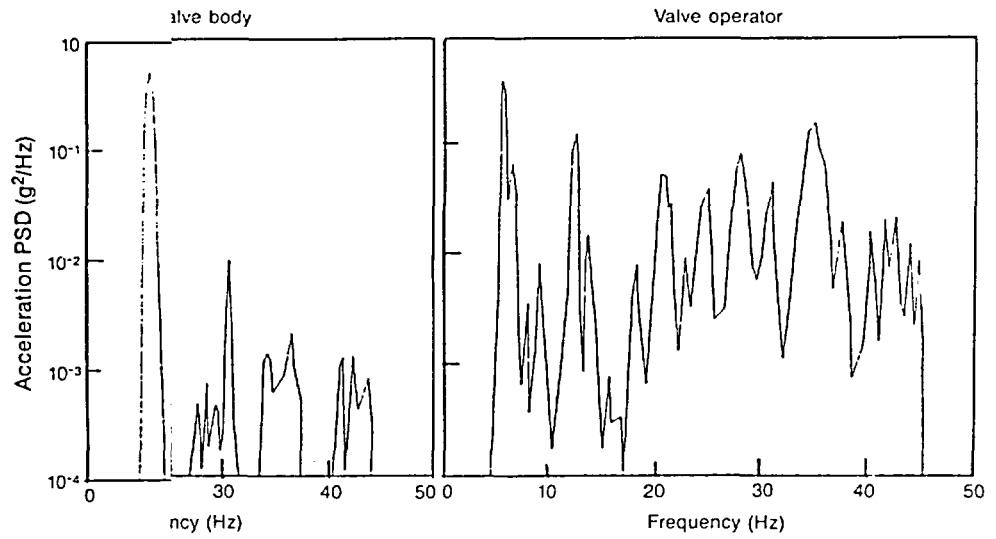
7-8897



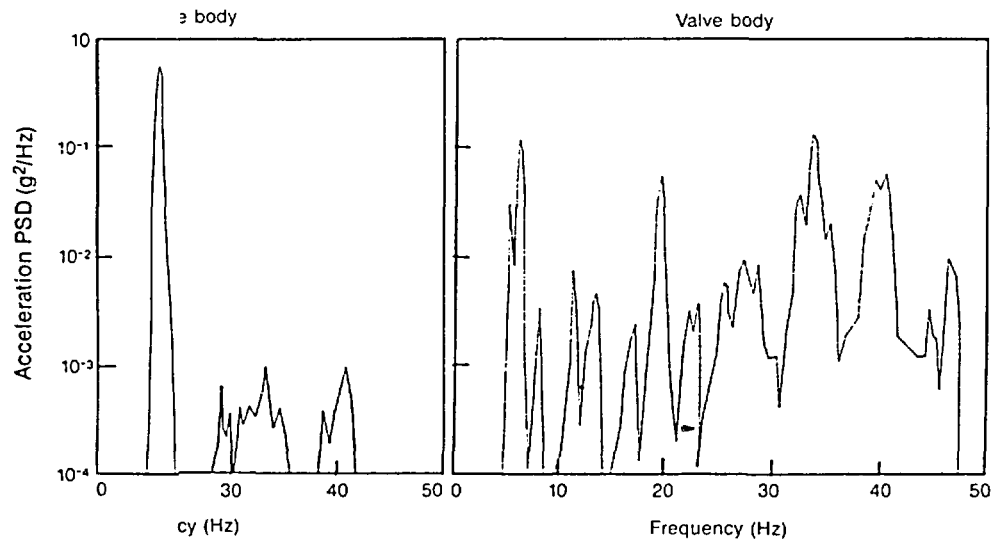
7-8898

e from the KfK flexible and U.S.

KFK flex



US stiff sy



HDR gl

7-8899

U.S.

in all of the PSD plots. However, since the resonance is independent of piping configuration, it may be caused by a local valve vibration mode. This mode was not detected during the bench fundamental frequency determination tests of the valve prior to installation in the VKL. Also, the 20 Hz mode is strongly present at the HDU top, which indicates the possibility of this being a mode of the HDU, transmitted through the VKL and amplified at the valve operator. An additional peak seen in the two valve operator PSDs occurs near 30 Hz. This resonance may be caused by a local valve vibration mode measured during the bench tests to occur at 28 Hz, where the difference between in situ installation and bench shaker mounting stiffness could account for the difference in frequency. Significant response amplification is seen for frequencies greater than 40 Hz, especially for the stiff configuration. The response peak located at 47 Hz may be owing to cross coupling between the Z and X axes, where a local valve resonance was found during bench tests to occur at 48 Hz (global Z axis).

Figure 50 presents global Y direction (vertical) acceleration response PSDs in a manner similar to the figure discussed above. Examination of the PSDs shown in this figure illustrates the source of the differences between the flexible and stiff system strain, displacement, and load responses. Comparison of the HDU and standard tee results indicates that their responses are independent of the support configuration. However, for the spherical tee and valve responses, there is significantly greater low-frequency (less than 10 Hz) acceleration for the flexible configuration. Since displacement, strain, and force are much more influenced by low-frequency acceleration than by the higher-frequency accelerations, differences in low-frequency vertical acceleration dominate the observed difference in load and strain between the two systems, as discussed in Section 3.3. The difference in observed response is probably primarily due to the presence of the vertical snubber (H-6) located at the spherical tee, which was not installed in the flexible configuration. Again, some high-frequency response is observed at the valve. However, there is little amplification of this response from the valve body to the operator; the valve vertical response appears to be primarily rigid body. This is as expected, since the valve assembly is extremely stiff in this direction.

Figure 51 presents acceleration PSD comparisons for response in the global Z direction. As in the X and Y directions, response of the HDU is very similar for both configurations. Significant high-frequency acceleration is observed for both configurations at the standard tee. Spherical tee responses have similar frequency distributions with somewhat different magnitude distributions. For lower and higher frequency

ranges, and for both configurations, the valve body has decreased response as compared to the standard tee. This may be because of anti-resonances at the valve body for frequencies within these ranges, or the Z-direction response is attenuated by horizontal supports located at the spherical tee. The valve operator responses, for both configurations, show significant high-frequency content and amplification when compared with all other Z-direction responses. This amplification is especially significant for frequencies between 35 and 45 Hz. Recall that bench test results indicate a local valve natural mode at 48 Hz, which may influence the observed amplification at the higher end of the frequency range.

Appendix E (Volume 2) reproduces all PSDs, including both the first and second 8-s data frames, and presents a more quantitative comparison of acceleration response and band integrated PSDs. Portions of the band-integrated data are graphically reproduced, showing valve-body-to-actuator amplifications and allowing frequency-distribution comparisons between the two support configurations for each response point.

In summary, all results presented show significant high-frequency (35- to 45-Hz) acceleration at the valve operator, and significant amplification of this acceleration from the valve body to the operator for the horizontal (X and Z directions) acceleration components. In the vertical direction (parallel to the valve actuator shaft), valve high-frequency content was significantly less, with little or no amplification between the valve body and operator. Even though the driving point (HDU top) acceleration records have been low-pass filtered at 30 Hz, there is evidence of some higher-frequency accelerations. We believe that the high-frequency acceleration experienced by the valve originated at the primary driving point, the HDU top, and was amplified by transmission through the VKL. Analysis results show that most amplification occurred between the valve body and valve operator. Bench frequency tests of the valve, prior to installation in the VKL, indicate that the valve assembly did not contain natural vibration modes in the frequency range of 30 to 45 Hz. Analysis also indicates that the high-frequency acceleration content and amplification present at the valve operator was experienced for both flexible and stiff configurations. However, the frequency distributions did differ for these configurations.

It is well known that the stiffness of a piping system changes its response frequency, and its response frequency changes the input to the line-mounted equipment within the system. The small variations in valve response between the flexible and stiff systems in the horizontal axes are insignificant. The primary difference appears in the piping system's low-frequency vertical response. The acceleration amplification across

the valve assembly contains a slightly different frequency distribution, but significant amplification is present in both piping support system responses.

To further verify the significant high-frequency valve operator acceleration response observed during the HDR SHAG tests, we performed a limited examination of the results of a similar but related study, the Containment Penetration System (CPS) dynamic test [see Reference 13 (NUREG/CR-4734)]. That examination, reported in Appendix E (Volume 2), showed that even though the CPS geometry and excitation method were very different from those of the VKL at HDR, the acceleration responses of the CPS gate and butterfly valves were strikingly similar to the VKL gate

valve responses. We conclude that the observed frequency-dependent behavior of the three valves is primarily a function of the valves' dynamic characteristics rather than the piping system geometries or the excitation methods.

The high frequency observed in the motor operator response during HDR tests is not accounted for in typical valve qualification. It is not expected that response in these frequency ranges will affect the valve structurally. However, they may affect valve operability by causing switches, relays, and other valve control and indication devices to chatter. The nuclear industry does not qualify these control devices to the frequencies that may be seen in an actual event.

4. CONCLUSIONS

The HDR presented a unique opportunity to research valve and piping system response in a reasonably typical in situ environment. In combination, the in situ loads input to the VKL system during the SHAG test series were sufficient in magnitude to provide understanding of valve and piping system responses. Analyses of the measured input and response data yield both confirmatory and conflicting evidence for support of current equipment qualification practices and piping system support technology. Following are INEL's several conclusions from its participation in the HDR SHAG Project.

4.1 Building and Piping System Responses

Pipe support system design can increase system reliability and reduce thermally induced stresses. A strong movement currently exists in the technical community to revise seismic design standards for piping in nuclear power plants. The philosophy behind present U.S. seismic design has been to raise the natural frequency of the piping system above the natural frequency of the building, thus reducing resonant interaction. The disadvantage of this type of design is that it may increase stresses caused by thermal expansion and independent building or anchor motion. The stiff piping support system typically uses snubbers, which have a history of locking up even without dynamic load. Locked up snubbers increase thermally induced stress, which can have serious consequences (the incident at Trojan with the reactor coolant loop is a case in point; see Reference 14).

A major portion of the HDR SHAG test series was concerned with measuring the piping system responses produced by various support configurations. A wide range of system stiffnesses were investigated, including a very flexible system, a moderately flexible system typical of nonnuclear power piping design, and a stiff system typical of U.S. nuclear design. Posttest analyses of very flexible and stiff system responses indicated, as would be expected, that stiff system dynamic response stresses were less than the corresponding flexible system stresses. However, the relative differences were not as great as would be expected. The moderately flexible system, with 50% fewer supports than the U.S. stiff design, responded with a smaller total system stress than any of the other systems tested. This may have been because the duration of the excitation, though conservatively representative of earthquake strong motion excitation duration,

was not long enough for the lower frequency modes of the moderately flexible system to reach maximum response.

Further analysis of experimental results is needed. KfK and ANL have the research assignments for indepth piping analyses. However, from the limited analysis we performed to understand equipment response issues, the results suggests the advantages of more flexible designs for nuclear piping systems.

4.2 Snubber Responses

Modern snubbers perform their function in a dynamic event; however, they may be susceptible to in-plant aging. The four INC snubbers installed during the preliminary tests at HDR failed to meet the manufacturer's specifications. Three of them failed to lock up, and one locked up with the pipe deflected 0.5 in. Post-test discussions with the staff of USNRC and with snubber vendors indicated that INC-designed snubbers have been removed from U.S. nuclear power plants, so these failures do not point out a safety problem.

The Pacific Scientific snubbers appear, with one exception, to meet the manufacturer's specifications. They also appear to have sufficient margin, as repeated testing at ASME Code Level C allowable loads did not degrade their performance. The one exception was pointed out in the snubber section of this report, where the snubber at H-1 failed to resist dynamic motion for 3 or 4 s during Test T40.30. This anomaly will be investigated in follow-on testing. We do not expect this to indicate a safety problem.

The snubbers used at HDR were not subjected to environmental aging as they are in nuclear plants. Aging problems were not experienced at HDR. We conclude from the HDR testing that when the mechanical components of the snubber are operable they resist motion at near load capacity.

4.3 Snubber Replacement Devices Compared

The snubber replacement devices tested on the VKL during the HDR experiments are all potentially more reliable than snubbers. There are fewer moving parts; hence, there is less chance for problems. However, one must also consider the effect that these devices may have on the response of the piping. The piping system peak response will occur when a piping system is excited at its natural or resonant frequencies. Piping

supports assist in establishing that natural frequency. The more flexible Bechtel support will lower the natural frequency of the piping system. The ANCO devices appear to be stiffer than snubbers. The Cloud device is the most flexible of all, since it does not restrain the pipe until impact. A problem that could result with the impacting type of support is that it can generate high frequency response. Line-mounted equipment typically is seismically qualified for 33 Hz and less. The high frequency response may well have an adverse effect on the control components for valves and other line-mounted equipment. High frequency response should be considered before use of the impact energy absorber.

These devices may increase the reliability of seismic restraints without increasing thermal induced stress. However, increased pipe reliability should not be traded for decreases of reliability in line-mounted equipment.

4.4 Valve Response

Valves are inherently rugged and, typically, are structurally not affected by seismic dynamic excitation. The naturally aged motor-operated valve obtained from the Shippingport Atomic Power Station was manufactured prior to equipment qualification requirements applied to valves procured today. However, the valve is still quite similar to valves procured today and is representative of units in the older plants and reasonably representative of the valves in newer plants. The motor operator manufactured by Limitorque (Model SMA) was manufactured from mid-1950s to mid-1960s and is representative of motor operators installed in the older plants (plants going on line up to the late 60s). The valve and operator were exposed to a significant number of dynamic excitations and performed as designed, with the exception of failure of the valve to close completely and to torque out on closing. HDR testing verifies that valve and piping systems are structurally inherently tough. Based on the loadings input at HDR and the measured system strains, considerably higher loadings could have been applied before reaching near yield stresses of the system. This is true for both the very flexible and the stiff support

configurations, which envelope most of today's operating systems.

The anomalous performance of the motor operator was not related to the seismic loads imposed during testing. Three factors contributed to the valve's anomalous performance: torque spring aging, motor heating, and undersized power cables. Test methods could be devised that would determine the condition of the torque spring and indicate whether the torque switch setting needed to be changed and whether the spring needed to be replaced. The failure of the motor operator to torque out was caused partly by motor heating and mostly by undersized power cabling. Current in-plant testing with no loads or with static pressure loads alone cannot detect these two problems.

Where these three problems exist undetected in the field, valves subjected to design flow and pressure loads might not completely close. If the thermal overload switches malfunction or if they have been bypassed in a motor that stalls, the motor could burn out.

|| Aging

4.5 Valve Dynamic Analysis

Valve qualification standards may not envelope actual response frequencies in a dynamic event. Valve seismic qualification tests verify design. Standards allow generic and family group testing, which is as it should be for these very rugged structures. The vulnerable components of typical valve assemblies, if any exist, are the operator controls and switches. The HDR and CPS dynamic testing results indicate that the qualification methods and requirements may not adequately envelope the magnitude and range of frequencies that the valve operator can experience. It is possible that high frequency responses at the operator could cause switches and relays to chatter. This may not be a problem, as the control devices may not be effected by these inputs, but we cannot conclude this from the subject testing. The information obtained from the HDR and CPS valve response will be presented to the ASME equipment Qualification Main and Valve Subcommittees for their consideration. The high-frequency response of the motor operator will be investigated further in the follow-on SHAM test series at HDR.

5. REFERENCES

1. S. H. Bush, P. G. Heasler, and R. E. Dodge, *Aging and Service Wear of Hydraulic and Mechanical Snubbers Used on Safety-Related Piping and Components of Nuclear Power Plants*, NUREG/CR-4279, PNL-5479, Vol. 1, February 1986.
2. *Mechanical Shock Arrestors, Standard Design Specification*, DR-1319, Pacific Scientific Company, 1346 South State College Boulevard, Anaheim, California 92803, April 1975.
3. J. E. Glauser, *Aerospace Technology Applied to Nuclear Power Plant Problems*, Pacific Scientific Company, 1346 South State College Boulevard, Anaheim, California 92803.
4. J. Glauser, "Application of Mechanical Snubbers for Seismic Restraint," *Nuclear Engineering International*, May 1978.
5. American Society of Mechanical Engineers, *Boiler and Pressure Vessel Code, Section III, Subsection NF, Component Supports*, 1986 Edition.
6. United States Nuclear Regulatory Commission, *USNRC Standard Review Plan, Section 3.9.3, ASME Code Class 1, 2, and 3 Components, Component Supports, and Core Support Structures*, NUREG-0800, 1981.
7. United States Nuclear Regulatory Commission, *Qualification and Acceptance Tests for Snubbers Used in Systems Important to Safety*, Draft Regulatory Guide SC 708-4, Rev. 1, 1981.
8. American Society of Mechanical Engineers, *Examination and Performance Testing of Nuclear Power Plant Dynamic Restraints (Snubbers)*, ANSI ASME OM4, 1982.
9. American Society of Mechanical Engineers, *Boiler and Pressure Vessel Code, Section XI, Subsection IWF, Requirements for Class 1, 2, 3 and MC Component Supports of Light-Water Cooled Power Plants*, 1979 and 1986 Editions.
10. Celesco Transducer Products, Inc., *Celesco Transducer Catalog*, 7800 Deering Avenue, Canoga Park, California 91304-5005.
11. American Society of Mechanical Engineers, *Functional Qualification for Power Operated Active Valve Assemblies for Nuclear Power Plants*, ANSI B16.41.
12. Idaho National Engineering Laboratory, *Valve Research HDR/VKL Phase II SHAG Testing Requirements*, EGG-REQ-7148, Rev. 2, May 1986.
13. Idaho National Engineering Laboratory, *Seismic Testing of Typical Containment Piping Penetration Systems*, NUREG/CR-4734, EGG-2470, December 1986.
14. Memorandum from C. E. Rossi to T. L. Chan Dated June 11, 1986, Subject Safety Evaluation of Inoperable Steam Generator Snubbers on the Trojan Nuclear Plant Reactor Coolant Loop (TAC #61405).

BIBLIOGRAPHIC DATA SHEET

(See instructions on the reverse)

1. REPORT NUMBER
(Assigned by NRC. Add Vol., Supp., Rev.,
and Addendum Numbers, if any.)
NUREG/CR-4977
EGG-2505
Vol. 1

2. TITLE AND SUBTITLE

SHAG Test Series

Seismic Research on an Aged United States Gate Valve and on a
Piping System in the Decommissioned Heissdampfreaktor (HDR):
Summary

3. DATE REPORT PUBLISHED

MONTH | YEAR
August | 1989

4. FIN OR GRANT NUMBER

A6322

5. AUTHOR(S)

R. Steele, Jr., J.G. Arendts

6. TYPE OF REPORT

Technical

7. PERIOD COVERED (Inclusive Dates)

8. PERFORMING ORGANIZATION - NAME AND ADDRESS (If NRC, provide Division, Office or Region, U.S. Nuclear Regulatory Commission, and mailing address; if contractor, provide name and mailing address.)

Idaho National Engineering Laboratory
EG&G Idaho, Inc.
Idaho Falls, ID 83415

9. SPONSORING ORGANIZATION - NAME AND ADDRESS (If NRC, type "Same as above"; if contractor, provide NRC Division, Office or Region, U.S. Nuclear Regulatory Commission, and mailing address.)

Division of Engineering
Office of Nuclear Regulatory Research
U.S. Nuclear Regulatory Commission
Washington, D.C. 20555

10. SUPPLEMENTARY NOTES

1. The Idaho National Engineering Laboratory (INEL) participated in an internationally sponsored seismic research program conducted at a decommissioned experimental reactor facility, the Heissdampfreaktor (HDR), located in the Federal Republic of Germany (FRG). The research program included the study of the effects of excitation, produced during a simulated seismic event, on (a) the operability and integrity of a naturally aged 8-in. motor-operated gate valve installed in the Versuchskreislauf (VKL), an existing piping system in the HDR, (b) the dynamic response of the VKL and the operability of snubbers, and (c) the dynamic responses of various piping support systems installed on the VKL. The INEL work, sponsored by the U.S. Nuclear Regulatory Commission (USNRC), contributes to earthquake investigations being conducted by the Kernforschungszentrum Karlsruhe (KfK) and is part of the general HDR Safety Program performed in behalf of the FRG, Federal Ministry for Research and Technology. This report presents the results of the KfK-designated SHAG (Shakergebäude) test series; these are the first in situ experiments involving an actual nuclear power plant and a full scale piping system under simulated seismic loading. Volume I presents a summary of the tests and results, and Volume II contains appendices that present details and specifics of the tests and results of Volume I.

12. KEY WORDS/DESCRIPTORS (List words or phrases that will assist researchers in locating the report.)

SHAG test series
seismic research program
aged gate valve
Piping system
Heissdampfreaktor (HDR)
simulated seismic loading

13. AVAILABILITY STATEMENT

unlimited

14. SECURITY CLASSIFICATION

(This Page)

unclassified

(This Report)

unclassified

15. NUMBER OF PAGES

16. PRICE

**UNITED STATES
NUCLEAR REGULATORY COMMISSION
WASHINGTON, D.C. 20555**

**OFFICIAL BUSINESS
PENALTY FOR PRIVATE USE, \$300**

SPECIAL FOURTH-CLASS RATE
POSTAGE & FEES PAID
USNRC
PERMIT No. G-67

NUREG/CR-4977, Vol. 1

SHAG TEST SERIES

AUGUST 1989